Unraveling details of CIN85/CD2AP assistance to SLP65-mediated B cell activation

Dissertation

for the award of the degree

"Doctor rerum naturalium"

Of the Georg-August-Universität Göttingen

within the doctoral program IMPRS Molecular Biology

of the Georg-August University School of Science (GAUSS)

submitted by

Arshiya Bhatt

From New Delhi, India

Göttingen, 2019

Thesis Committee

Prof. Dr. Jürgen Wienands, Institute of Cellular and Molecular Immunology, University Medical Center, Göttingen

2nd Referee: Prof. Dr. Blanche Schwappach, Department of Molecular Biology, University Medical Center, Göttingen

Prof. Dr. Steven Johnsen, Clinic for General, Visceral and Pediatric Surgery, University Medical Center, Göttingen (Former position)

Members of the Examination Board

Referee: Prof. Dr. Jürgen Wienands, Institute of Cellular and Molecular Immunology, University Medical Center, Göttingen

2nd Referee: Prof. Dr. Blanche Schwappach, Department of Molecular Biology, University Medical Center, Göttingen

Further members of the Examination Board

Prof. Dr. Christian Griesinger, Department of NMR-based Structural Biology, Max Planck Institute for Biophysical Chemistry, Göttingen

Prof. Dr. Thomas Meyer, Department of Psychosomatic medicine and Psychotherapy, University Medical Center, Göttingen

Prof. Dr. Dieter Kube, Department of Hematology and Oncology, University Medical Center, Göttingen

Prof. Dr. Henning Urlaub, Department of Bioanalytical Mass Spectrometry, Max Planck Institute for Biophysical Chemistry, Göttingen

Date of oral examination: September 17th, 2019

सर्वतीर्थमयी माता सर्वदेवमयः पिता

मातरं पितरं तस्मात् सर्वयत्नेन पूजयेत् ।

To my parents…

Abstract

The hallmark of adaptive immunity is the production of specific antibodies. This process is initiated upon the ligation of the B cell antigen receptor (BCR) which activates multiple intracellular signaling cascades through the phosphorylation of the B cell 'master regulator': SLP65. Our lab found that in order to function, SLP65 interacts constitutively – in a stimulation independent manner, with molecules of the CIN85/CD2AP-family of adaptor proteins, harbouring multiple protein interaction domains.

Mouse models with B-cell specific CIN85 deletion and patients with a germline deletion in CIN85 encoding gene have shown that CIN85 is mandatory for B cell activation and the subsequent B cell responses. The molecular basis of the mechanism driving this, however, needed further elucidation. The primary cells pose a limitation to the scope of genetic and mechanistic studies due to the scarce availability of the reserve. I addressed these aspects through the generation of CIN85-deficient B cells from the established B cell lines, followed by subsequent deletion of CD2AP.

The cellular system thus created was used to conduct genetic and biochemical functional assays to assess how these proteins work. I observed that CIN85 significantly impacts the Ca^{2+} flux upon BCR-ligation. Moreover, CIN85 could additionally affect an upstream NF-κB pathway signaling element called PKCβ. I also used the abovementioned CIN85/CD2AP-double deficient cells to investigate further binding partners of SLP65 employing SILAC-based mass spectrometry to look for possible functional redundancies.

In our collaboration with Prof. C. Griesinger's group, we found that CIN85 and SLP65 undergo phase-separation into supramolecular-clusters, representing the more recent and exciting intracellular compartments of membrane-free, mini-organelles, that orchestrate signaling in B cells. Due to their capacity to interact with multiple signaling elements, droplet signalosomes could be the modus operandi for CIN85/CD2AP-family of adaptor proteins for scaffolding of relevant signaling proteins.

Table of Contents

Chapter 1: Introduction

1.1 Basic concepts in Immunology, a brief overview of the Immune system and identifying the B lymphocytes

The immune system is the host's defence system, the loyal battalion bestowed with the ardent task of protecting the host against the pathogenic invaders or occasionally, the cellular-traitors within, like tumour cells. Ready to combat, are the soldiers that comprise of a vastly complex network of circulating molecules and cells that extend up to the higher ranks of specialised tissues and organs. In the strategic defence for the purpose of deterring, resisting, and repelling a strategic offensive, the immune system employs two components: the innate and the adaptive components, with much crosstalk between the two branches. The innate branch of the immune system provides the first line of defence. It consists of pre-existing systems, for example, the anatomical barrier of the epithelial layer and the mucosa lining that provide physical obstruction to the pathogen invasion. It is a conserved, germline encoded-strategy to mount a set of non-specific immune responses, to recognize a broad range of conserved pathogenic patterns. They act rapidly, bypass the need for previous exposure to elicit a full response and mediate pathogen clearance (Medzhitov & Janeway, 2000).

The adaptive immune system evolved to mount a more specific-immune response against the diverse pathogens and confers memory for subsequent similar encounters with that pathogen (Flajnik & Masanori, 2008; Parkin & Cohen, 2001). It may take several days or weeks to become fully activated and utilizes both cell-mediated and humoral responses, mediated by the T lymphocytes and the B lymphocytes respectively (Coico R. et al., 2003). These cells express receptors that recognize specific structures on pathogens called 'antigens'. On binding with the cognate antigen, the cells undergo proliferation, resulting in expansion of the antigen-specific clonal population. In the case of T lymphocytes, this results in either direct killing of intracellular pathogens by the cytotoxic T cells, or provision of support to B-lymphocytes mediated by the helper T cells (Zúñiga-Pflücker, 2004). In contrast, B lymphocytes present the host with humoral immunity by production of the

soluble mediators called 'antibodies'. Antibodies are produced by the terminally differentiated B cells called plasma cells. The important effector functions of the antibodies include direct pathogen masking/neutralization or opsonisation mediated subsequent activation of effector cells. The effector cell mediates phagocytosis or killing of antibody-coated target cells – expressing tumor or pathogen derived antigens on their surface in a process called antibody dependent cellular toxicity (ADCC) (Cooper, 2015; Flajnik & Masanori, 2008).

1.2 BCR signal transduction: A labyrinth of signaling cascades

The generation of mature B cells continues throughout life in the adult bone marrow. This serves a critical purpose. During the lifetime of an individual, the capacity to recognize diverse antigenic structures requires diverse, high-affinity antigen recognizing assemblies rendered by the random re-arrangement of the immunoglobulin genes in a process called somatic recombination (as opposed to genetic recombination). This, in addition to the ability of a selected B cell to clonally proliferate in response to an infection, are the primary hallmarks of adaptive immunity (Yam-Puc et al., 2018).

For combating the myriad pathogens in the environment by the production of antibodies, the B cells are equipped with a sample of the protective antibody produced by each clone as a component of the cell's antigen receptor called the 'B-cell antigen receptor' (BCR). Depending on the developmental stage, the signals initiated by the BCRs play a decisive role in determining the ultimate fate of the B cells: activation, proliferation and differentiation into antibody secreting plasma cells or alternatively, anergy, apoptosis for autoreactive B cells (Niiro & Clark, 2002).

A single BCR is a complex of multiple proteins, the membrane bound immunoglobulin (mIg) responsible for recognition of the cognate antigen and the Igα (CD79α)/Igβ (CD79β) heterodimer as the signal transduction units for the subsequent relay of the signal to the intracellular effector proteins (Reth M., 1992). As mentioned above, somatic recombination in the gene segments encoding the antigen recognizing region of mIg, during B cell development in bone marrow, results in BCRs that can recognise their cognate antigens with

significantly higher affinity (Honjo et al., 2002; Brack et al., 1978).

The naïve B cells are characterized by the expression of either mIgM and/or mIgD class of BCRs on the surface of their cells (Havran et al., 1984). On antigen-encounter, in addition to exhibiting respective antibody secretions, these B cells undergo class-switching to a different Ig isotype in specialised regions in lymphoid organs called the germinal centres (GCs). This produces B cells expressing IgG, IgA or IgE class of BCRs and secreted antibodies (Honjo et al., 2002). Class-switching enables the B cells to mount a response directed towards a specific class of pathogens thus mediating varying effector functions. For instance, soluble IgG is associated with antiviral responses (Hangartner et al., 2006), IgE is known to elicit a response against parasites such as helminths (Fitzsimmons et al., 2014) and IgA present primarily in mucosal secretions inhibits pathogen invasion from the respiratory and gastrointestinal lumen (Woof & Kerr, 2004).

For the general purpose of antigen-specific activation of the BCR, two models have been suggested. The dissociation activation model (DAM) proposes that BCRs in resting cells exist as signaling inactive oligomers and undergo dissociation into an activated state upon antigen ligation (Fiala et al., 2013; Reth M., 2001). Proponents of the more established model, the cross-linking model (CLM) propose that BCRs are dispersed on the surface of B cells as inert monomers and the antigen mediated BCR dimerization initiates signaling from the receptor. Regardless of the questions raised about the factual accuracy of either of the two models, the downstream signal transduction events are fairly similar.

The antigen ligation to the BCR results in phosphorylation of the immunoreceptor tyrosine-based activation motifs (ITAMs) in the cytosolic chains of Igα and Igβ. Src-family kinases, Lyn and the spleen tyrosine kinase (Syk) are responsible for the phosphorylation of the ITAM (Dal Porto et al., 2004). Additionally, this interaction further enhances the activity of Syk (Rowley et al., 1995). Syk then phosphorylates a non-ITAM tyrosine residue in the cytoplasmic tail of Igα. This serves as a docking site for the SH2 domain of the central B cell adaptor, SH2 domain-containing leukocyte protein of 65 kDa (SLP65).

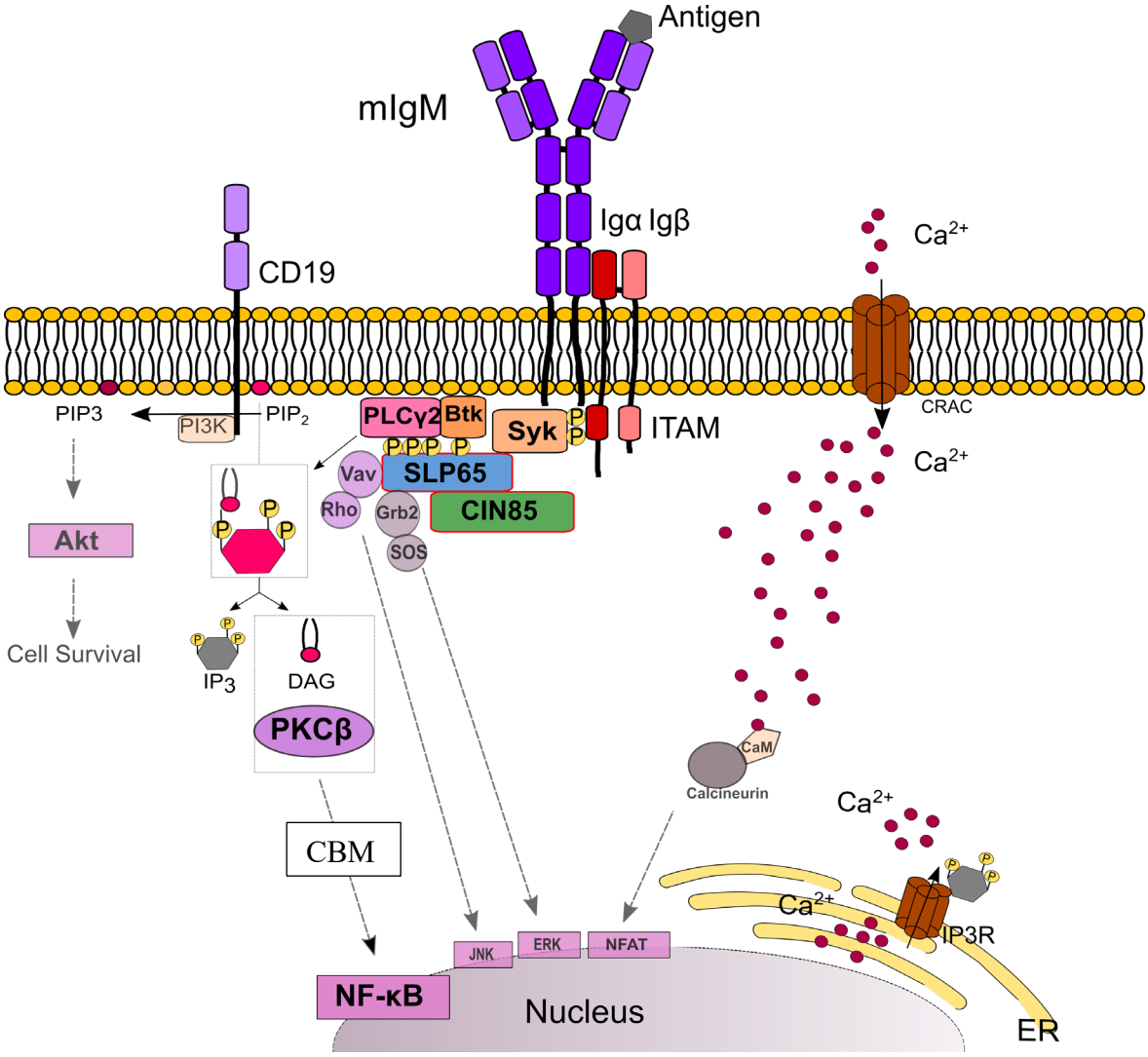

Figure 1: Intracellular signaling cascades initiated on ligation of the B cell antigen receptor (BCR). Antigen mediated BCR activation results in activation of Src-family kinases such as Lyn and Syk, which in turn phosphorylate the ITAMs in Igα/Igβ heterodimer and a non-ITAM tyrosine in Igα. The translocation of Syk to the phosphorylated ITAMs assists the assembly of the trimolecular Ca^{2+} initiation complex. This complex consists of SLP65, Btk and PLCγ2. PLCγ2 hydrolyzes PIP2 to release IP3 and DAG second messengers. The release of IP3 commences the biphasic Ca^{2+} flux with the release of Ca^{2+} from the ER stores in the first phase, followed by the influx of Ca^{2+} across the plasma membrane in the second phase, all culminating in NFAT transcription factor activation. Membrane bound DAG and the cytosolic Ca^{2+} additionally facilitate the plasma membrane recruitment and activation of the enzyme PKCβ. Activated PKCβ phosphorylates and activates further downstream signaling elements, essentially the CBM complex eventually leading to the release and nuclear translocation of the NF-κB transcription factors. The ERK signaling pathway is activated along the Grb2-SOS axis. CD19 provides the necessary co-stimulatory signals. Recruitment of PI3K results in production of PIP3, leading to the activation of the PKB/Akt pathway. The diverse pathways converge in the nucleus with the activated transcription factors initiating specific gene transcription. Indirect effects are represented by the dashed lines and direct effects are represented by the solid lines. CaM – Calmodulin.

SLP65 undergoes Syk mediated phosphorylation at multiple sites (Engels et al., 2001; Wienands et al., 1998; Zhang et al., 1998). Phosphorylated SLP65 recruits Bruton's tyrosine kinase (Btk) and its substrate Phospholipase C-gamma-2 (PLCγ2) to assemble the Ca^{2+} initiation complex (Kurosaki & Tsukada, 2000). Important to note here is that the adaptor protein CIN85 has been reported to be a constitutive interactor of SLP65 resulting in a steady complex formation. This interaction is a prerequisite for the plasma membrane recruitment of SLP65 and its phosphorylation (Oellerich et al., 2011).

PLCγ2 present in the Ca^{2+} initiation complex hydrolyzes the membrane bound phosphatidyl-4,5-bisphosphate (PIP2) into membrane-bound diacylglycerol (DAG) and soluble inositol-1,4,5-trisphosphate (IP3). IP3 binds the IP3 receptor (IP3R) on the ER membrane which initiates the release of Ca^{2+}into the cytosol along the concentration gradient, marking the first phase of the biphasic-Ca^{2+} flux. Reduction of Ca^{2+} in the ER is sensed by an ER membrane protein called the stromal interaction molecule 1 (STIM1).

STIM1 can then induce Ca^{2+} influx across the plasma membrane via opening of Ca^{2+} release activating channels (CRAC) in the plasma membrane culminating the second phase of Ca^{2+} mobilization in B cells (Engelke et al., 2007). The surge in cytosolic Ca^{2+} concentrations presents an essential indicator for B cell activation and is commonly used as a valuable readout system for the flowcytometric experiments. Ca^{2+}-bound Calmodulin then activates the phosphatase Calcineurin, which in turn dephosphorylates Nuclear factor of activated T cells (NFAT) transcription factor, also present in B cells. NFAT then translocates into the nucleus and induces gene transcription (Bhattacharyya et al., 2011; Winslow et al., 2006). Extracellular signal regulated kinase (ERK)-mitogen activated protein kinase (MAPK) pathway is another pathway activated downstream of the BCR. The adaptor protein Grb2 steps into the picture, interacts with the guanine nucleotide exchange factor (GEF) Son of sevenless (Sos), and facilitates the activation of ERK through a series of downstream signaling steps involving activation of the small G-protein Ras (Coughlin et al,, 2005). Additionally, c-Jun N-terminal kinase (JNK) pathway, also a MAPK pathway is activated on BCR-stimulation (Sutherland et al., 1996).

CD19 provides essential co-stimulatory signals. Phosphorylated motifs of CD19 recruit signaling proteins, for instance, Phosphoinositide-3-kinase (PI3K) which catalyzes the production of membrane bound phosphatidylinositol-3,4,5-trisphosphate (PIP3). PIP3 facilitates pleckstrin homology (PH) domain mediated recruitment and activation of protein kinase B (PKB or Akt) (Okkenhaug & Vanhaesebroeck, 2003). Cell survival is promoted by the PKB/Akt activation (Pogue et al., 2000).

DAG and Ca^{2+} second messengers also activate the canonical NF-κB pathway. Membrane bound DAG facilitates the recruitment and activation of protein-kinase C-β (PKCβ) (Nishizuka, 1992). PKCβ subsequently phosphorylates a protein called CARD-containing MAGUK protein 1 (CARMA1) (Sommer et al., 2005). CARMA 1 forms part of a trimolecular complex with adaptor proteins Mucosa-associated lymphoid tissue lymphoma translocation protein 1 (MALT1) and B-cell lymphoma/leukemia 10 (Bcl10). This complex is therefore denoted as the CBM complex (Shinohara et al., 2007). Via a poorly understood mechanism, the CBM complex recruits the transforming growth factor beta-activated kinase (TAK) complex, which further recruits the Inhibitor of κ B kinase (IKK) complex (Wang et al., 2001). The IKKβ subunit phosphorylates IκB which marks it for proteasomal degradation and releases the NF-κB subunit dimers. Initially sequestered in the cytoplasm, bound to IκB, the NF-κB subunits upon release, translocate to the nucleus and activate gene transcription. In contrast, non-canonical NF-κB pathway is activated by stimulation of the members of the tumor necrosis factor receptor superfamily (TNFR) including CD40, Lymphotoxin beta receptor and the B cell activating factor receptor (BAFF) (Coope et al., 2002). The NF-κB family of transcription factors are crucial regulators of B cell proliferation, differentiation and apoptosis. Constitutive NF-κB activation has been found in several types of cancers, suggesting their pro-proliferative/anti-apoptotic effects mediate transformation resulting in lymphoid malignancies (Nagel et al., 2014).

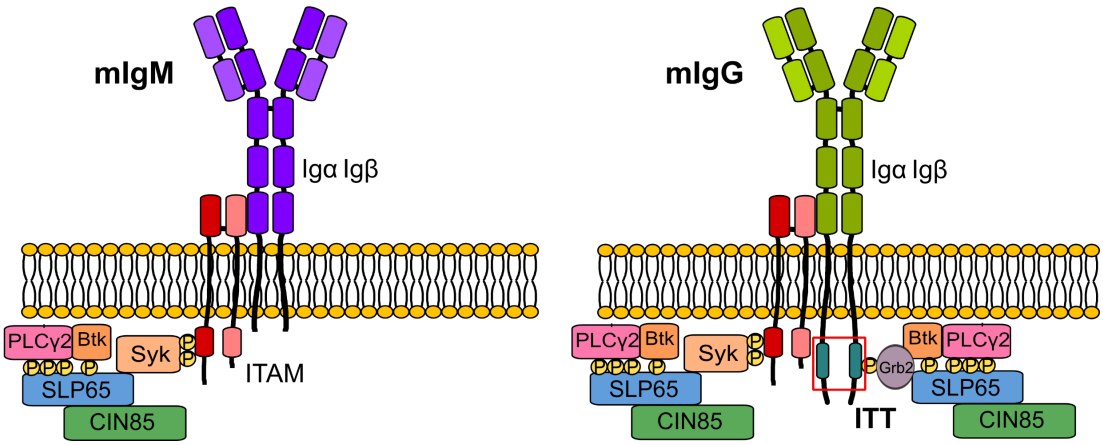

Figure 2: Differences in the membrane bound immunoglobulin structures. The differences in the structures of the mIg aid mIgM-BCRs and IgG-BCRs in deploying varying signaling modules that exhibit differing immune response intensity. The short cytoplasmic tail of the mIgM-BCR makes it dependent on the ITAM motifs of the Igα/Igβ heterodimer for signal transduction and the subsequent Ca^{2+} mobilization as part of the primary immune response. Unlike the mIgM-BCRs, mIgG-BCRs are equipped with an immunoglobulin tail tyrosine or ITT motif (enclosed in red square). Engagement of the mIgG-BCRs results in activation of the canonical ITAM-based signaling pathway as illustrated for the mIgM-BCR. This signal is fortified by the additional Grb2-Btk mediated signaling from the ITT motif. Thus, mounting the secondary immune response.

Affinity maturation and class-switching modifies the sensitivity and threshold for the activation of BCRs and subsequently the intensity and duration of their immune function. Naïve B cells mount a primary response marked by moderate serum IgM titers. Post class-switching and affinity maturation, this initial encounter results in B cells that can confer long-lived humoral memory, called the memory B cells expressing cell surface IgG-BCRs (Figure 2). Re-encounter with the same antigen then initiates the secondary response, marked by early onset and significantly high serum levels of high affinity, class switched, IgG antibodies (Arpin et al., 1995). Therefore, the BCR-isotype is critical in determining the nature of immune response mounted by the B cell.

1.3 Members of the BCR transducer complex: steady complex formation of SLP65 with CIN85 and/or CD2AP

After the processes of affinity maturation and class-switching equip a B cell with a functional, antigen-specific receptor, the intracellular effector proteins come into the picture and provide necessary regulation checkpoints. The ultimate physiological action of the B cells is thus dependent on the three aspects coming together in a carefully regulated manner.

The BCR-proximal and distal effector proteins carefully regulate the downstream signaling events, enabling either signal relay, amplification or inhibition of the signal. These critical steps of signal regulation are marked by protein complexes. Protein complexes constitute members that can either covalently modify the substrates with their enzymatic activities, or, a second class of molecules call the adaptor proteins, which instead provide a platform to facilitate interactions between various molecules (Gavin et al., 2006). Adaptor proteins lack inherent enzymatic activity but enable multimolecular complex formations with their versatile protein-protein and/or protein-lipid interaction domains (Kurosaki T., 2002). The adaptor proteins are thus capable of controlling the spatio-temporal dynamics of the signaling events during B cell activation (Good et al., 2011).

1.3.1 SLP65: the master regulator

As depicted in the canonical BCR-signaling scheme (Figure 1), SLP65 phosphorylation and the assembly of the Ca^{2+} initiation complex is a critical upstream signaling step for the various signaling pathways mentioned. Also called the central B cell linker (BLNK) or B cell adaptor containing SH2 domain (BASH), SLP65 is expressed exclusively in B cells. It was identified by virtue of being heavily phosphorylated upon BCR activation (Bonilla et al., 2000; Fu et al., 1998; Goitsuka et al., 1998; Wienands et al., 1998). SLP65 is essential for both B cell development and activation. However, SLP65-deficiency presents varying phenotypes depending on the species under investigation. Mice lacking SLP65 exhibit partial hinderance to B cell development, with the presence of immature B cells that show reduced Ca^{2+} mobilization compared to the wildtype mice (Hayashi et al., 2000; Jumaa et al., 1999; Minegishi et al., 1999; Xu et al., 2000). In humans, the absence of SLP65 results in severe immunodeficiency manifested as agammaglobulinemia (Minegishi et al., 1999). Finally, in chicken DT40 cells, SLP65 absence renders B-cells incapable of exhibiting BCR-mediated Ca^{2+} mobilization (Ishiai et al., 1999).

As depicted in the figure 3, SLP65 consists of a positively charged N-terminal region proposed to form a leucine zipper capable of anchoring SLP65 molecule to the membrane. The N-terminus thus serves as an important lipid interaction moiety, facilitating the membrane recruitment of SLP65 (Engelke et al., 2014). Adjacent to the basic amino-

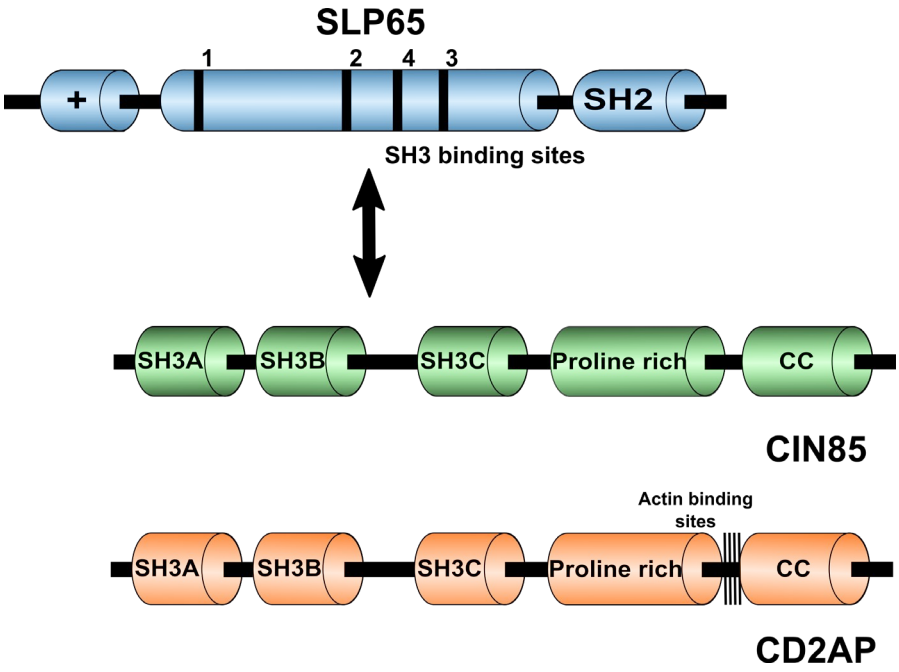

Figure 3: Modular architecture and interactions between SLP65 and/or CD2AP. SLP65 molecule consists of a positively charged N-terminal region, constituting the basic effector domain (labelled as +, encompassing the first 50 amino acids). This is followed by the proline rich region with the proline rich motifs marked as 1, 2, 3 and 4. Proline rich motifs (PRM) 1, 2 and 3 are of the PXXXPR type and PRM 4 is of the PXPXXR type. These proline rich motifs serve as binding sites for CIN85 and CD2AP. The C-terminus of the protein constitutes the SH2 domain. CIN85 and CD2AP exhibit high structural and sequence similarity, with the domain organization of the two proteins being almost identical. In each protein, there are three N-terminal SH3 domains, followed by a proline-rich region and a C-terminal coiled-coil domain (labelled as CC).

terminal domain is the central proline rich region (PRR). This region consists of several tyrosine residues which serve as targets for phosphorylation, in addition to the multiple proline rich motifs (PRM) (Oellerich et al., 2011). The PRM 1, 2, and 3 are of PXXXPR type, providing docking sites for CIN85 and/or CD2AP (Oellerich et al., 2009). In terms of functional significance, the second and third PRM are critical for CIN85 interaction while the PRM 1 is dispensable (Oellerich et al., 2011). Recently, an additional PRM (PRM 4) of PXPXXR type has been identified by Prof. Griesinger's group which has been tested *in vitro* to be capable of participating in the interaction of SLP65 with CIN85. The functional significance of the SLP65-CIN85 interaction mediated by the PRM 4 within B cells is however, yet to be established. Finally, the C-terminus of SLP65 consists of an SH2 domain which is responsible for facilitating the recruitment of SLP65 to the plasma membrane and the BCR, where it binds the non-ITAM pY204 in the tail of Igα (Abudula et al., 2007; Engels et al., 2001; Kabak et al., 2002).

1.3.2 CIN85/CD2AP: the loyal assistants.

CIN85 was first identified as the Cbl-interacting protein of 85 kDa by isolating and cloning the gene from humans (Take et al., 2000) and subsequently as Ruk (regulator of ubiquitous kinase) (Gout et al., 2000), SETA (SH3 domain-containing gene expressed in tumorigenic astrocytes) from rats (Borinstein et al., 2000) and SH3KBP1 (SH3 domain kinase binding protein 1) when isolated from the mice (Narita et al., 2001). CD2AP is another adaptor protein that displays high structural and sequence similarities to CIN85 (Dustin et al., 1998). It was originally identified as a scaffold protein required for organization of the immunological synapse between a T lymphocyte and an antigen-presenting cell (Dustin et al., 1998). Due to their sequence and structural similarities, CIN85 and CD2AP form part of a family of adaptor proteins, officially designated as the CIN85/CMS family, CMS being the human homologue of the mouse CD2AP gene (Dikic I., 2002)

The overall domain organization of CIN85 and CD2AP is identical. Homology searches based on the deduced amino acid sequence gave information about the domain organization of CIN85 (Take et al., 2000). At the amino-terminus, CIN85 consists of three SH3 domains known to mediate protein–protein interactions by binding to proline-rich motifs. Adjacent to the third SH3 domain is a proline-rich region, providing potential recognition sites for other SH3-domain containing proteins. The C-terminal domain assumes a coiled-coil structure (Figure 3). It has been established that this domain facilitates homo-oligomerization of CIN85 or hetero-oligomerization with CD2AP, due to its ability to form stable coiled-coil trimers (Kühn J., 2015).

CIN85 and CD2AP adaptor proteins exhibit multi-functional properties. The SH3 domains can bind to atypical proline rich motifs of the PXXXPR type (Kowanetz et al., 2003; Kurakin et al., 2003). CIN85 also presents multiple functional protein isoforms (created as splice variants or from internal promoter usage) capable of regulating numerous cellular processes in cell-type specific or developmental stage specific manner (Dikic I., 2002; Havrylov et al., 2009). For a long time after discovery, majority of CIN85 studies focussed on its function in the epidermal growth factor receptor (EGFR) signaling (Soubeyran et al., 2002). Upon EGFR activation, CIN85 mediates clustering of c-Cbl and endophilin and thus drives

receptor internalization. Similar receptor downregulation mechanisms have been reported for other receptor tyrosine kinases (Petrelli et al., 2002; Soubeyran et al., 2002; Szymkiewicz et al., 2002). Similarly, CD2AP is a rather well-established regulator of kidney glomerular functions in mice and humans. CD2AP-deficient mice, exhibit a strong nephrotic defect (Shih et al., 1999).

Few studies report the function of CIN85 and CD2AP in immune cells. It has been shown that CIN85 and CD2AP can interact with a transmembrane protein called CD2 in T cells (Dustin et al., 1998; Tibaldi & Reinherz, 2003). CIN85 links CD2 to cytoskeleton owing to its interaction with the actin capping protein CapZ. This implicates CIN85 in promoting cytoskeletal reorganization events upon TCR-activation (Hutchings et al., 2003). Additionally, CD2AP-deficient T cells showed prolonged phosphorylation of the Zap70 kinase and Ca^{2+} mobilization, associated with a defect in TCR degradation (Lee et al., 2003). In mast cells, CIN85 has been shown to downregulate signaling via the FcεRI due to receptor internalization, thus inhibiting degranulation of mast cells (Molfetta et al., 2005).

Recently, it was shown that mice with T cell-specific deletion of CIN85 or CD2AP, showed hyperresponsiveness in terms of proliferation and IL-2 production, thus implicating CIN85 in inhibitory interactions (Kong et al., 2019). Along similar lines, another report suggests negative regulatory functions of CIN85 in B cells. CIN85 has been reported to interact with SHIP-1 that downregulates PIP3 levels in B cells (Damen et al., 2001) and thereby inhibits BCR signaling. Furthermore, CIN85 has also been described to inhibit Syk and PLCγ2 phosphorylation in addition to the reduction in BCR-induced Ca^{2+} mobilization (H. Niiro et al., 2012).

In stark contrast to these reports, the positive regulatory significance of the constitutive interaction between SLP65 with CIN85 and/or CD2AP has been established by our group. SLP65-deficient DT40 cells and primary B cells when expressing a SLP65 variant with the CIN85 and CD2AP docking sites disrupted showed a defect in BCR-stimulated Ca^{2+} mobilization (Oellerich et al., 2011). Additionally, in the absence of the steady interaction in these cells, SLP65 showed reduced phosphorylation.

Furthermore, these cells showed a defect in the NF-κB signaling pathway upon BCR-activation (Oellerich et al., 2011). Similar reports appeared from studies in the primary mouse B cells deficient in CIN85, where the NF-κB pathway activation upon BCR stimulation is reduced. It was shown that CIN85 links BCR to IKKβ activation. Interestingly, in this report, the BAFF-mediated non-canonical NF-κB pathway was shown to remain unaffected (Oellerich et al., 2011).

Patients exhibiting antibody deficiency were identified by our group and analyzed in collaboration with the Human genetics department, Göttingen. These male siblings were diagnosed with antibody deficiency marked by diminished serum antibody titers to various extents. This resulted in common consequences of recurring severe bacterial infections. The older brother with all immunoglobulin isotypes reduced, died of a septic shock. The younger brother shows reduced IgM and IgG4 levels and served as the index patient. The whole exome sequencing analysis (WES) revealed that the patients harboured an inactivating germline deletion within the *CIN85* gene on the X chromosome. However, in contrast to the reduced serum antibody levels, the peripheral B cell and T cell compartments of the younger sibling appeared undisturbed. Despite the previously mentioned involvement of CIN85/CD2AP in T-cell functions, analysis of the of the patient's T cell responses showed wild type levels of activation upon TCR/CD28 stimulation. This is in contrast to the patients´ B cells, which showed reduced Ca^{2+} mobilization and a defect in NF-κB activation upon BCR stimulation, indicating that the deletion mutation resulted in B-cell specific effects. Additionally, no such defects were seen upon activation of the B cells by Phorbol myristate acetate (PMA), CD40 ligand or CpG oligodeoxynucleotides, which is indicative of a role of CIN85 specifically downstream of the BCR (Keller et al., 2018). The study of these patient-conditions, calls for a system that could provide molecular details about how these proteins work inside the cells, which was one the aims of my thesis.

To encapsulate, several studies suggest an involvement of CIN85/CD2AP adaptor proteins in a plethora of intracellular signaling pathways. These include imparting both positive and negative regulatory functions. More specifically, with respect to B cells, equipped with the adequate understanding of the significance of the preformed transducer complex, it became necessary to explore the molecular mechanism propelling these signaling events.

1.4 Scope of the thesis

Based on the reported significance of SLP65-CIN85 interaction in B cell development and function in mice and humans, we were interested in exploring the facets of this complex-assembly and its functions further.

To accomplish our main objectives, I pursued the following specific aims:

- Generation of CIN85-deficient human and mouse B cell lines, followed by subsequent deletion of CD2AP from the two respective cell lines, making use of the CRISPR/Cas genome editing technology. The cellular system thus created, was used to conduct genetic and biochemical functional assays to elucidate the role of these adaptor molecules in both BCR-proximal and downstream signaling events.

- Making use of the aforementioned cell lines to employ mass spectrometric analyses for the identification of thus far unreported interaction partners of SLP65, facilitated by the absence of the significant constitutive binding partners, CIN85 and CD2AP.

- Combining the techniques of structural biology with mutational analyses, and imaging approaches, to garner an understanding of the nature and biophysical properties of the phase separated SLP65-CIN85 droplets/micro-clusters.

Chapter 2: Results

2.1 CIN85 and CD2AP regulate BCR-proximal signaling events

As mentioned in the previous section, considering the significance of SLP65/CIN85 interaction observed in the patients and the mouse models, it became necessary to create model systems from established B cell lines, the use of which could provide mechanistic details for the function of CIN85/CD2AP adaptor proteins within B cells. In this regard, I used CRISPR/Cas9-gene editing technique as described in Cong & Zhang, 2014 to first knock-out CIN85 from the human DG75 B cell line. DG75 human burkitt's lymphoma cell line originated from a boy and the CIN85 gene locus on account of being positioned on the X-chromosome proved helpful such that disruption of only one allele resulted in successful inactivation of the gene. For the purpose of designing CRISPR-guide sequences, exon 3 in the *CIN85* gene was targeted. This exon is present in almost all CIN85 isoforms (Figure 4, A) and is early in the order amongst exons in the genomic sequence such that an INDEL mutation mediated by Cas9-cleavage resulted in a premature stop codon early enough for the translated protein product to be rendered functionally inactive.

After electroporation with the CRISPR-constructs and subsequent cell sorting for GFP (simultaneously encoded by the CRISPR-construct) positive cells, the genomic DNA was isolated and a segment of exon 3 encompassing the targeted sequence was amplified via PCR. Subsequent cleavage with the restriction endonuclease HpyCHV, the binding site of which overlapped with the Cas9 cutting site, indicated the successful activity of CRISPR/Cas9 system in the transfected cells. For explanation: Cas9 cleavage-mediated insertion/deletion mutation modified the binding site of the HpyCHV restriction endonuclease, thus preventing DNA restriction digestion in cells successfully targeted by the CRISPR/Cas system. The DNA bands thus appearing at a different positions, post agarose gel electrophoresis, when compared to the unmodified DNA of the homogenous population of parental cells (Figure 4, B). Post subsequent sub-cloning, the clones were screened for CIN85-absence via western blotting. The CIN85-deficient clones are depicted in figure 5, A. It was additionally observed that knocking-out CIN85 does not disturb the expression levels of CD2AP and SLP65 proteins (Figure 5, A).

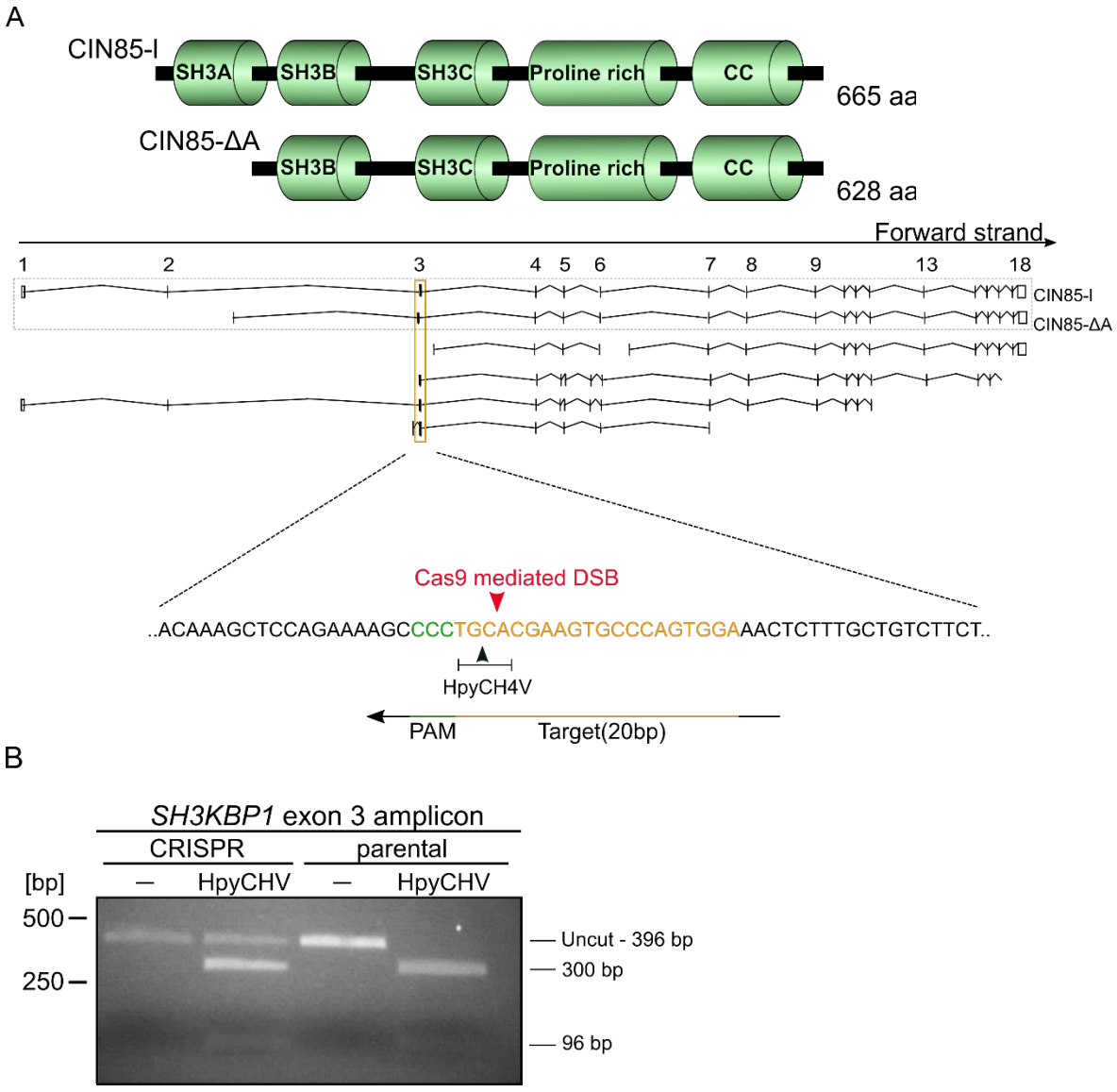

Figure 4: Exon 3 in the *CIN85* gene was targeted for CRISPR/Cas9-mediated gene editing.
(A) Upper panel: Domain architecture of the predominant CNI85 isoforms in B cells. CIN85-l is the long isoform of CIN85 consisting of 3-SH3 domains on the N terminus followed by a proline rich region and a coiled-coil domain on the C-terminus. CIN85-ΔA lacks the first SH3 domain (labelled as SH3A). **Lower panel**: schematic representation of the *CIN85* genomic locus indicating the targeted exon and the nucleotide sequence against which the guide sequence was designed **(B)** To test cleaving activity mediated by the CRISPR/Cas constructs transfected into the cells, amplification of the Exon 3 was carried out via PCR. The PCR amplicon was subjected to restriction digestion with the HpyCH4V endonuclease, the binding site of which overlapped with the Cas9 cutting site. Once modified due to Cas9 induced insertion/deletion mutation, the target site undergoes modification, affecting restriction endonuclease's binding capacity, thus resulting in only a fraction of DNA in the sample undergoing restriction digestion.

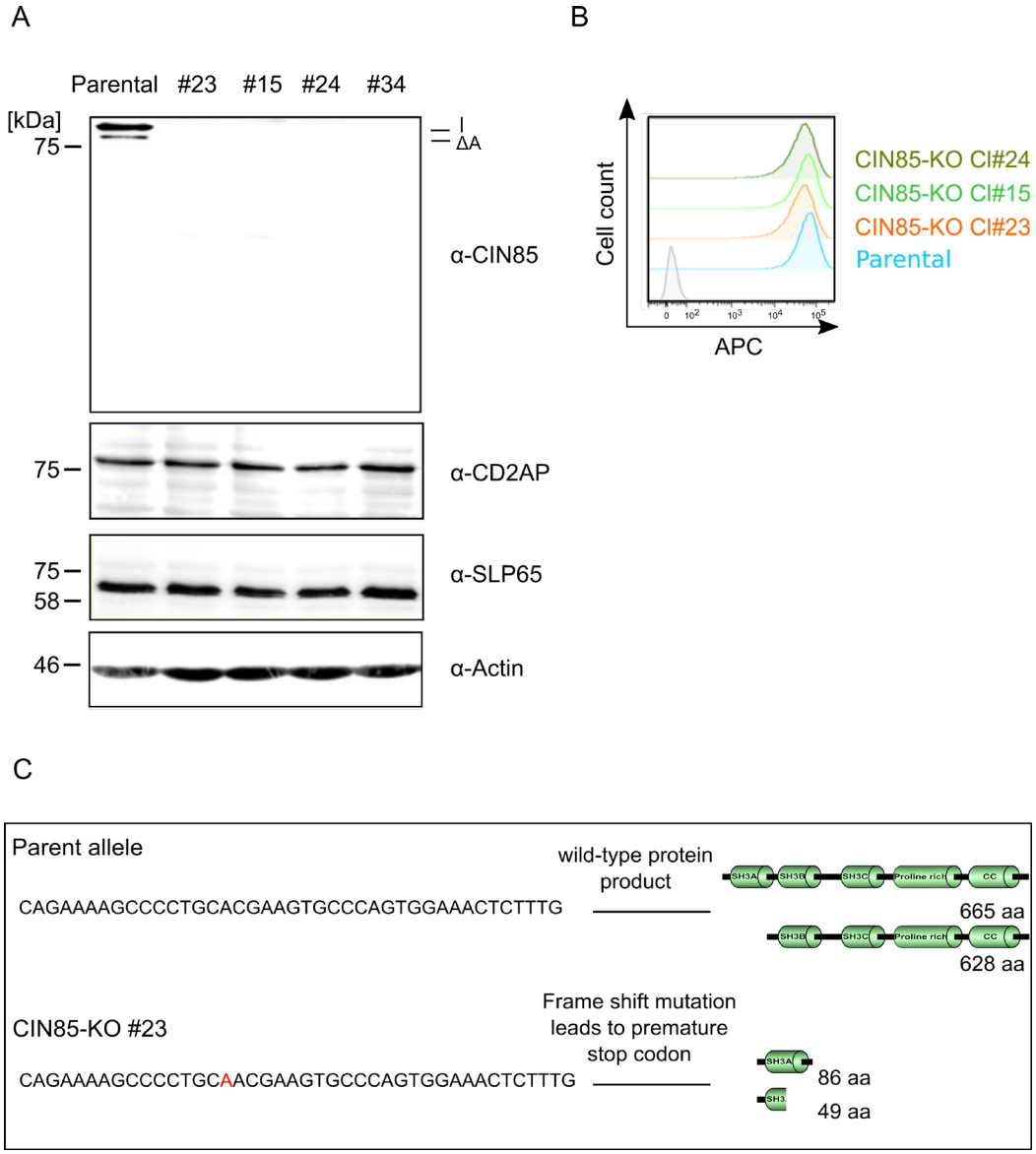

Figure 5: Identification of CIN85-KO clones of the human DG75 cell line. (A) Cleared cellular lysates of DG75 parental and putative CIN85-KO clones were tested for CIN85 expression via western blot analyses using antibodies against CIN85. Similarly, CD2AP and SLP65 expression levels were compared using antibodies against the respective proteins. Actin was used as the loading control. **(B)** The histogram represents the flowcytometric analyses of surface BCR levels, detected using anti-hIgM-CY5 antibody **(C)** Sequencing results indicating the target site modification compared to the sequence of the wild type *CIN85* allele have been depicted, along with the changes that the sequence modification confers to the biological product

CIN85 has been known to be indirectly associated with RTKs via its interaction with Cbl such that it promotes their internalization upon receptor ligation. I proceeded to check whether deletion of CIN85 could also impact the cell surface expression levels of BCRs in the resting cells. It was observed that the expression of mIgM-BCR in the representative CIN85-deficient clones was similar to that of the parental cells (Figure 5, B), indicating that

wild-type levels of cell surface IgM is expressed in CIN85-KO DG75 cells. This additionally ruled out the possibility of clonal variations or CRISPR/Cas off target affects that could impact the cell surface BCR levels. The deletion of CIN85 in the knock-out clones was additionally validated at the level of nucleotide sequence. The sequencing results of one such representative CIN85-KO clone, clone #23 revealed insertion of a nucleotide at the Cas9 cleavage site which in turn resulted in a shift in the translation reading frame, thus rendering a premature stop codon (Figure 5, C). This clone represents the DG75 CIN85-KO cells that were used during the course of the study.

To monitor the effect of CIN85 expression on BCR-mediated Ca^{2+} mobilization, I transduced the CIN85-KO cells with constructs as depicted in figure 6, A. I tested three CIN85-KO clones for their capacity to support Ca^{2+} flux while expressing either wild-type or full length CIN85 protein (wt), a variant of CIN85 lacking its C-terminal coiled-coil domain (ΔCC), or while expressing EGFP (mock) protein.

Interestingly, it was observed that at high stimulating $F(ab')_2$ concentrations, the impact of CIN85-presence or absence on BCR-mediated Ca^{2+} mobilization was negligible. The CIN85-KO cells promoted Ca^{2+} flux to the same extent as the cells expressing wild type CIN85, ΔCC variant or the mock. However, at low stimulating $F(ab')_2$ concentrations, it was observed that the CIN85 expression governs the onset as well as the amplitude of Ca^{2+} mobilization. This was observed in all three CIN85-deficient clones that were tested. CIN85 thus significantly increased the capacity of cells to get activated, supporting Ca^{2+} influx levels that were higher than those in cells lacking CIN85 or expressing the ΔCC variant. CIN85 expression reduces the stimulation threshold for BCR-and thus positively regulates Ca^{2+} mobilization in human DG75 B cells.

The signaling defect seen for the ΔCC variant of CIN85 is plausible, because the C-terminal coiled-coil domain of CIN85 is the critical effector unit of CIN85. It mediates homo (with other CIN85 molecules) and hetero-oligomerization (with proteins like CD2AP), to form clusters of CIN85, thereby increasing the local concentration of its interaction partner SLP65 and an inability to do so, hampers the SLP65-mediated Ca^{2+} mobilization in the cells.

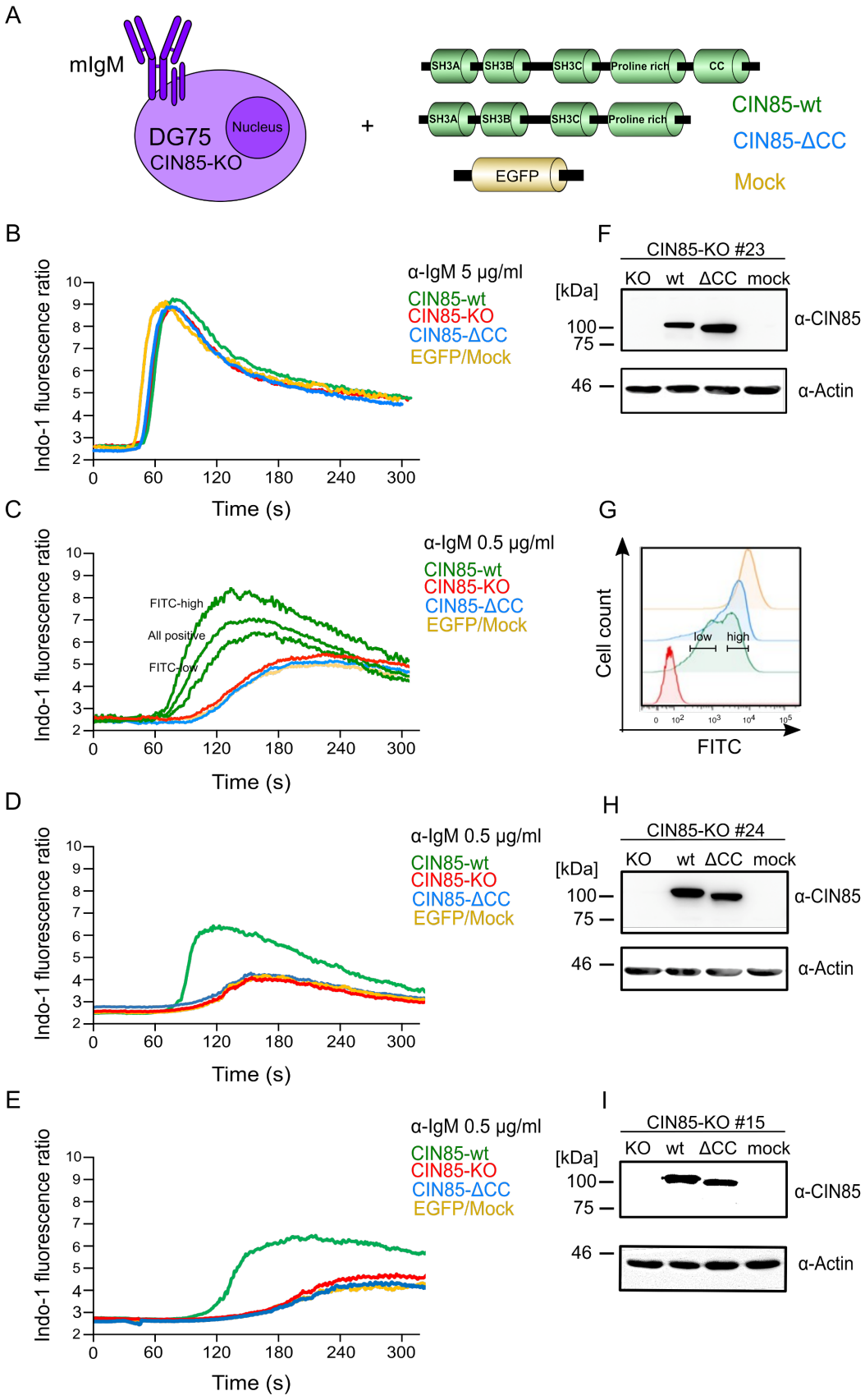

Figure 6: CIN85 expression in cells enables them to respond to low stimulating F(ab´)$_2$ concentrations.
(A) CIN85-KO DG75 clones: # 23, 34 and 15 were transduced with citrine-tagged CIN85-wt (green line),

variant of CIN85 lacking the C-terminal coiled-coil domain (blue), or the EGFP/mock protein (yellow) as depicted. The Ca^{2+} influx in the transduced citrine positive cells of clone #23 was monitored upon stimulation with **(B)** 5 µg/ml α-human IgM $F(ab')_2$ or **(C)** 0.5 µg/ml α-human IgM $F(ab')_2$ via flow cytometry. **(D-E)** The Ca^{2+} influx in transduced CIN85-KO clones #24 and #15 was monitored upon stimulation with 0.5 µg/ml α-human IgM $F(ab')_2$ by flow cytometry. **(F)** The western blot depicts the expression levels of CIN85 or its ΔCC-variant in the transduced cells of CIN85-KO clone #23. **(G)** The histograms confirm similar expression levels of the citrine-tagged proteins along with the EGFP-mock protein in the respective cell populations. **(H-I)** The western blots depict the expression levels of CIN85 or its variant in the retrovirally transduced populations of clone #34 and clone #15.

Identical strategy of CRISPR/Cas-mediated gene disruption was applied to the Exon 3 of mouse CIN85 encoding gene in the IIA1.6 cell line. IIA1.6 cells are a descendant of the more commonly used A20 murine cell line. It is important to note that unlike DG75 cells that express cell surface IgM-BCRs, IIA1.6 cells express the class-switched IgG-BCRs (refer section 1.1) representing memory B cells – a different B cell developmental stage. As mentioned in the earlier, the structural differences between the two BCR molecules equips them to mount immune responses of varying intensities, with IgM transducing the signal via the ITAM motif. The IgG in addition to mounting the canonical ITAM mediated response also harbours an ITT motif that plays additional role in BCR-mediated signaling within the B cells. It is of significance therefore, to be able to compare the signaling events in these mIgG-expressing cells with those of DG75 cells expressing cell surface IgM.

The guide sequence was selected using the previously-mentioned CRISPR online tool. The Cas9-cleaving activity in the transfected cells was tested by treating the Exon 3 PCR amplicon with the restriction enzyme HpyCHV, the binding site of which overlapped with the cleavage site of the Cas9 enzyme, resulting in its inability to bind to the modified binding site, thus ensuring successful Cas9-mediated cleavage. After western blot screening to identify CIN85-KO clones, the knock-outs were validated at the nucleotide-sequence level. Unlike DG75 cell line, there are two X chromosomes in IIA1.6 cells harbouring two CIN85 coding alleles. In the representative sequencing results from CIN85-KO clone #22, there were two mutations identified, corresponding to the two alleles: one was the 25-nucleotide deletion surrounding the Cas9 cutting site, and the other was the insertion of a nucleotide at the said position. Both resulted in a shift of the translation reading frame which in turn resulted in a premature stop codon, giving rise to a functionally inactive, truncated protein product.

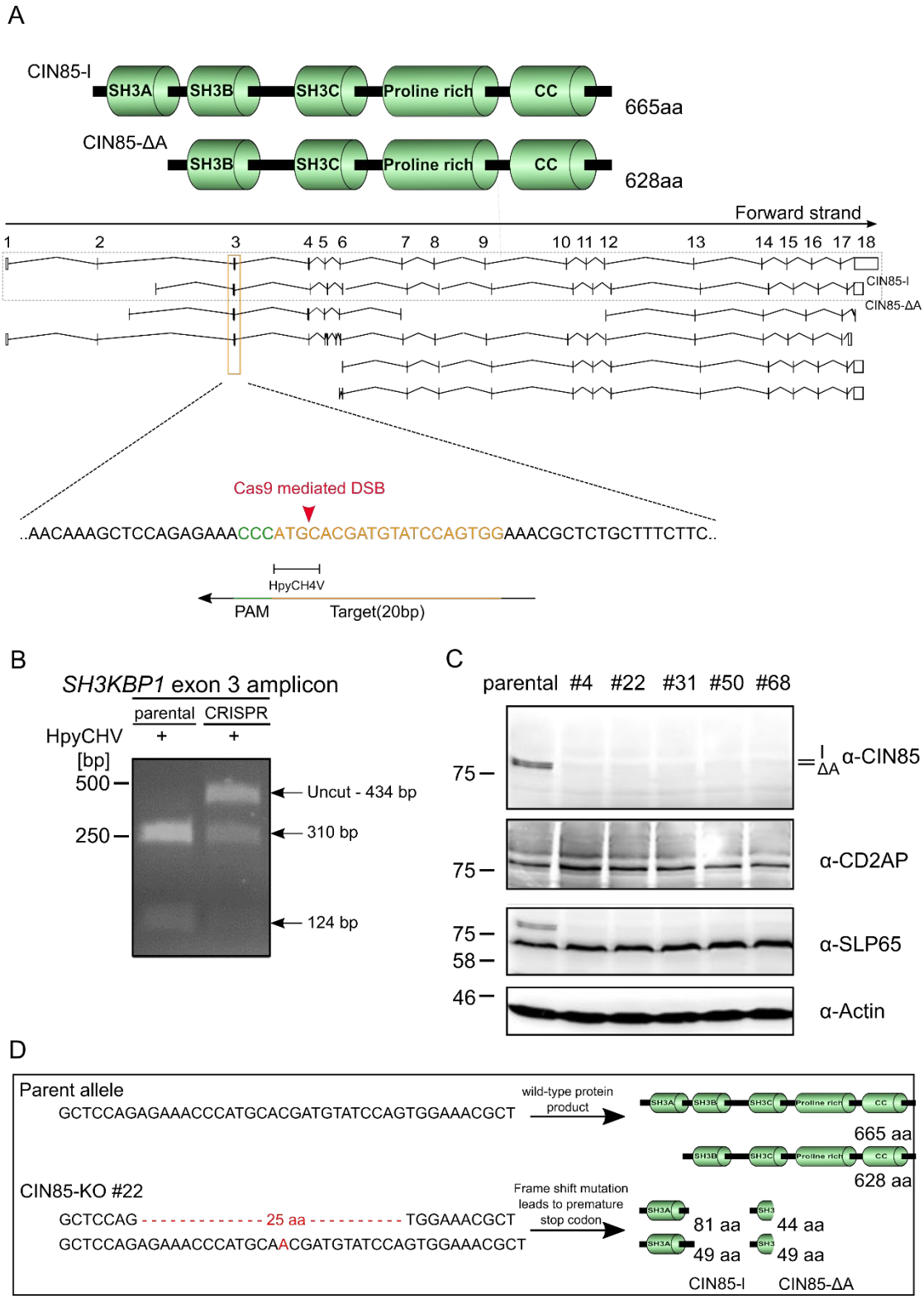

Figure 7: Creation and identification of CIN85-KO IIA1.6 clones using CRISPR/Cas9-mediated gene editing technology and western blot analyses. (A) Upper panel: Domain architecture of CIN85 isoforms found in IIA1.6 cells**. Lower panel**: schematic representation of the *CIN85* genomic locus in mice indicating the targeted exon and the nucleotide sequence against which the guide sequence was designed.

(B) To test cleaving efficiency mediated by the CRISPR/Cas constructs transfected into the cells, the PCR amplicon was cleaved with the restriction enzyme HpyCH4V, the binding site of which overlaps with the Cas9 cutting site. Once modified due to Cas9 induced insertion/deletion mutation, the restriction endonuclease is unable to bind to its target site. **(C)** Cleared cellular lysates of IIA1.6 parental and putative CIN85-deficient clones were tested for CIN85 expression via western blot analyses using antibodies against CIN85. Similarly, CD2AP and SLP65 expression levels were compared using antibodies against the respective proteins. Actin was used as the loading control. **(D)** Sequencing results indicating the target site modification compared to the sequence of the wild type *CIN85* allele have been depicted along with the changes they confer to the protein product.

On monitoring the Ca^{2+} mobilization capacity of the cells transduced with either CIN85-wt, CIN85-ΔCC or the EGFP-mock, similar results, as for the DG75 cells were observed (Figure 8). At high stimulating concentrations, no difference in Ca^{2+} flux onset or amplitude were observed amongst the different cell populations. However, at 10-fold lower stimulating F(ab´)2 concentrations, the wild type or full length-CIN85 expressing cells were capable of mounting a stronger Ca^{2+} response. Additionally, similar to the respective constructs expressed in DG75 cells, the CIN85-ΔCC variant expressing IIA1.6 cells mediated signaling to the same level as the CIN85-KO cells or KO cells expressing the mock protein, indicating that similar to the observations made in the human DG75 cells, this variant is incapable of promoting Ca^{2+} signaling in the mouse IIA1.6 cells.

The observations made have critical physiological implications. They depict that B cells when expressing full length CIN85 protein are better capable of sensing even the small doses of circulating antigen concentrations, get activated and have the capacity to mount a robust immune response. This would aid early clearance of the pathogen from the system before it renders any significant harm to the host. Furthermore, the combined observations made in the human and mouse CIN85-deficient cell lines corroborate the Ca^{2+} phenotype observed in the case of the immunodeficient patients (explained in section 1.3.2) wherein a similar Ca^{2+} defect was observed for the patient's B cells when compared to the healthy controls.

It has been reported that CD2AP bears high structural and functional similarity to CIN85 (Section 1.3.2). It has a domain architecture almost identical to that of CIN85 (with additional actin binding motifs), and similar to its counterpart, CD2AP is a ubiquitously expressed protein that has been implicated in several cell surface receptor-associated functions. We were therefore curious to test if within B cells, CD2AP provides functional redundancies in terms of the intracellular signaling.

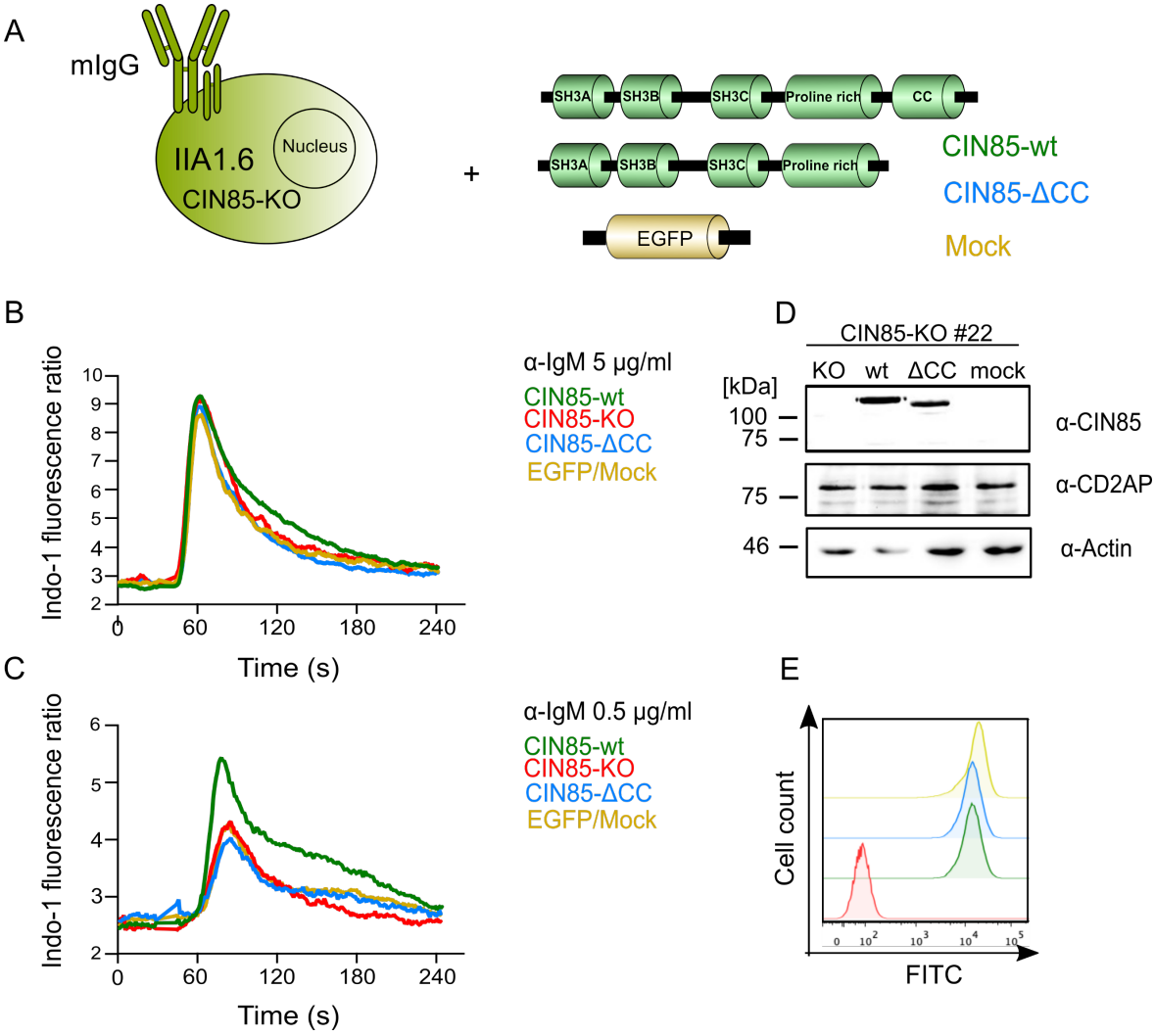

Figure 8: CIN85 mediated positive regulatory effects on Ca^{2+} mobilization in IIA1.6 mouse B cells are similar to DG75 cell. **(A)** CIN85-KO IIA1.6 clone #22 was transduced with citrine-tagged CIN85-wt (green line), variant of CIN85 lacking the coiled-coil domain (blue), or the EGFP/mock protein (yellow) as depicted. The Ca^{2+} influx in transduced citrine-positive cells was monitored upon stimulation with **(B)** 5 µg/ml α-mouse IgG $F(ab')_2$ or **(C)** 0.5 µg/ml α-mouse IgG $F(ab')_2$ via flow cytometry. **(D)** The western blot depicts the expression levels of CIN85 or its variant in the transduced populations of clone #22, along with the expression levels of CD2AP, detected with antibodies directed against the respective proteins. **(E)** The histogram confirms similar expression levels of the citrine-tagged proteins and the EGFP-mock protein in the respective cell populations as specified.

To this extent, CRISPR/Cas9-mediated gene editing was performed to target Exon 2 of the gene encoding CD2AP within the CIN85-KO DG75 cells and the clones with the combined absence of CIN85 and CD2AP were identified. The targeting and the protein-deletion confirmation steps have been explicitly explained in the figure 9.

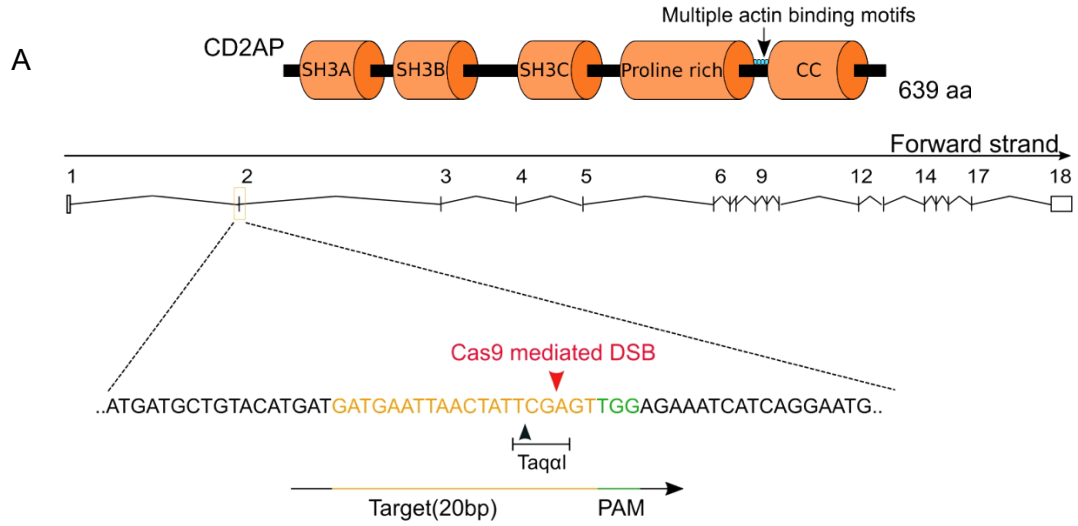
A
CD2AP
SH3A
SH3B
SH3C
Proline rich
CC
Multiple actin binding motifs
639 aa
Forward strand
1
2
3
4
5
6
9
12
14
17
18
Cas9 mediated DSB
..ATGATGCTGTACATGATGATGAATTAACTATTCGAGTTGGAGAAATCATCAGGAATG..
TaqαI
Target(20bp)
PAM

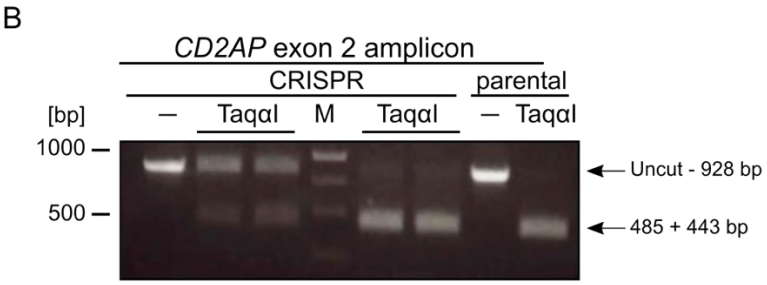
B
CD2AP exon 2 amplicon
CRISPR
parental
[bp]
–
TaqαI
M
TaqαI
–
TaqαI
1000
500
Uncut - 928 bp
485 + 443 bp

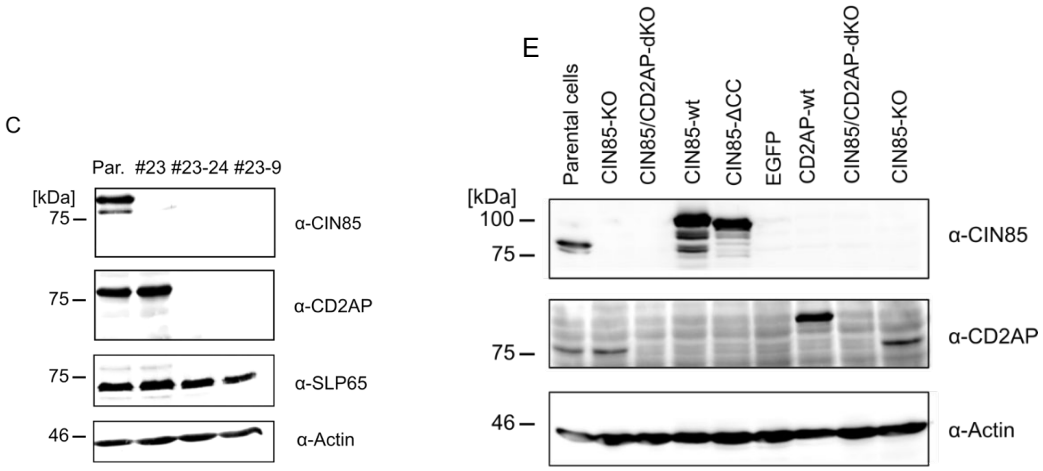
C
Par. #23 #23-24 #23-9
[kDa]
75
α-CIN85
75
α-CD2AP
75
α-SLP65
46
α-Actin
E
Parental cells
CIN85-KO
CIN85/CD2AP-dKO
CIN85-wt
CIN85-ΔCC
EGFP
CD2AP-wt
CIN85/CD2AP-dKO
CIN85-KO
[kDa]
100
75
α-CIN85
75
α-CD2AP
46
α-Actin

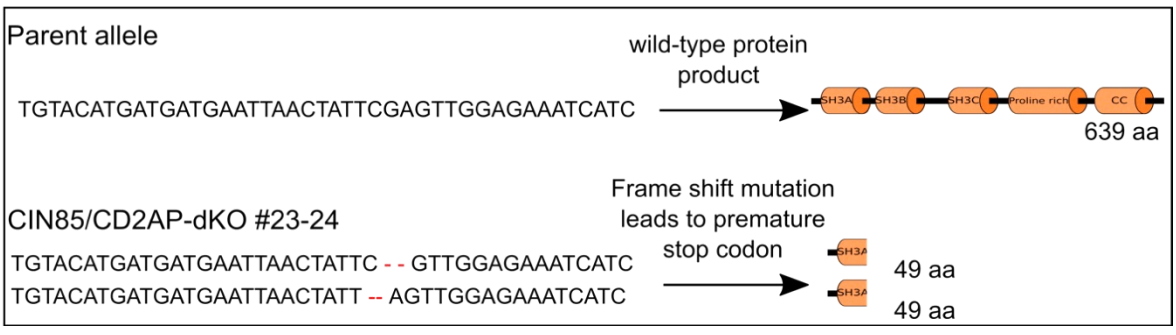
D
Parent allele
TGTACATGATGATGAATTAACTATTCGAGTTGGAGAAATCATC
wild-type protein product
SH3A
SH3B
SH3C
Proline rich
CC
639 aa
CIN85/CD2AP-dKO #23-24
TGTACATGATGATGAATTAACTATTC - - GTTGGAGAAATCATC
TGTACATGATGATGAATTAACTATT -- AGTTGGAGAAATCATC
Frame shift mutation leads to premature stop codon
SH3A
SH3A
49 aa
49 aa

Figure 9: Exon 2 of *CD2AP* in human CIN85-KO DG75 B cells was targeted for CRISPR/Cas9-mediated gene disruption and the CIN85/CD2AP-dKO clones were identified. (A) Upper panel: Domain architecture of the CD2AP protein in human DG75 B cells. Similar to CIN85, it consists of 3-SH3 domains on the N terminus followed by a proline rich region and a coiled-coil domain on the C-terminus. However, unlike CIN85, CD2AP has 4 actin binding motifs (blue circles). **Lower panel**: schematic representation of the *CD2AP* genomic locus indicating the targeted exon and the nucleotide sequence against which the guide sequence was designed **(B)** To test cleaving efficiency mediated by the Cas9 enzyme encoded by the CRISPR constructs transfected into the cells, amplification of the Exon 2 was carried out via PCR. The PCR amplicon was subjected to restriction digestion with the enzyme Taqα1, the binding site of which overlapped with the Cas9 cutting site, thus enabling effective testing for the success of the transfected CRISPR/Cas9 system **(C)** Cleared cellular lysates of DG75 parental and putative CIN85/CD2AP-dKO clones were tested for CIN85 and CD2AP expression via western blot analyses using antibodies against CIN85 and CD2AP respectively. Similarly, SLP65 expression levels were compared using antibodies against the respective proteins. Actin was used as the loading control. **(D)** Sequencing results indicating the target site modification compared to the sequence of the wild type *CIN85* allele have been depicted along with the changes they confer to the protein product. **(E)** The western blot depicts the CIN85 and CD2AP expression levels in parental and CIN85-KO DG75 clone as well as the CIN85/CD2AP-dKO cells that were retrovirally transduced with constructs expressing either CIN85-wt, the ΔCC variant of CIN85, CD2AP or the EGFP-mock. Antibodies directed against CIN85 and CD2AP were used and the detection of actin served as the loading control.

On comparing the Ca^{2+} mobilization capacity of CIN85-deficient and CIN85/CD2AP-double deficient cells, it was observed that knocking-out CD2AP from previously CIN85-depleted cells, does not reduce the Ca^{2+} flux levels further to a significant extent. A very mild effect on Ca^{2+} mobilization capacity of the cells lacking both the proteins was observed. On the contrary, when these cells were transduced to over-express the wild type CIN85 and CD2AP proteins, it was observed that BCR-mediated Ca^{2+} mobilization capacity of the cells significantly increases compared to the cells that lacked both CIN85 and CD2AP (Figure 10, A-D).

The patients and the mouse models discussed previously additionally exhibited a B cell-specific defect in the BCR-mediated NF-κB pathway activation. I therefore proceeded to monitor BCR-distal signaling events in these cells by monitoring the phosphorylation of IκBα which is part of the activation of NF-κB pathway and ERK (Figure 10, E). I observed that while the phosphorylation of ERK appeared to be dependent on the stimulating antigen concentrations, only the stimulation independent, basal levels of phosphorylated IκBα were detected in the DG75 cells. These levels were the same in both CIN85 expressing and the CIN85-KO cells.

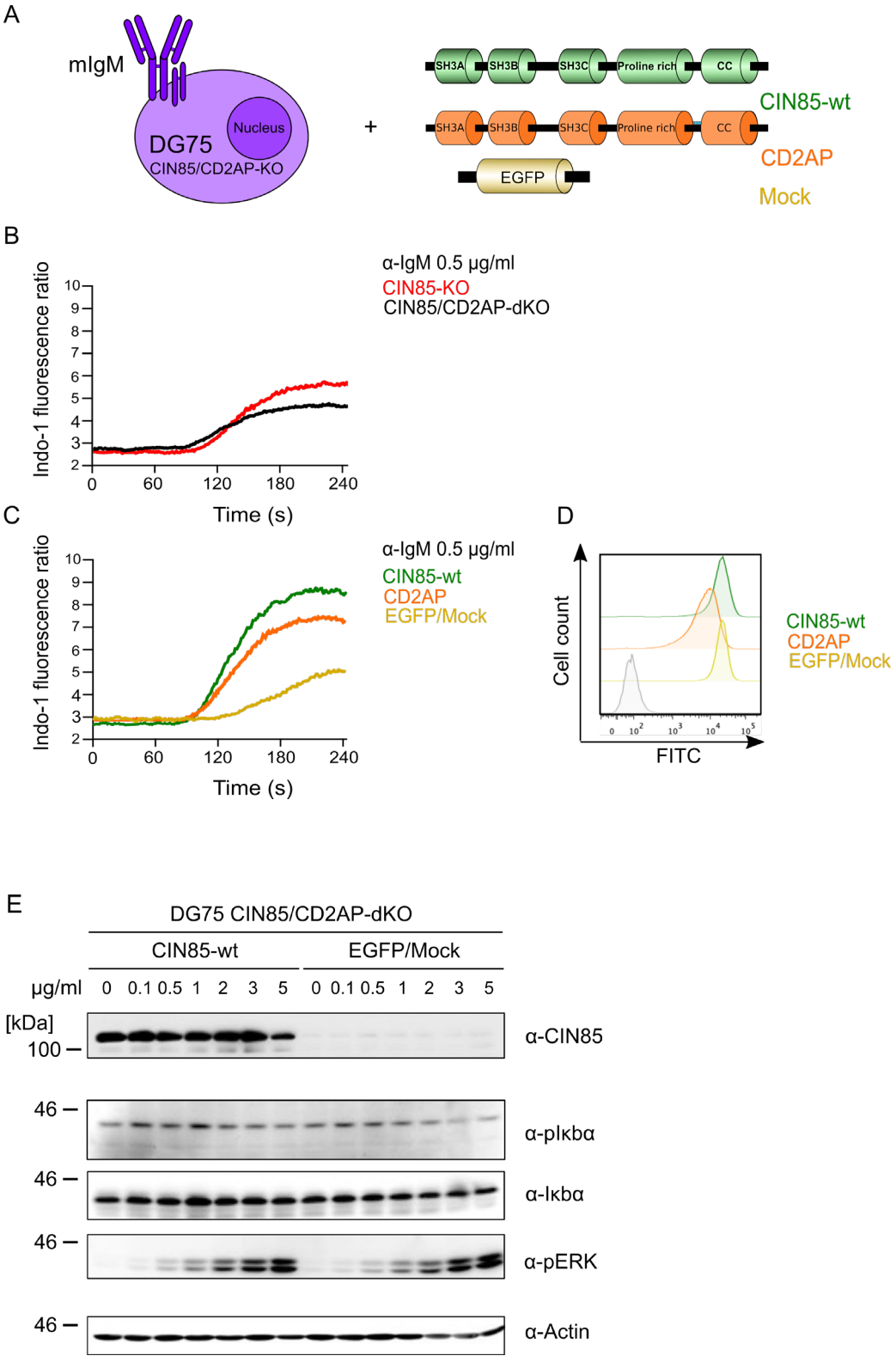

Figure 10: Over expression of CD2AP in CIN85/CD2AP-double deficient DG75 B cells improves their Ca^{2+} signaling capacity. (A) CIN85/CD2AP-double deficient DG75 cells were transduced with citrine-tagged CIN85-wt (green line), CD2AP (orange), or the EGFP/mock protein (yellow) as depicted. **(B)** The Ca^{2+} influx in the CIN85-KO and CIN85-dKO was monitored upon stimulation with 0.5 µg/ml α-human IgM $F(ab')_2$

via flow cytometry. **(C)** The Ca^{2+} influx in the CIN85-dKO expressing either wild type CIN85, wild type CD2AP or EGFP was monitored upon stimulation with 0.5 µg/ml α-human IgM $F(ab')_2$ via flow cytometry. **(D)** The histogram confirms similar expression levels of the citrine-tagged proteins and the EGFP-mock protein in the respective cell populations as specified. **(E)** Cell lysates were prepared after stimulation of CIN85/CD2AP-dKO cells either expressing wild type CIN85 or EGFP with indicated concentrations of α-human IgM $F(ab')_2$. IκBα phosphorylation was analysed by SDS-PAGE and immunoblotting with antibodies against phospho-IκBα (p-IκBα) or total IκBα. ERK phosphorylation was also monitored with antibodies directed against phospho-ERK (p-ERK). Actin served as the loading control.

The BCR-activated ERK phosphorylation levels were also similar in the observed cell populations. Therefore, despite the significant differences in the levels of Ca^{2+} influx in the CIN85 expressing and the CIN85-deficient cells, similar signaling differences were not observed for the activation of NF-κB pathway and the MAPK/ERK pathway. This hinted towards possible redundancies conferred by additional signaling elements in the cells. Moreover, it was concluded that DG75 cells, despite serving as a well-established cellular system to monitor Ca^{2+} signaling, do not serve as a suitable model system to study the activation of BCR-mediated the NF-κB pathway.

Although extremely robust in terms of culture growth and maintenance, even the established cell lines can present inconsistencies in signaling observations owing to multiple factors. To rule out any impact of the inadvertent differences in sample handling or culture conditions of the independent cell populations, I additionally monitored the Ca^{2+} signaling in cells that were cultured in a co-culture set up, as explained below (Figure 11). The CIN85/CD2AP-dKO cells which lacked any fluorescently tagged proteins were cultured in a 1:1 ratio with the cells either expressing cintrine-tagged wild type-CIN85 or citrine-tagged ΔCC-variant of CIN85 or EGFP/mock protein. Therefore, each pair of cell populations analysed (dKO with transduced-dKO) came from the same culture dish, underwent the same sample preparation procedures and were subjected to stimulation in the same sample tube, thus giving more reliable Ca^{2+} flux measurement results. In this way the previous Ca^{2+} influx differences in the CIN85 expressing cells, compared to the cells expressing ΔCC-variant of CIN85 or the mock control, were corroborated to confirm a role of CIN85 in BCR-mediated Ca^{2+} mobilization.

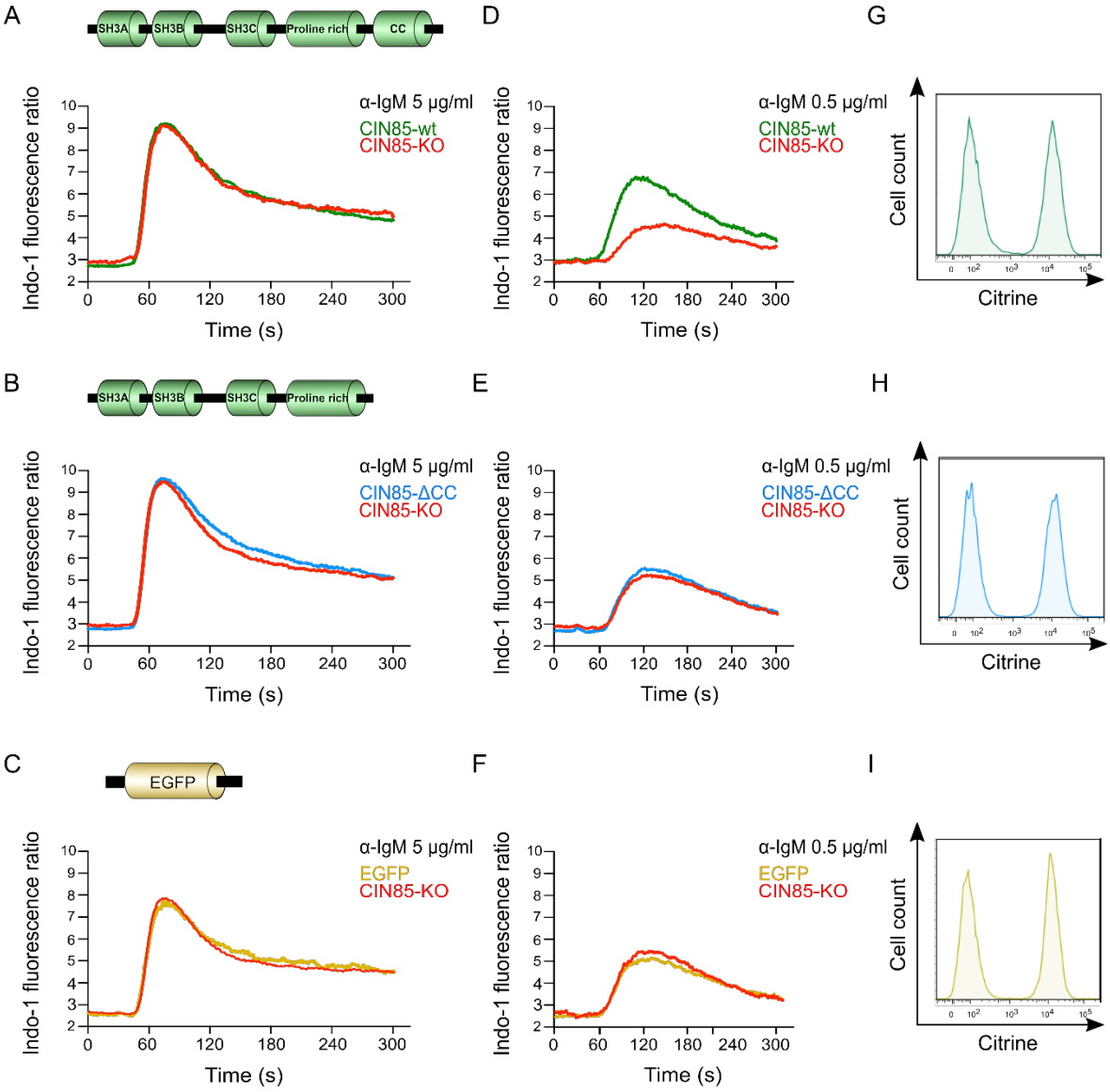

Figure 11: CIN85 expression positively regulates the Ca^{2+} influx levels in a co-culture setup. The co-culture set up consisted of DG75 CIN85/CD2AP-dKO cells mixed in equal proportions with the dKO-transfectants expressing exogenous citrine-tagged CIN85 (A), ΔCC variant of CIN85 (B) or the EGFP-mock (C). The cells were co-cultured under optimum culture conditions and the Ca^{2+} flux monitored after stimulation with 0.5 µg/ml α-human IgM F(ab´)$_2$ via flowcytometry. (G-I) The histograms confirm equal proportion of the two cell populations at the time of Ca^{2+} flux measurement in the co-cultured system.

To draw species-comparative conclusions, identical CRISPR/Cas9-mediated gene editing was performed for the CD2AP locus in the CIN85-KO mouse IIA1.6 cells (Figure 12), the dKO clones were identified and validated by sequencing. Monitoring the Ca^{2+} mobilization in these cells, the observations that were made for the DG75 cells were corroborated.

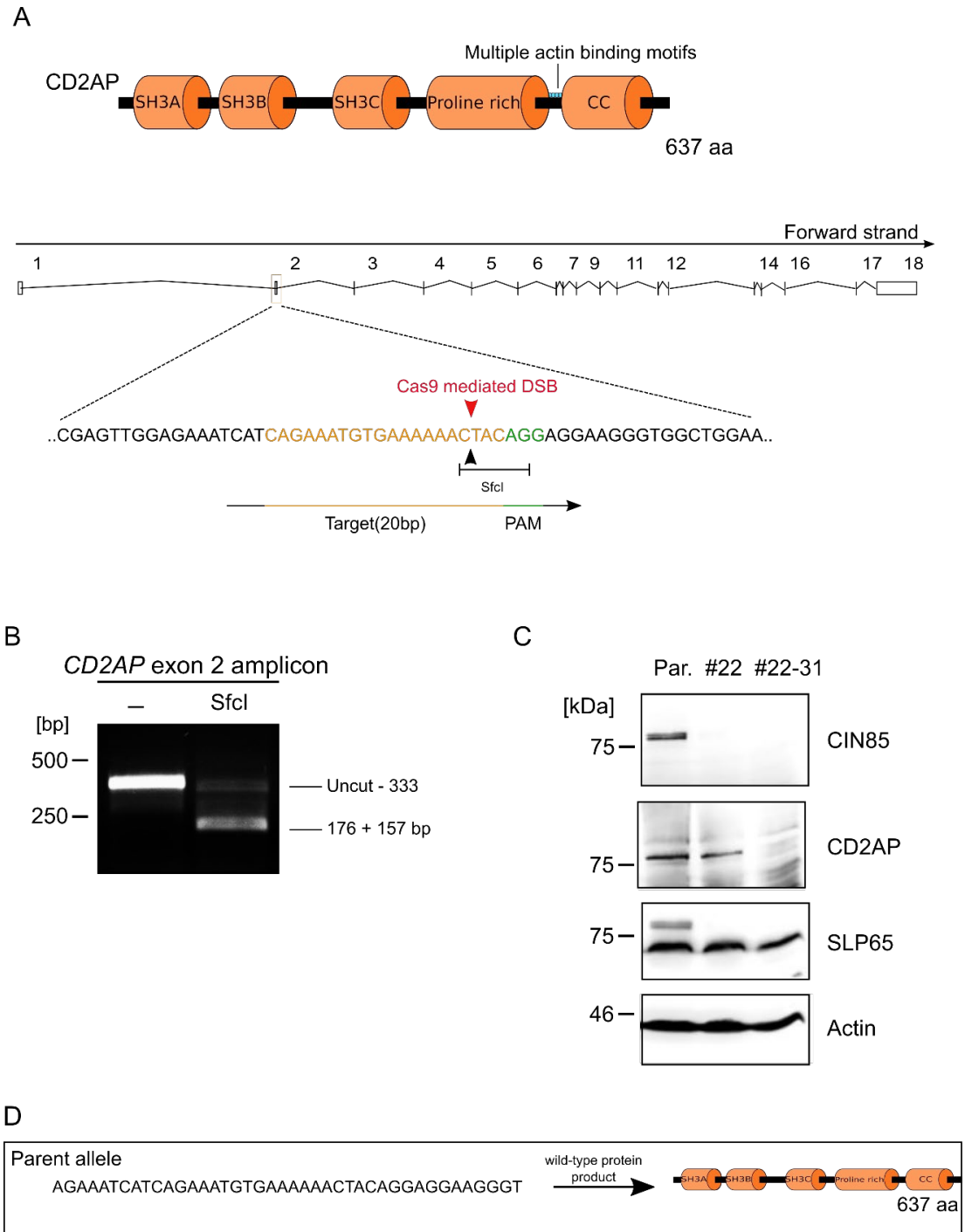

Figure 12: Exon 2 of *CD2AP* in mouse CIN85-KO IIA1.6 cells was targeted for CRISPR/Cas9-mediated gene editing and CIN85/CD2AP-dKO cells were identified. (A) Upper panel: Domain architecture of the CD2AP protein in mouse IIA1.6 cells **Lower panel:** schematic representation of the *CD2AP* genomic locus indicating the targeted exon and the nucleotide sequence against which the guide sequence was designed

(B) To test cleaving efficiency mediated by the Cas9, the amplification of the Exon 2 was carried out via PCR. The PCR amplicon was subjected to restriction digestion with the enzyme Sfc1, the binding site of which overlapped with the Cas9 cutting site, resulting in incomplete digestion of the DNA sample. **(C)** Cleared cellular lysates of IIA1.6 parental and putative CIN85/CD2AP-dKO clones were tested for CIN85 and CD2AP expression via western blot analyses using antibodies against CIN85 and CD2AP respectively. Similarly, SLP65 expression levels were compared using antibodies against the respective proteins. Actin was used as the loading control. **(D)** Sequencing results indicating the target site modification have been depicted along with the changes they confer to the protein product.

IIA1.6-dKO cells showed a very mild effect of CD2AP deletion on Ca^{2+}mobilization, however the over-expression of CD2AP significantly increased the Ca^{2+} flux level in the cells, almost to the level of CIN85 expressing cells. (Figure 13, B). Additionally, unlike the DG75 cells, the IIA1.6 cells showed a stimulation dependent activation of the NF-κB pathway. There was almost no phosphorylated IκBα (pIκBα) detected for the unstimulated cells and upon stimulation with increasing concentrations of the antibody, the levels of pIκBα also increased. A moderate reduction in pIκα levels was observed for the dKO cells when compared to the cells expressing wild type CIN85. In the case of ERK phosphorylation, the results were similar to those observed for the DG75 cells.

Equipped with these KO and dKO cells, I proceeded further to perform genetic and biochemical functional assays to explore the function of CIN85 in B cells.

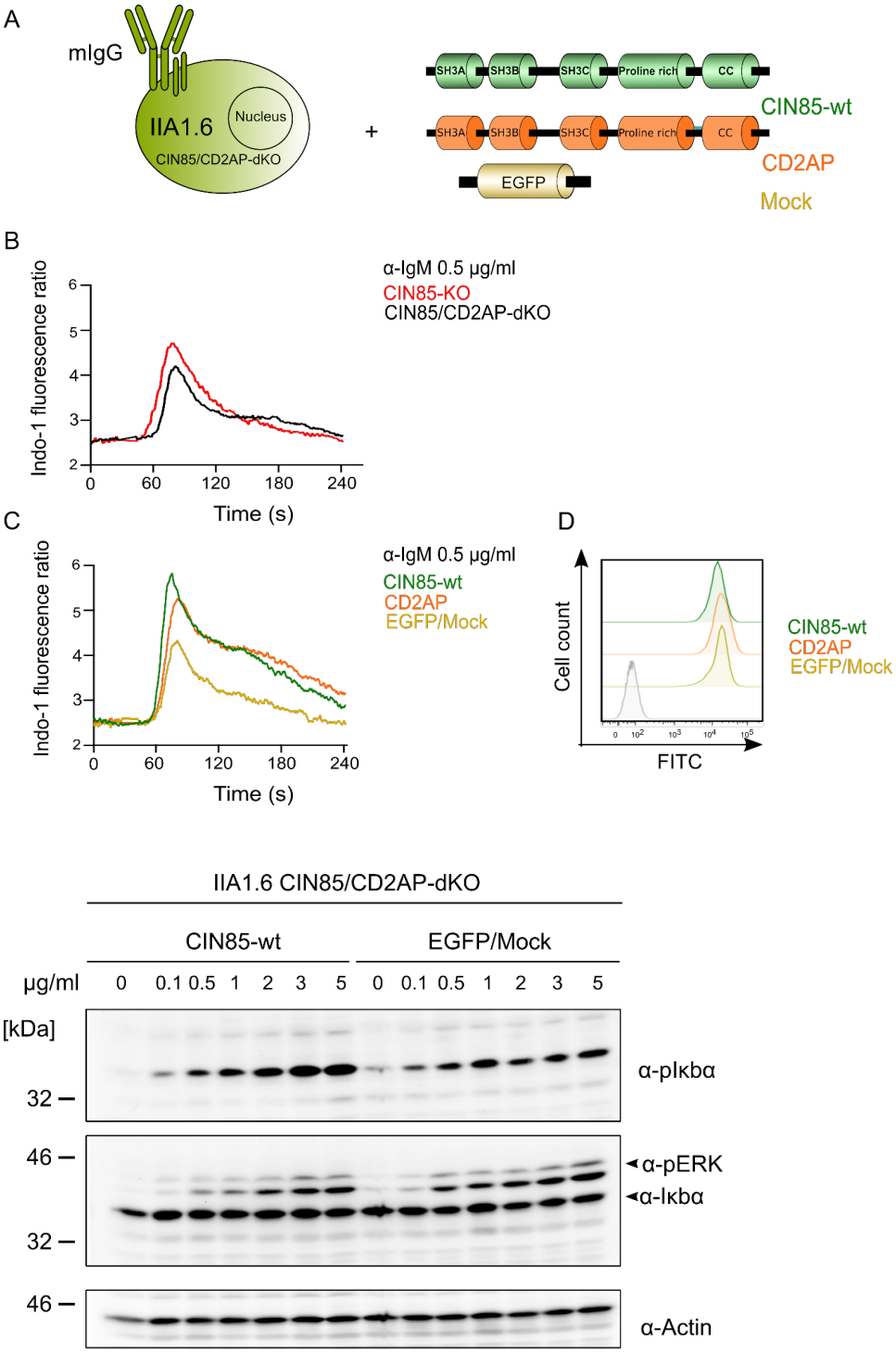

Figure 13: Over expression of CD2AP in CIN85/CD2AP-dKO IIA1.6 B cells significantly improves their Ca^{2+} signaling capacity. (A) CIN85/CD2AP-dKO IIA1.6 cells were transduced with citrine-tagged CIN85-wt (green line), CD2AP (orange), or the EGFP/mock protein (yellow) as depicted. (B) The Ca^{2+} influx in the CIN85-KO and CIN85/CD2AP-dKO cells was monitored upon stimulation with 0.5 µg/ml α-mouse IgG $F(ab')_2$ via flow cytometry. (D) The Ca^{2+} influx in the CIN85-dKO cells expressing either wild type CIN85, wild type CD2AP or EGFP was monitored upon stimulation with 0.5 µg/ml α-mouse IgM $F(ab')_2$ via flow cytometry. (D) The histogram confirms similar expression levels of the citrine-tagged proteins and the EGFP-mock protein in the respective cell populations as specified. (E) Cell lysates were prepared after stimulation of CIN85/CD2AP-dKO cells either expressing wild type CIN85 or EGFP with indicated concentrations of

α-mouse IgG F(ab´)$_2$. IκBα phosphorylation was analysed by SDS-PAGE and immunoblotting with antibodies against phospho-IκBα (p-IκBα) or total IκBα. ERK phosphorylation was also monitored with antibodies against phospho-ERK (p-ERK). Actin served as the loading control.

2.1.1 The human CIN85/CD2AP-dKO cell line serves as a model system to test the functional relevance of mutations found in CIN85 encoding gene of immunocompromised patients.

After corroborating the Ca^{2+}-defect phenotype of the patients mentioned in chapter 1 with the help of knock-out cell lines I generated, the subsequent course of action was to screen for any additional mutations in CIN85 gene that render the biological product functionally inactive in humans. I proceeded to test the signaling capacity of the prevailing variants of CIN85 reported in several patients. We identified these patients in collaboration with the human genetics department in Göttingen. All the reported patients are males and exhibit an immunocompromised condition, akin to the male siblings mentioned previously. Each of the three amino acid substitutions identified are positioned such that, they present a high probability of affecting the function of CIN85. The Q541E substitution falls close to PRR before the C-terminal coiled-coil domain. This mutation was reported in two patients. The T266I mutation was reported in 4 patients and lies right at the beginning of the third SH3 domain. Finally, the R413Q mutation which was reported in 2 patients is present in the LSRPGALPRR sequence in the proline rich region which is an optimum SH3 binding site. We were interested in screening for mutations that inhibited or modified, in any manner, the interaction of CIN85 with SLP65 thereby influencing the Ca^{2+} mobilization. The CIN85/CD2AP-dKO cells that I generated from the human DG75 cell line in the previous section thus served as a proficient cellular system to screen for such mutations and thus indicate their clinical significance with regard to the immunocompromised condition of the patients.

I therefore utilised the technique of site directed mutagenesis to create constructs that mimicked the abovementioned patient mutations. I then retrovirally transduced each of these constructs into the CIN85/CD2AP-dKO DG75 cells and monitored BCR-stimulated Ca^{2+} mobilization at 0.5 and 0.1 μg/ml α-human IgM F(ab´)$_2$ concentrations.

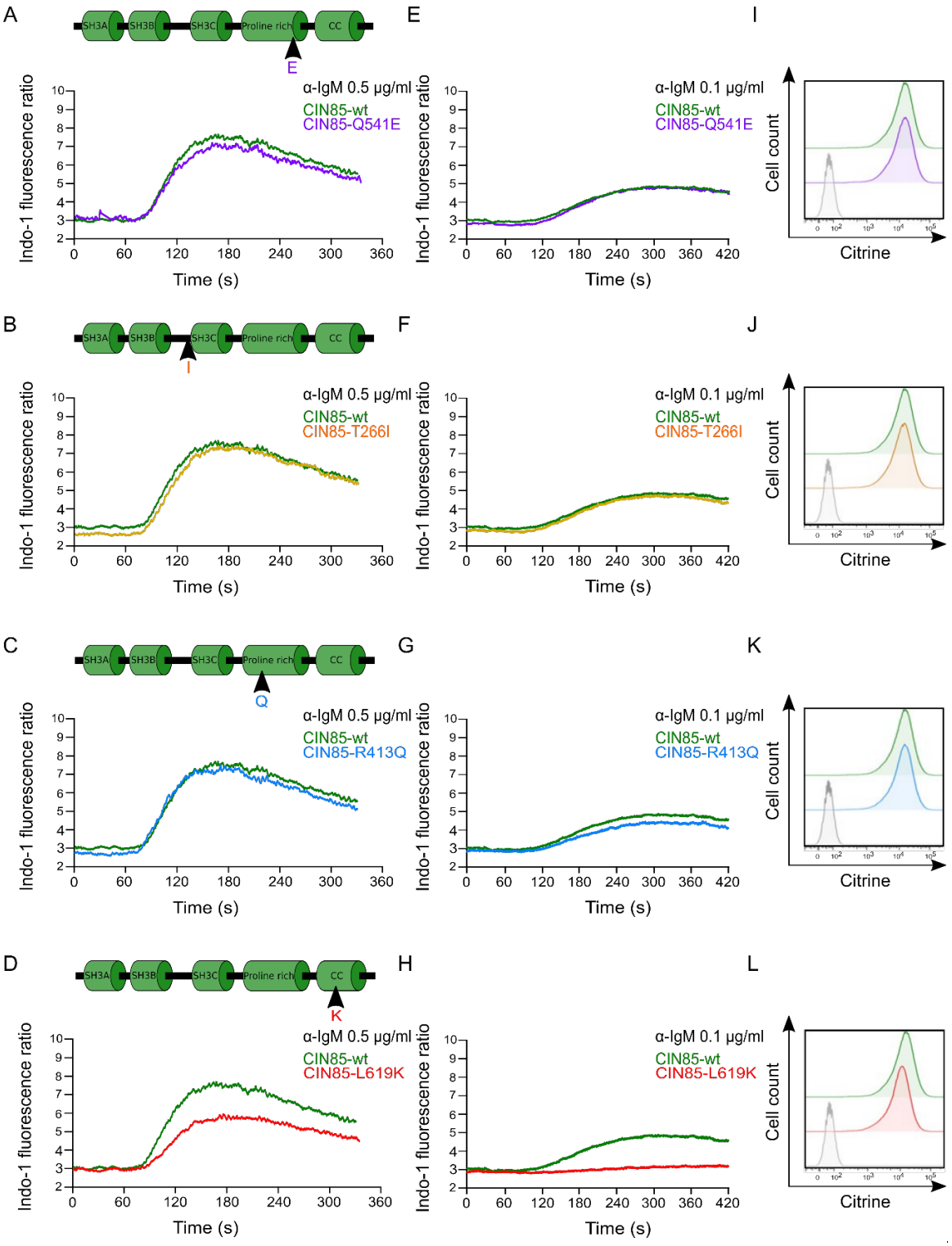

Figure 14: Testing the functional relevance of point mutations in the gene encoding CIN85 reported in immunocompromised patients. CIN85/CD2AP-dKO DG75 cells were transduced with citrine-tagged CIN85-wt (green line), Q541E mutant (purple), T266I mutant (yellow line), R413Q mutant (blue line) or L619K mutant (red line) as depicted. The Ca^{2+} influx in transduced and sorted citrine positive cells upon stimulation with **(A-D)** 0.5 µg/ml α-human IgM F(ab´)$_2$ or **(E-H)** 0.1µg/ml α-human IgM F(ab´)$_2$ was monitored by flow cytometry. **(I-L)** The histograms confirm similar expression levels of the two citrine-tagged proteins in the respective cell populations.

Additionally, I expressed an L619K variant of CIN85 as a negative control: the NMR studies in Kühn et al., 2016 established that replacing the hydrophobic residue Leu^{619} with the hydrophilic residue lysine impacts the stability of the coiled-coil domain, such that, the trimerization gets disrupted.

In my results, I observed that none of these mutations hampered the capacity of CIN85 to promote calcium mobilization (Figure 14). It appeared that these mutations are "silent" or "quiet" mutations that although change the amino acid sequence of the protein, fail to alter the biological function. The CIN85 variants function similar to wild type-CIN85 in terms of SLP65 clustering, mediating Ca^{2+} flux to the wild type levels. The negative control showed a decreased calcium flux compared to wild type-CIN85.

These point mutations therefore, cannot be directly implicated for the immunocompromised condition of the patients, as these CIN85 variants do not show any defect in the capacity of B cells to get activated upon BCR-stimulation. Presently it is difficult to rule out the possibility of additional/alternative combination of factors which could be responsible, however these results demonstrate that inefficient CIN85-mediated clustering of the master regulator SLP65 can be ruled out.

2.1.2 CIN85 influences the plasma membrane localization of PKCβ upon BCR-mediated stimulation of cells

Beyond its well-established role in constitutive interaction with the key adaptor protein SLP65 and driving its multimerization to subsequently regulate its capacity to conduct Ca^{2+} mobilization, CIN85 has been implicated to play a role in NF-κB pathway activation in B cells (Keller et al., 2018, Kometani et al., 2011). Earlier we attempted to investigate this by monitoring the effect of the absence or presence of CIN85 on the extent of phosphorylation of IκBα, a key signaling step in the pathway in the established cell lines. Considering the sequence of events in the NFκB signaling pathway, this step appears way downstream of the BCR-antigen ligation. We were therefore interested in setting up a read-out system at a relatively upstream-level that could give us hints as to the involvement of

Ratio H/L normalized	No. Of Peptides	Gene name	Protein ID	Protein name
4.0219	3	TSPAN14	Q8NG11-2	Tetraspanin-14
3.3134	2	RPF2	Q5VXN0	Ribosome production factor 2 homolog
3.017	9	SPECC1L	F8WAN1	Cytospin-A
2,7318	4	MAGED1	Q9Y5V3	Melanoma-associated antigen D1
2,7071	4	METTL5	B8ZZY8	Methyltransferase-like protein 5
2,6042	26	MYH10	P35580	Myosin-10
2,4268	7	VLDLR	P98155-2	Very low-density lipoprotein receptor
2,4143	2	KIAA0020	Q15397	Pumilio domain-containing protein KIAA0020
2,3803	3	PIK3CD	O00329	PtdIns(4,5)P23-kinase catalytic subunit delta isoform
2,3716	2	MICU1	Q9BPX6-2	Calcium uptake protein 1, mitochondrial
2,2859	3	MFN2	O95140	Mitofusin-2
2,2577	1	VLDLR	P98155-2	Very low-density lipoprotein receptor
2,148	25	DBN1	Q16643	Drebrin
2,0973	13	MYH14	Q7Z406	Myosin-14
1,9008	14	PPAT	Q06203	Amidophosphoribosyltransferase
1,8133	17	UQCRC1	P31930	Cytochrome b-c1 complex subunit 1, mitochondrial
1,2099	14	SH3KBP1	Q96B97	SH3 domain-containing kinase-binding protein 1

Table 1: PKCβII interactome analysis in the human DG75 B cell line. Strep-tagged version of human PKCβII was introduced into the DG75 cells via electroporation. The selected positive clones were mixed to avoid clonal variations and were cultured in SILAC medium containing heavy amino acids Lysine D4 (Lys+4), Arginine 13C6 (Arg+6). For control, DG75-wt cells were cultured in SILAC medium containing light amino acids. The two cell populations were stimulated for 5 minutes with α-human IgM $F(ab')_2$ fragments and the lysates from these cells were subject to affinity purification by streptavidin-coated beads. The purified light and heavy labeled samples were pooled in a 1:1 ratio and subsequently analyzed by mass spectrometry. The mass spectrometry analysis and preliminary data processing was done in collaboration with the Proteomics Core Facility of University Medicine Göttingen. Data are from one experiment.

CIN85 in the NF-κB pathway. Studying PKCß activation served as an appealing option in this regard owing to several reasons. Multiple studies have highlighted a crucial role of PKCß in NFκB pathway activation specifically in B cells. It has been shown that IκB degradation is abrogated in PKCß-deficient B cells activated by IgM ligation but not in the case of stimulation with CD40 (Saijo et al., 2002; Su et al., 2002). This bears stark resemblance to the CIN85-deficient patient's B cells where, BCR stimulation of the primary B cells could not induce NF-κB activation whereas other stimuli (PMA, CD40) did (Keller et al., 2018).

Our very initial endeavour was to get a more exhaustive view of the interaction partners of PKCβ in B cells in an attempt to check for its interaction with CIN85. For this, a strep-tagged version of PKCβII was used to pull down interaction partners from stimulated SILAC-labeled B cell lysates, which were then identified via mass spectrometry (done in collaboration with the Proteomics Core Facility of University Medical Center Göttingen).

Table 1 enlists the prominent interaction partners with around 2.0-fold enrichment ratio for proteins that fulfilled the significance conditions. It is important to note that these proteins include both direct and indirect interaction partners. Additionally, however, in these affinity purification procedures, certain labile protein interactions can be lost owing to the use of harsh detergent conditions. Although mentioned in the list, CIN85 does not make the 2.0-fold enrichment ratio cut-off which suggests that it is unlikely that CIN85 is involved in direct interaction with PKCβII in these cells or if it does, the interaction is highly unstable and cannot be studied by means of conventional affinity purifications.

Our next technical approach was to retrovirally transduce the citrine-tagged version of protein kinase C β II (PKCβII) into DG75 cells. Of the two isoforms PKCβI and PKCβII which are simultaneously expressed in several B cell lines, DG75 cells lack the expression of PKCβII. This allows us to study the functioning of the exogenously expressed citrine-tagged variant of the protein without the interference from any endogenously expressed protein. Expression of the citrine-tagged version of PKCβII in parental DG75 cells allowed for visualizing of the protein within the cell with confocal laser scanning microscopy (Figure 15, A). PKCβII is localized in the cytoplasm in resting B cells and undergoes translocation to the plasma membrane upon BCR stimulation (Su et al., 2002). This could be confirmed by our confocal microscopy experiments that showed a ring like appearance on recruitment of the citrine-tagged protein to the plasma membrane upon BCR-mediated activation, the ring being most prominent around 30 secs of stimulation showing maximum recruitment, and fades thereafter.

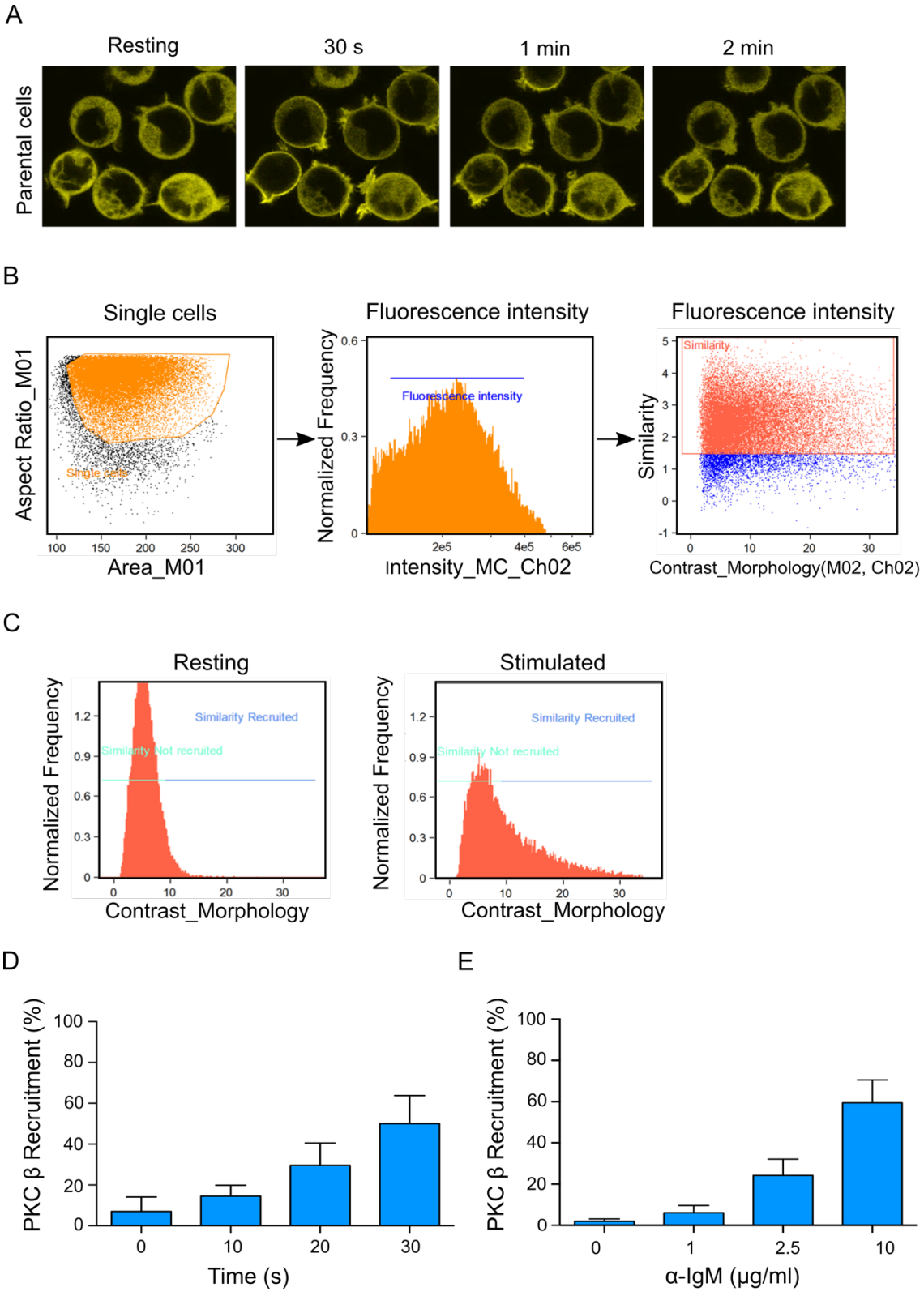

Figure 15: BCR-mediated activation induced PKCβII plasma membrane translocation in DG75 cells. **(A)** Parental DG75 cells were retrovirally transduced with Citrine-tagged human PKCβII. The cells were then sorted to achieve a homogenous sub-cell population consisting of cells with similar expression levels of

exogenously expressed Citrine-tagged PKCβII. The cells were subsequently subjected to confocal laser scanning microscopy and the plasma membrane localization of the Citrine-tagged PKCβII was monitored in resting cells and cells stimulated with 10µg/ml α-human IgM F(ab´)2 fragments, over the time course of 2 mins. These cells were then analysed at the AMNIS imaging flow cytometer to subsequently make quantitative measurements. After the data acquisition with imaging flow cytometer, the analysis was performed using the co-localization wizard of the Image Data Exploration and Analysis Software from AMNIS called IDEAS® according to the given analysis strategy**: (B**) the dot plot represents the gating strategy used to identify single cells. The single cells are further subjected to above depicted gating strategy to obtain cells falling within a specific range of their Citrine-fluorescence intensity. Subsequently, the similarity feature of the wizard is used to specifically compare the co-localization of Citrine tagged-PKCßII and the membrane dye to define membrane recruitment. Similarity >1.5 between membrane dye and PKCßII represented cells with membrane localized PKCβII. **(C)** These histograms depict the resting and stimulated cell populations respectively where the contrast Morphology >9 equals PKCßII membrane recruitment. **(D)** BCR activation-mediated PKCßII membrane recruitment kinetic profile for DG75 parental cells. The cells were stimulated with 10µg/ml α-human IgM F(ab´)2 fragments. The Y-axis indicates the percentage of cells with membrane localized PKCßII. **(E)** Effect of increasing concentration of α-human IgM F(ab´)2 fragments on PKCßII membrane recruitment in parental DG75 cells. The cells were stimulated for 30 secs. The Y-axis indicates the percentage of cells with membrane localized PKCßII. Standard deviations were calculated with recruitment values from 3 biological replicates, each further representing three technical replicates.*.These experiments were conducted in collaboration with Dr. Marcel Liebick.

Confocal microscopy, although a conventionally trusted imaging technique spatially restricts the visual observations to merely a few cells at a time and does not give a quantitative indication of the behaviour of cells in a given population. To overcome this challenge, I collaborated with a Post Doc. colleague from my department Dr. Marcel Liebeck and decided to shift to a technically more sophisticated system that combines the power of imaging and flowcytometry called, Amnis® imaging flow cytometer, a high-throughput system that allowed us to make quantitative, statistically robust measurements in addition to the conventional imaging studies. A detailed analysis strategy explains the selected parameters and the gating system used to quantify the cells for their PKCβII membrane recruitment (Figure 15, B and C).

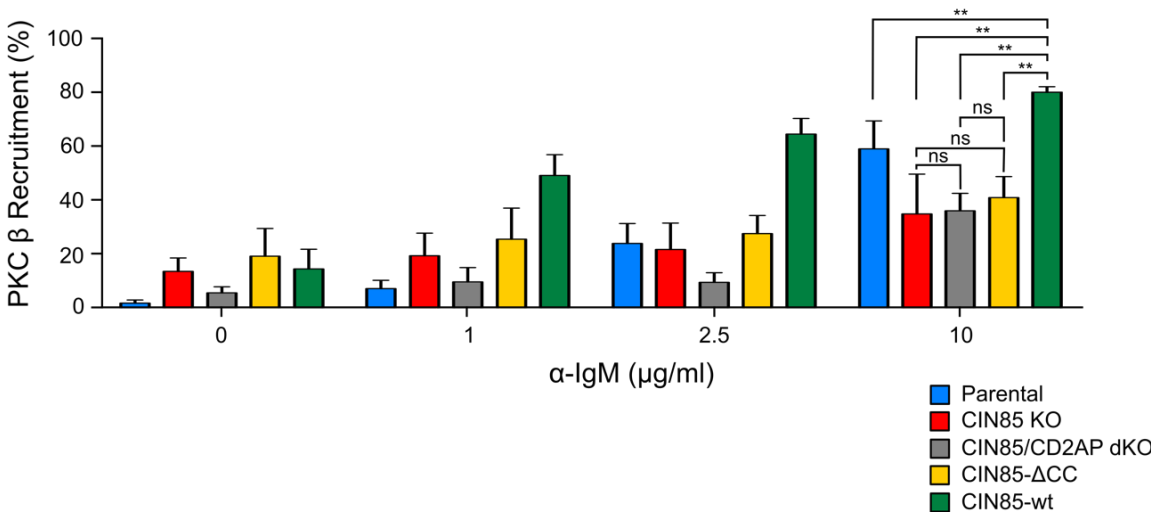

Figure 16: CIN85 can regulate PKCβII membrane translocation upon B cell activation. DG75 parental cells(blue), CIN85-KO cells(red), CIN85/CD2AP-dKO cells(grey), cells expressing the C-terminal deletion variant of CIN85(yellow) and finally cells overexpressing the wt-version of CIN85(green) were tested for the extent of PKCβII membrane translocation upon stimulation with increasing doses of α-human IgM F(ab´)2 fragment concentrations. Each cell population was stimulated for 30 secs. The analysis was performed using the co-localization wizard of the Image Data Exploration and Analysis Software from AMNIS called IDEAS® with which the percentage of cells displaying co-localization of the Citrine fluorescence signal with the signal from the plasma membrane stain CellMask™ was quantified. The Y-axis indicates the percentage of cells with membrane localized PKCßII. Standard deviations were calculated with recruitment values from 3 biological replicates, each further representing three technical replicates. ** $P \leq 0.01$. These experiments were conducted in collaboration with Dr. Marcel Liebick.

Initial experiments with the parental DG75 cells established that PKCβII membrane recruitment response from the majority of cells in a population occurs 30 secs post-stimulation (Figure 15, D). Additionally, the membrane localization is antigen-concentration dependent with increasing percentage of cells showing PKCβII recruitment with increasing concentrations of α-human IgM F(ab´)$_2$ fragments (Figure 15, E).The established AMNIS imaging flowcytometry-based PKCßII membrane translocation assay allowed for comparative quantitative visualization of membrane recruitment of the citrine-tagged protein in multiple cell-populations. Therefore, I used this assay to test the PKCßII plasma membrane localization in CIN85-deficient cells and the several transduced sub-cell lines that were created. It was observed that a significantly higher proportion of cells were capable of recruiting PKCßII to their plasma membrane when over-expressing CIN85-wt as compared to those expressing either the ΔCC-variant or the EGFP mock (Figure 16). This indicated that the presence of CIN85 is capable of impacting the plasma membrane translocation of PKCßII in the cellular systems tested.

2.1.3 Ibrutinib downregulates BCR-mediated NF-κB pathway activation in IIA1.6 cells but not in DG75 cells.

I made use of ibrutinib, an irreversible inhibitor of Bruton's tyrosine kinase (integral member of the calcium initiation complex) to confirm its capacity to inhibit Ca^{2+} mobilization and test if it affects the canonical NF-κB pathway activation in the CIN85/CD2AP-dKO DG75 and IIA1.6 cells (Figure 17). As expected, ibrutinib successfully inhibits Ca^{2+} flux in both DG75 and IIA1.6 cells almost entirely. This result also highlights the fact that there is no BCR-induced increase in the levels of pIκBα in DG75 cells.

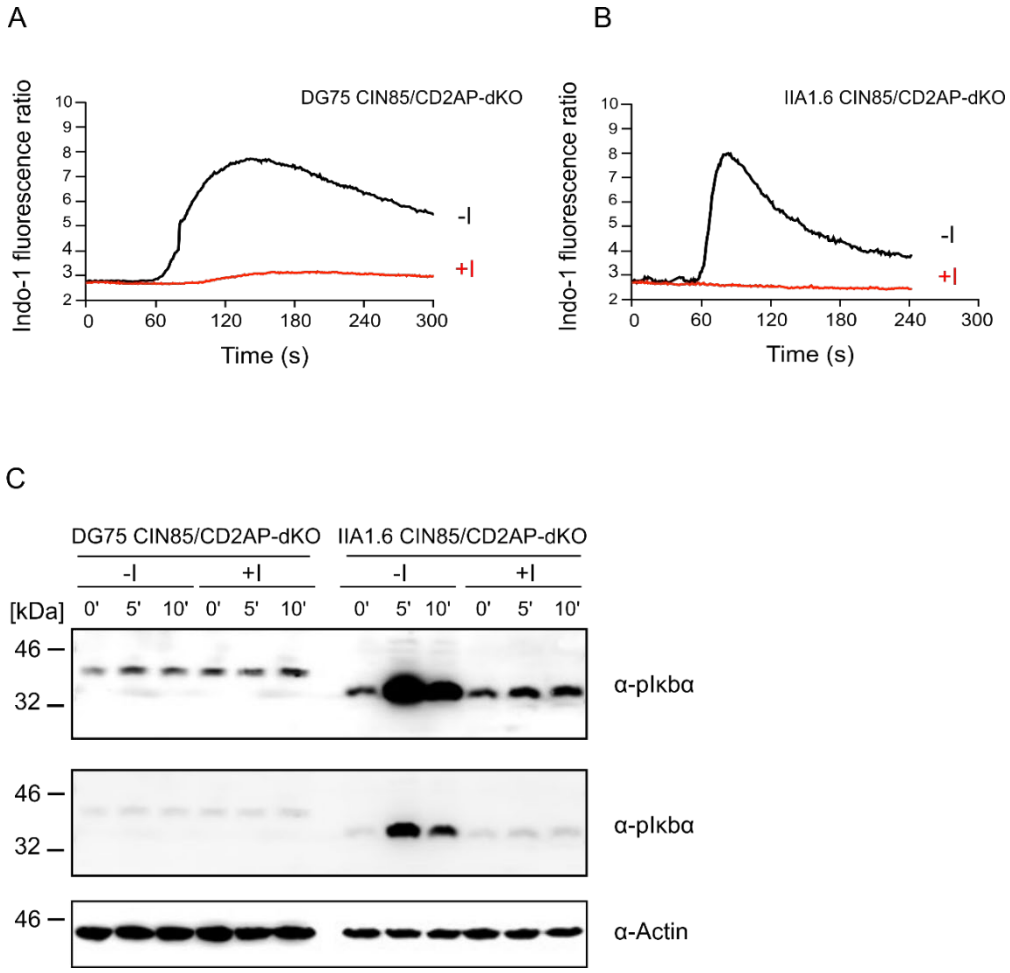

Figure 17: Ibrutinib inhibits Ca^{2+} signaling in DG75 and IIA1.6 cells but has a varying effect on NF-κB pathway activation in the two cell lines. CIN85/CD2AP-dKO DG75 cells (A) or IIA1.6 cells (B) were

treated with 1µM Ibrutinib prior to stimulation with 5 µg/ml α-IgM F(ab´)2 for DG75 and α-IgG F(ab´)2 for IIA1.6 cells and the Ca^{2+} flux was monitored by flowcytometry. (C) Cell lysates were prepared after stimulation of respective cell lines either treated with 1µM Ibrutinib (+I) or not treated with Ibrutinib (-I) and IκBα phosphorylation was analyzed by SDS-PAGE and immunoblot analyses with antibodies against phospho-IκBα (pIκBα). The upper panel shows the immunoblot post longer time exposure and high contrast settings and the lower panel shows the same blot with lower contrast settings. Actin was used as the loading control.

For both IIA1.6 and DG75 cells, there is stimulation independent, similar basal levels of phosphorylated IκBα which is unaffected by ibrutinib's presence. There is a spike in the levels of pIκBα upon BCR-stimulation in IIA1.6 cells, indicating activation of the canonical NF-κB pathway which was not the case for DG75 cells. This indicated that apart from basal levels, there is was no additional activation of the pathway upon the stimulation of cells.

2.1.4 The CIN85-KO impact on the viability of cells in a co-culture set up is specific to the cell line being investigated.

An additional method of monitoring the involvement of these adaptor proteins in intracellular signaling pathways was to test the effect of their depletion on cell viability and cell growth. This would give an indication of their involvement with regard to the low level, constitutive signaling in the basal state (tonic signaling) that does not require BCR-mediated signals but are required for survival of the cells. The main advantage of this set-up however, was that it aims to partially mimic the B cell compartment of the mother of the patients harbouring deletion in their *CIN85* gene, positioned on the X chromosome (see chapter 1). Considering the Lyon Hypothesis and the random X chromosome inactivation, it is reasonable to believe that the mother's B cell compartment is a heterogenous mixture of CIN85 expressing and CIN85-deficient B cells, and under competitive conditions, differential survival advantages might play a role in determining which population takes over and mediates the immune responses.

Equipped with the human and mouse knock-out B cell lines which could be transduced to express fluorescent-tagged proteins, we devised a means to monitor the viability of cells and the rate of cell growth in the presence or absence of fluorescently tagged-CIN85 expression over the course of 4 days in a co-culture set up.

For this, I mixed the CIN85/CD2AP-double deficient cells lacking any fluorescence and cells reconstituted with citrine-tagged CIN85 in equal proportion and monitored the changes in the abundance of the non-fluorescent and fluorescent populations of the cells in the culture at 24 hrs time points (Figure 18). The cell count comparisons for the non-florescent and fluorescent cells (high citrine), gave indication of the abundance of each of the two cell populations in the culture at that time point.
It was observed that for the human DG75 B cells (Figure 18), there was no difference in the viability or the rate of cell growth for the dKO and citrine-tagged CIN85 expressing populations of cells in the culture and that an equal abundance of the two populations was maintained over the course of 72 hours.

Unlike the DG75 cells, contrasting observations were made for the mouse IIA1.6 cells (Figure 19). After 24 hrs of co-culture, cell count peak for the cells lacking CIN85 (non-fluorescent cells) started to reduce in comparison to the cells expressing citrine-tagged CIN85. Post 72 hrs of co-culture, the differences in the abundance of the two cell populations became more prominent. This indicates that CIN85 in the mouse IIA1.6 cells somehow impacts the tonic signals that serve a maintenance function. Biologically, this holds significance as it hints to the possibility that, over the years, one B cell compartment takes over the other in a heterogenous peripheral B cell population of the mother, because of a possible survival advantage conferred owing to the presence of CIN85.

A

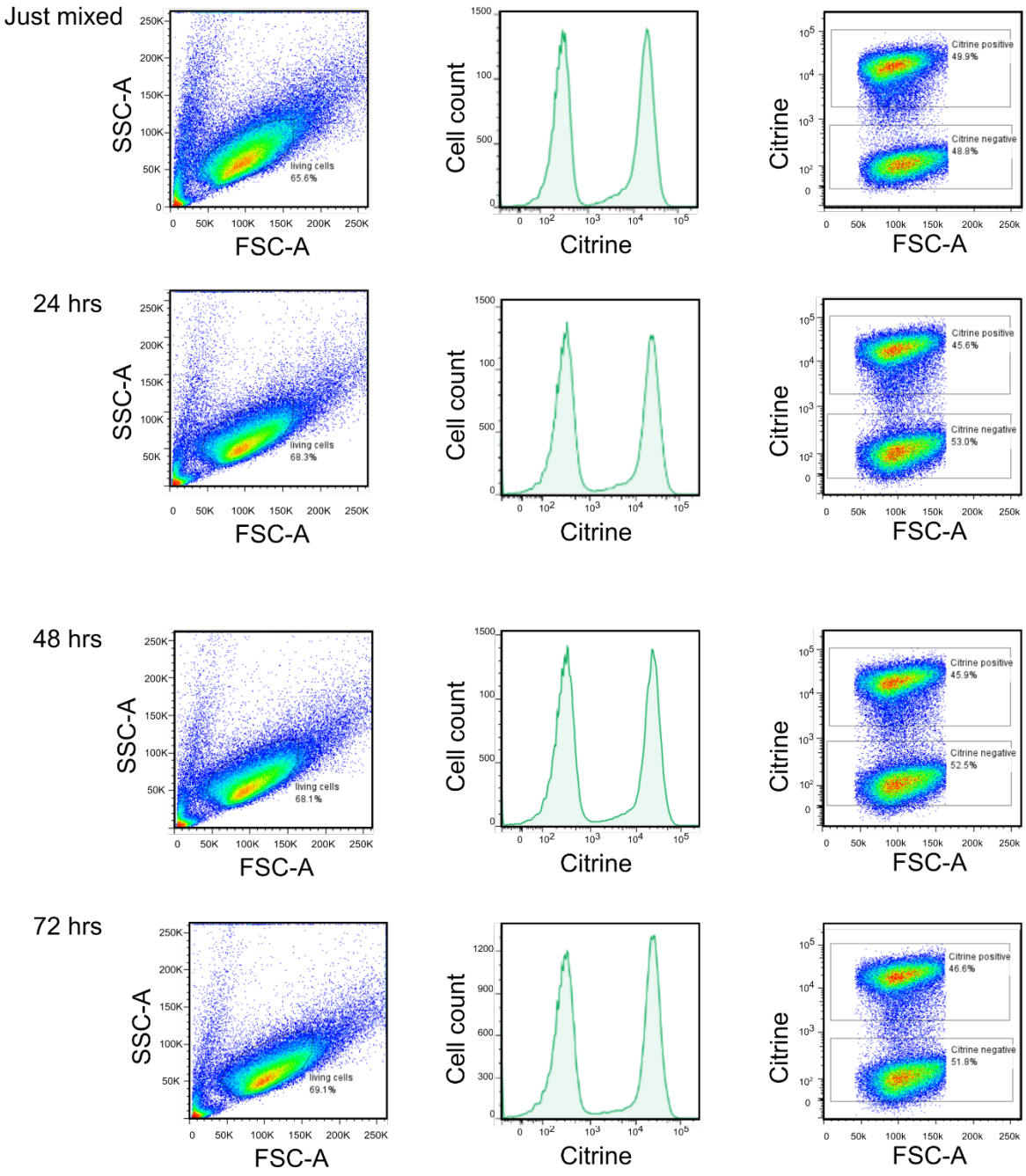

Figure 18: Absence of CIN85 and CD2AP in DG75 cells does not impact the cell viability or growth rate in a co-culture set up. The co-culture set up consisted of DG75 CIN85/CD2AP-dKO cells mixed in equal proportions with the DG75 dKO-transfectants expressing exogenous citrine-tagged CIN85 and co-cultured under optimum culture conditions. The fraction of non-fluorescent (dKO) and fluorescent (expressing citrine-tagged CIN85) cells was monitored via flowcytometry over the course of 72 hrs at every 24 hrs time point.

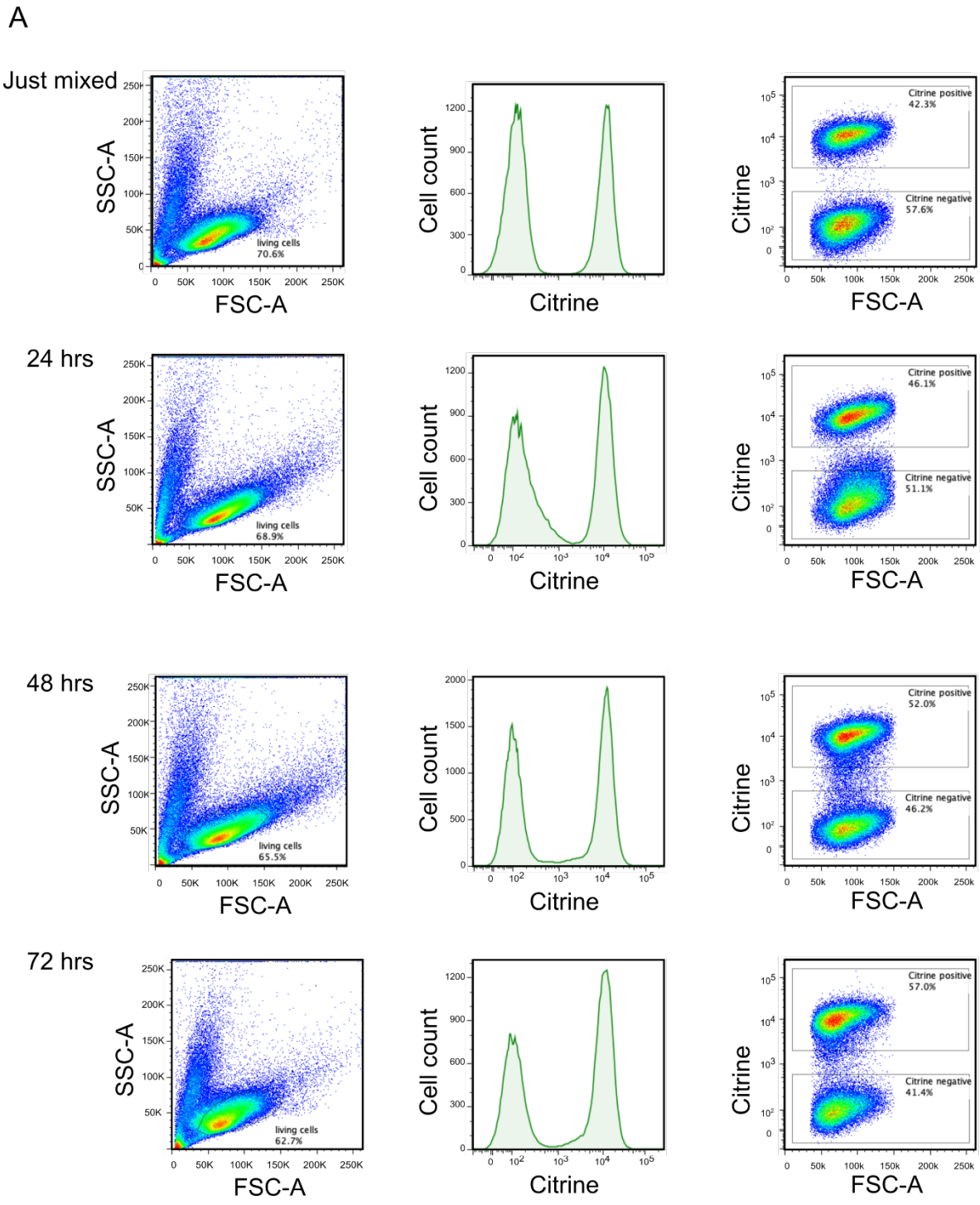

Figure 19: Absence of CIN85 and CD2AP in IIA1.6 cells has a negative impact on the cell viability or growth rate in a co-culture setup. The co-culture set up consisted of IIA1.6 CIN85/CD2AP-dKO cells mixed in equal proportions with the IIA1.6 dKO-transfectants expressing exogenous citrine-tagged CIN85 and co-cultured under optimum culture conditions. The fraction of non-fluorescent (dKO) and fluorescent (expressing citrine-tagged CIN85) cells was monitored via flowcytometry over the course of 72 hrs at every 24 hrs time point.

2.1.5 Combined deletion of CIN85 and CD2AP does not influence the stimulation triggered-BCR internalization.

In several reports, CIN85 has been implicated in receptor downregulation functions. In fact, for several years after discover, the function of CIN85 that received the most widespread attention was its capacity to facilitate ligand induced internalization of receptors such as the EGFR, thus dampening the effector functions (Soubeyran, et al., 2002). Moreover, with the ability to interact with actin capping proteins and CD2AP being especially equipped with actin binding sties, it was fair to assume that CIN85 and CD2AP could connect the cell surface BCRs to components of the actin cytoskeleton, playing an important role in receptor endocytosis. We were therefore curious to check if the above-mentioned receptor internalization activity of CIN85 is specific with regard to the receptor tyrosine kinases, or if similar effects are exerted on the cell surface BCRs.

I tested this in both human and mouse established B cell lines using the CIN85/CD2AP-dKO cells I had generated. I retrovirally transduced the double deficient-cells with constructs encoding either wild type CIN85 or the mock control EGFP. This system could give us reliable information about the impact of the presence or absence of CIN85 on antigen induced BCR internalization without any possible compensatory effects of CD2AP. I then proceeded to analyse the BCR levels using flowcytometry, prior (0 min) and post antigen stimulation over the course of 120 mins (Figure 20). The cells were appropriately stimulated with either biotinylated anti-human IgM or anti-mouse IgG which initiated the BCR internalization. The remaining BCRs localised on the cell surface were stained with APC fluorophore-conjugated streptavidin. Monitoring the levels of the residual BCRs left at the B cell surface at several time points after stimulation in this manner, gives us an indirect means to examine the extent and rate of BCR internalization.

The DG75 and IIA1.6 cells, after stimulation for 120 mins showed a decrease in surface BCR levels of up to 70 and 80% respectively, compared to the unstimulated cells. Additionally, the expression of CIN85 in the CIN85/CD2AP-dKO cells does not alter the kinetics of BCR internalization. This indicates that perhaps in B cells, CIN85 is prioritised in participating in other signaling pathways and is thus not involved in BCR internalization.

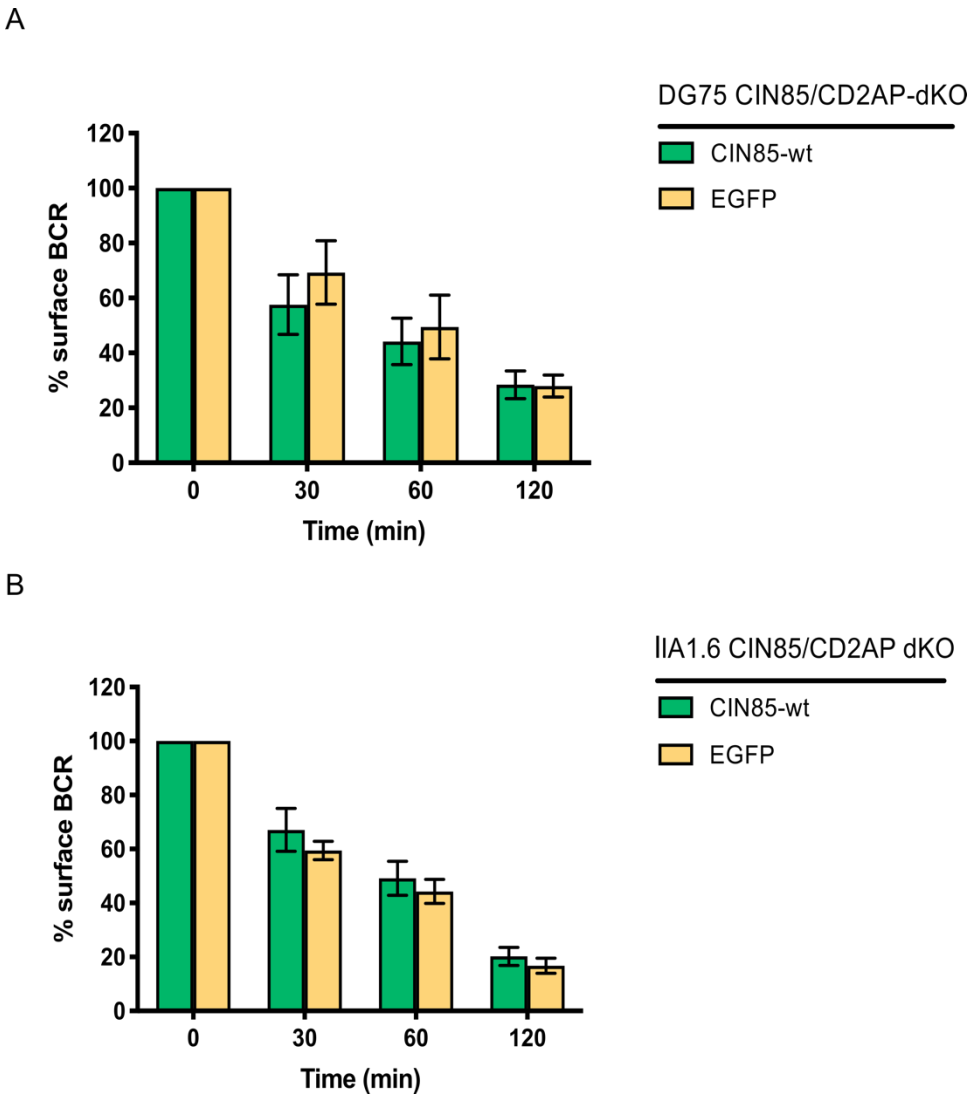

Figure 20: Deletion of CIN85 and CD2AP does not influence BCR internalization. (A) DG75 or **(B)** IIA1.6 CIN85/CD2AP-dKO cells expressing either wild type CIN85 (green) or EGFP mock (yellow) were analyzed for stimulation-mediated receptor internalization by staining of the remnant cell surface IgM for DG75 cells or IgG for IIA1.6 cells over the course of 120 mins. The percentage values of the surface BCR are relative to those of the resting cells and were calculated form the mean fluorescence intensity of the APC fluorophore-conjugated streptavidin that bound to biotinylated α-human IgM or α-mouse IgG primary antibodies. The 0 min time point depicts the total BCR levels on the surface of resting cells followed by 30, 60 and 120-min time points post stimulation with 1 µg/ml primary antibody. Standard deviations were calculated from three independent experiments.

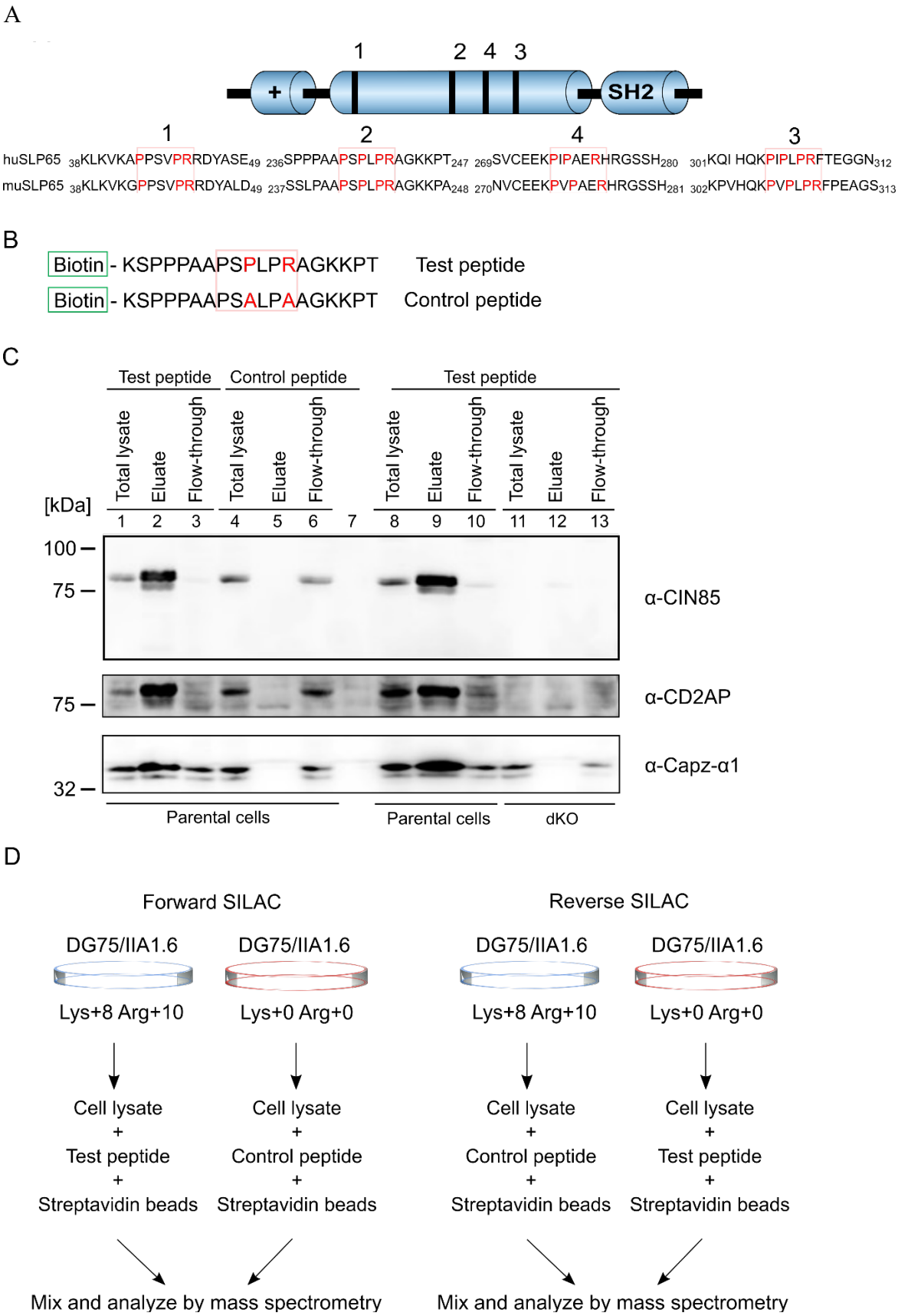

Figure 21: Experimental outline for mass-spectrometric identification and relative quantification of all the PXXXPR ligands.

(A) Domain architecture of SLP65 with the four atypical proline/arginine motifs (indicated 1-4) and their amino-acid sequences in human and murine SLP65. **(B)** Amino-acid sequence of the N-terminally biotinylated peptides encompassing the central proline/arginine motif of SLP65 as either wild-type (Test peptide) or binding-inactive version (Control peptide) for affinity purification experiments. **(C)** The binding capacity of the peptides was tested by subjecting the lysates from IIA1.6 parental or CIN85/CD2AP dKO cells to affinity purification tests with the aforementioned peptides, followed by SDS-PAGE and immunoblotting analyses of the purified proteins. The blot was probed with antibodies against known interaction partners namely, CIN85, CD2AP and a co-purification protein CapZ-α1. **(D)** Schematic representation of the independent forward and reverse pull-down approaches for comparative analyses of the ligands binding to the biotinylated peptides. In the forward pull-down experiment, the test peptides are immobilized on streptavidin beads and incubated with the lysate from DG75 CIN85/CD2AP dKO cells or IIA1.6 CIN85/CD2AP dKO cells metabolically labelled with heavy (Lys+8/Arg+10) amino acids. For control, the control peptides are incubated with lysate from the respective cell lines cultured in light (Lys+0/Arg+0) SILAC medium. The heavy and the light purified proteins(eluates) were mixed at a 1:1 ratio, digested with trypsin and identified by quantitative LC-MS/MS analysis using MaxQuant software. In the reverse pull-down experiment, the test peptides are incubated with the light lysate and the control peptides are incubated with the heavy lysate. The subsequent steps for protein purification and mass-spectrometric analyses were the same as in the forward SILAC-labeling experiment. Binding candidates give large H/L enrichment values in the forward experiment and small H/L enrichment ratios in the reverse experiment.

2.2 Amphiphysin 2/Bin 1 can bind atypical SH3-binding motifs on SLP65

In Oellerich et al. 2011, it was established that steady ligands CIN85 and CD2AP constitute the stimulation-independent preformed signalosomes. Moreover, the interaction was shown to be highly selective, with the central proline/arginine motif of SLP65 exclusively purifying CIN85 and CD2AP from the B cell lysates.

The human and mouse CIN85/CD2AP-double deficient cell lines I created gave us an opportunity to study additional, thus far unreported, PXXXPR ligands that bind to SLP65 via the same interaction module as the CIN85 and CD2AP adaptor proteins. Figure 21, B shows the synthetic biotinylated peptides encompassing the central proline/arginine motif of SLP65 and the surrounding amino acids to purify its interaction partners from the human and mouse B cell lines. These peptides are referred to as the test peptides. Additionally, peptides carrying a mutated version of the proline/arginine motif designed to be incapable of interacting with CIN85 and CD2AP was used as a control and these peptides are referred to as the control peptides. I then proceeded to confirm the capacity of the peptides to interact with known interactors CIN85 and CD2AP and their close associates like the CapZ-α1 in both the parental cells and the CIN85/CD2AP-double deficient cells. I also confirmed the binding incompetence of the control peptides (Figure 21, C).

A

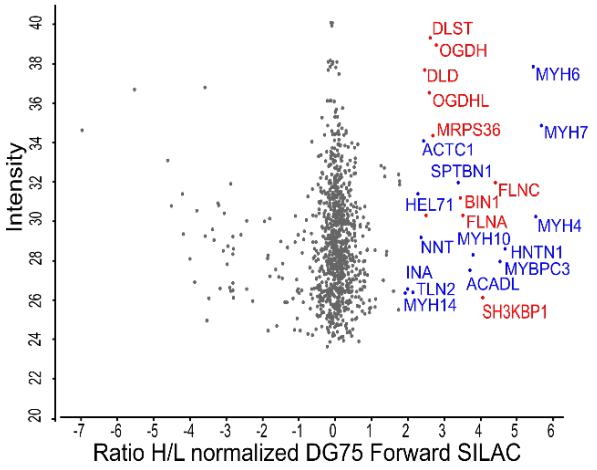

B

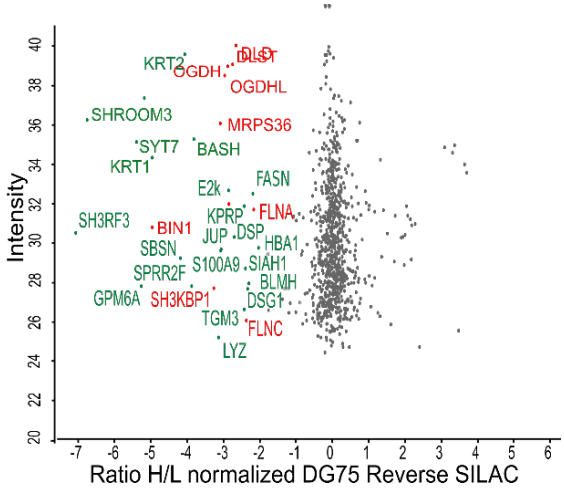

C

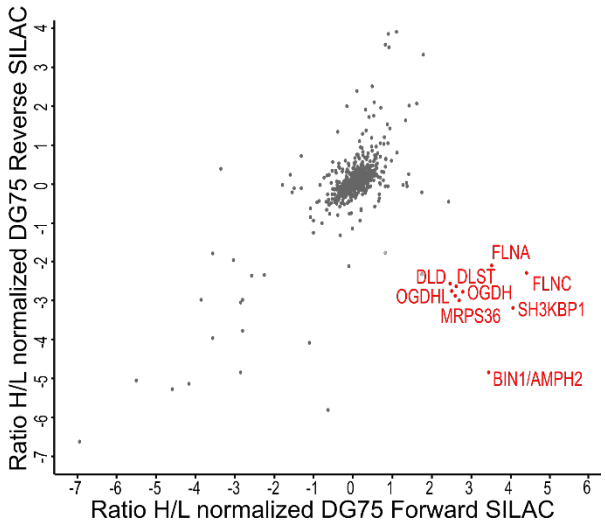

D

Ratio H/L normalized Forward SILAC	Ratio H/L normalized Reverse SILAC	No. Of Peptides	Gene name	Protein ID	Protein name
3.443076	-4.845391	10	BIN1	B7Z6Y2	Myc box-dependent-interacting protein 1
4.05693	-3.18128	2	SH3KBP1	B7Z6E8	SH3 domain-containing kinase-binding protein 1
4.399035	-2.289263	37	FLNC	Q14315-3	Filamin-C
3.513112	-2.09068	34	FLNA	Q5HY54	Filamin-A
2.688941	-3.003351	7	MRPS36P2	P82909	28S ribosomal protein S36, mitochondrial
2.782387	-2.765033	88	OGDH	Q02218	2-oxoglutarate dehydrogenase, mitochondrial
2.616169	-2.635047	42	DLST	A0A024R6C9	Dihydrolipoamide S-succinyltransferase
2.456885	-2.572351	43	DLD	A0A024R713	Dihydrolipoamide dehydrogenase
2.590937	-2.883422	78	OGDHL	Q9ULD0	2-oxoglutarate dehydrogenase-like, mitochondrial

Figure 22: Interaction partners of the central proline/arginine motif of SLP65 in human DG75 B cells. The scatter plot represents the values of 'heavy' versus 'light' ratio of enrichment (H/L) of the identified and quantified proteins, plotted against their intensity measured in the mass spectrometer. These values are plotted on logarithmic scales in the forward SILAC-labeling experiment **(A)** and the Reverse SILAC-labeling

experiment **(B)** respectively. Proteins with a normalized H/L ratio of about 2.0-fold or greater in the forward labeling-experiment and about -2 or smaller in the reverse labeling-experiment are highlighted with their gene names. Identified proteins significant only in forward SILAC-labeling experiment are highlighted in blue, those identified and significant only in reverse SILAC-labeling experiment are highlighted in green and the identified proteins satisfying significance requirements in both forward and reverse pull-down experiments are highlighted in red**. (C)** The results from the forward and reverse pull-down approaches are combined and the identified proteins fulfilling significance requirements in both the approaches are highlighted in red with their gene names. **(D)** Proteins highlighted in (C) are represented in tabular format with values for normalized H/L ratio, number of peptides, gene name, protein ID and protein name. The mass spectrometry analyses and preliminary data processing was done in collaboration with the Proteomics Core Facility of University Medicine Göttingen.

Finally, the figure 21, D, illustrates the experimental scheme used for purification, detection and subsequent analyses of the binding partners. Forward and reverse pull-down approaches for the comparative analyses of the ligands binding to the biotinylated peptides was adopted In the forward pull down experiment, the binding proficient test peptides were immobilized on streptavidin beads and incubated with the lysate from DG75 CIN85/CD2AP-dKO cells or IIA1.6 CIN85/CD2AP-dKO cells metabolically labelled with heavy amino acids after being cultured in the heavy SILAC medium. For control, the binding incompetent peptides were incubated with lysate from the respective cell lines cultured in light SILAC medium. The heavy and the light purified proteins (eluates) were then mixed at a 1:1 ratio and analysed via mass spectrometry (done in collaboration with the Proteomics Core Facility of University Medical Center Göttingen).

In the reverse pull-down experiment, the test peptides were incubated with the light lysate and the control peptides are incubated with the heavy lysate. The subsequent steps for protein purification and mass-spectrometric analyses were the same as in the forward SILAC-labeling experiment. Binding candidates give large H/L enrichment values in the forward experiment and small H/L enrichment ratios in the reverse experiment. Therefore, combined together, the forward and reverse labeling approaches can provide more reliable quantification results.

I considered the proteins that satisfied significance conditions and presented a 2.0-fold and higher enrichment ratio in the forward SILAC labeling approaches and proteins that presented a -2.0-fold and smaller enrichment ratio values in the case of reverse SILAC labeling approach. The results of the mass spectrometry analyses are presented in the figure 22 for DG75 cells and figure 23 for the IIA1.6 cells respectively.

A

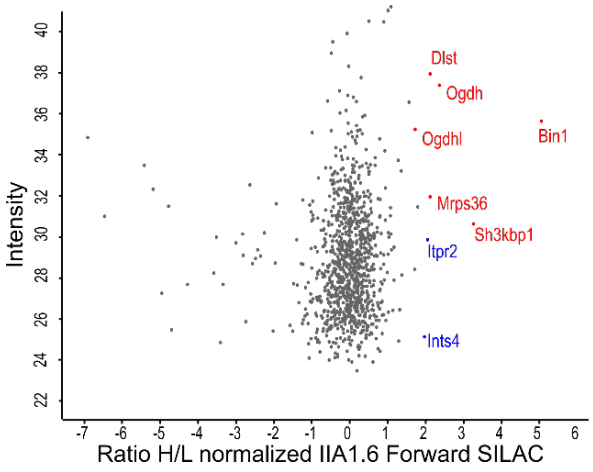

B

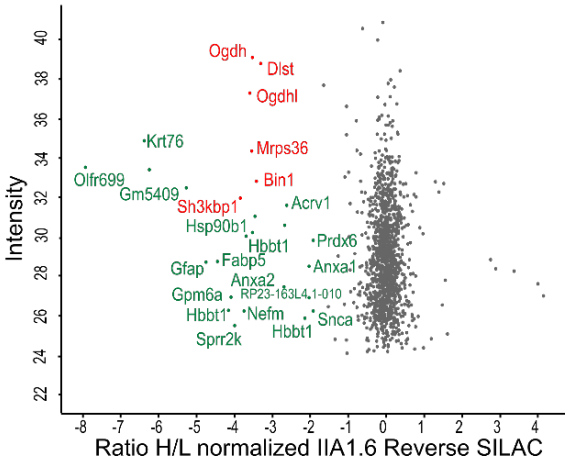

C

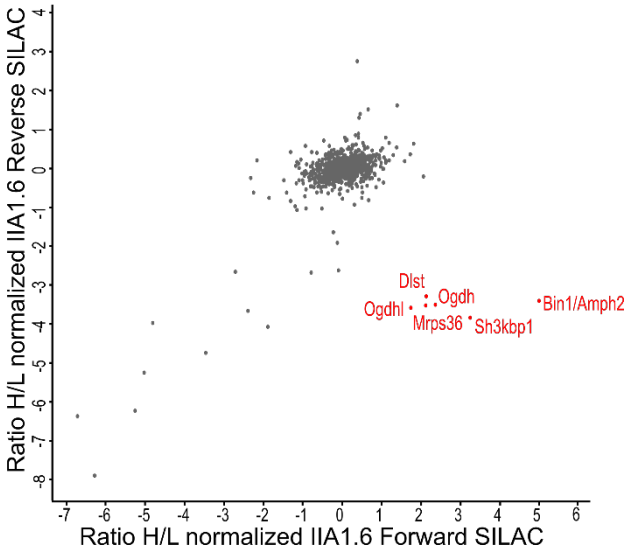

D

Ratio H/L normalized Forward SILAC	Ratio H/L normalized Reverse SILAC	No. Of Peptides	Gene name	Protein ID	Protein name
5.01556	-3.393107	25	Bin1	Q6P1B9	Myc box-dependent-interacting protein 1
3.251643	-3.824208	27	Sh3kbp1	Q3TA88	SH3 domain-containing kinase-binding protein 1
2.382252	-3.500691	96	Ogdh	Q60597	2-oxoglutarate dehydrogenase, mitochondrial
2.134024	-3.513469	4	Mrps36	Q9CQX8	28S ribosomal protein S36, mitochondrial
2.138421	-3.280685	37	Dlst	Q9D2G2	Dihydrolipoamide S-succinyltransferase
1.752577	-3.580146	86	Ogdhl	B2RXT3	Oxoglutarate dehydrogenase-like

Figure 23: Interaction partners of the central proline/arginine motif of SLP65 in murine IIA1.6 B cells. The scatter plot represents the values of 'heavy' versus 'light' ratio of enrichment (H/L) of the identified and

quantified proteins, plotted against their intensity measured in the mass spectrometer. These values are plotted on logarithmic scales in the forward SILAC-labeling experiment **(A)** and the Reverse SILAC-labeling experiment **(B)** respectively. Proteins with a normalized H/L ratio of about 2.0-fold or greater in the forward labeling-experiment and about -2 or smaller in the reverse labeling-experiment are highlighted with their gene names. Identified proteins significant only in forward SILAC-labeling experiment are highlighted in blue, those identified and significant only in reverse SILAC-labeling experiment are highlighted in green and the identified proteins satisfying significance requirements in both forward and reverse pull-down experiments are highlighted in red. **(C)** The results from the forward and reverse pull-down approaches are combined and the identified proteins fulfilling significance requirements in both the approaches are highlighted in red with their gene names. **(D)** Proteins highlighted in (C) are represented in tabular format with values for normalized H/L ratio, number of peptides, gene name, protein ID and protein name. The mass spectrometry analyses and preliminary data processing was done in collaboration with the Proteomics Core Facility of University Medicine Göttingen.

In both the cell lines, the forward and reverse labeling approaches confirmed that Amphiphysin 2 also called the Bridging integrator-1 (Bin1) was purified along with proline/arginine motif and consistently showed the highest enrichment in both the cases.

As depicted in the figures above, SH3KBP1 or CIN85 was also detected in the Mass spectrometry results, despite the cellular system created with the intention to be deficient in both CIN85 and CD2AP. There was no CD2AP detected which meant that the CRISPR/Cas-mediated deletion of CD2AP was successful. The detection of CIN85 however, indicated a remnant/residual CIN85 expression in these cells owing possibly to alternative splice variants or variants of CIN85 expressed due to the usage of alternative internal promoters, rendering isoforms of CIN85 that expressed in much smaller quantity than the more significant wild type version.

It is however, imperative to note that despite the leaky expression of this CIN85 variant, Amphiphysin 2/Bin 1 is still observed to be the more significant interaction partner owing to significantly reduced level of CIN85 expression. Amphiphysin 2/Bin 1 has been described to have an N-terminal BAR domain with a predicted coiled-coil structure and C-terminal SH3 domain (Sakamuro et al., 1996) via which it can possibly interact with the atypical proline rich motifs of SLP65.

I then attempted to validate the mass spectrometry results biochemically, by testing for the binding of Amphiphysin 2/Bin 1 to the central proline rich motif of SLP65 taking the approach of western blotting (Figure 24). I made use of the same control and test peptides as mentioned above and purified binding partners from cell lysates of both parental IIA1.6 cells and the IIA1.6 CIN85/CD2AP-dKO cells.

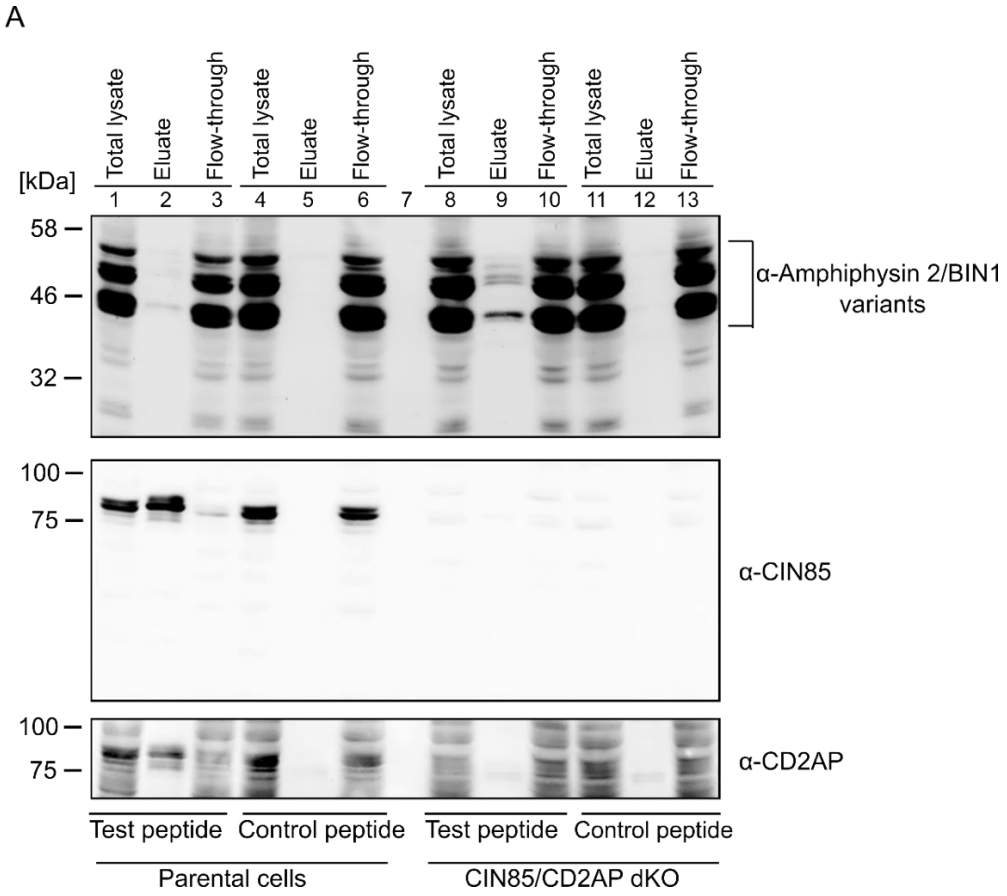

Figure 24: Amphiphysin 2 variants are capable of interacting with the isolated central proline rich motif of SLP65. Parental mouse IIA1.6 B cells or IIA1.6 CIN85/CD2AP-dKO cells were lysed and subjected to affinity purification experiments with the test or the control peptides. Obtained proteins were analyzed by immunoblotting with antibodies directed against Amphiphysin 2, CIN85 and CD2AP.

The prominent bands seen on the blot for the eluate for binding proficient peptide treated with the dKO cell-lysate confirmed this interaction. Moreover, relatively faint bands seen in the eluate lane for the test peptide treated with the paternal cells' lysate indicate a competition of Amphiphysin 2 for the same binding site with the adaptor proteins CIN85 and CD2AP, such that, CIN85 and CD2AP are the significantly stronger interaction partners. The significance of these findings, in context of the structural properties of Amphiphysin 2 has been further discussed in chapter 3.

2.3 SLP65 and CIN85 micro-clusters phase separate into signaling competent complexes

In the previous sections, it was established that CIN85 is capable of reducing the stimulation threshold for BCR-mediated Ca^{2+} signaling in human and mouse B cells. Moreover, comparative Ca^{2+} flux analyses of the CIN85-deficient B cells transfected with either wild type-CIN85 or the ΔCC-deletion mutant of CIN85 indicated that the effector functions of the CIN85 protein emanate from its C-terminal coiled-coil domain. This is in conjunction with the previously established findings by our department, where it was shown that the intracellular localization directed simultaneously but independently by both CIN85 interaction and the N terminus of SLP65 is essential for SLP65 function in B cells (Engelke et al. 2014). This revealed a two-fold regulation mechanism deployed to carefully control the SLP65 activation. We were interested in exploring these facets further:

2.3.1 Introduction to phase separation: SLP65-CIN85 interaction mediates the liquid-liquid phase-separation of the two proteins *in vitro*

During the course of our collaboration with the Prof. Griesinger's group, we tried to understand the underlying biophysical mechanism for CIN85-mediated multimerization based micro-clusters of SLP65. It was seen that when SLP65 and CIN85 are mixed in equimolar concentrations *in vitro*, they reorganise into tiny phase-separated droplets.

Following were some of the fascinating *in vitro* observations made (Figure 25 and Figure 26), I went on to work with genetic culture systems that allowed mutational analyses to test if these observations also held true in live cells, connecting the ability of phase separation with the signaling capacity in B cells.

In the *in vitro* analyses it was found that the concentration threshold for this phase separation was governed by the trimerization capacity of CIN85 and the presence of lipid vesicles. SLP65 underwent phase-separation with the $CIN85_{1-333}$ construct lacking its C-terminal coiled-coil domain, hence monomeric, at and above 60 μM concentration of both proteins

(Figure 25, A). The concentration for phase separation was reduced to 10 μM when SLP65 was mixed with the CIN85$_{\Delta 57}$ construct, lacking a 57 amino acid segment in the middle but capable of efficient Ca^{2+} mobilization. Finally, it was seen that the threshold concentration for phase-separation is reduced even further when small unilamellar vesicles (SUVs) were added to the SLP65-CIN85 mixture (Figure 25, C).

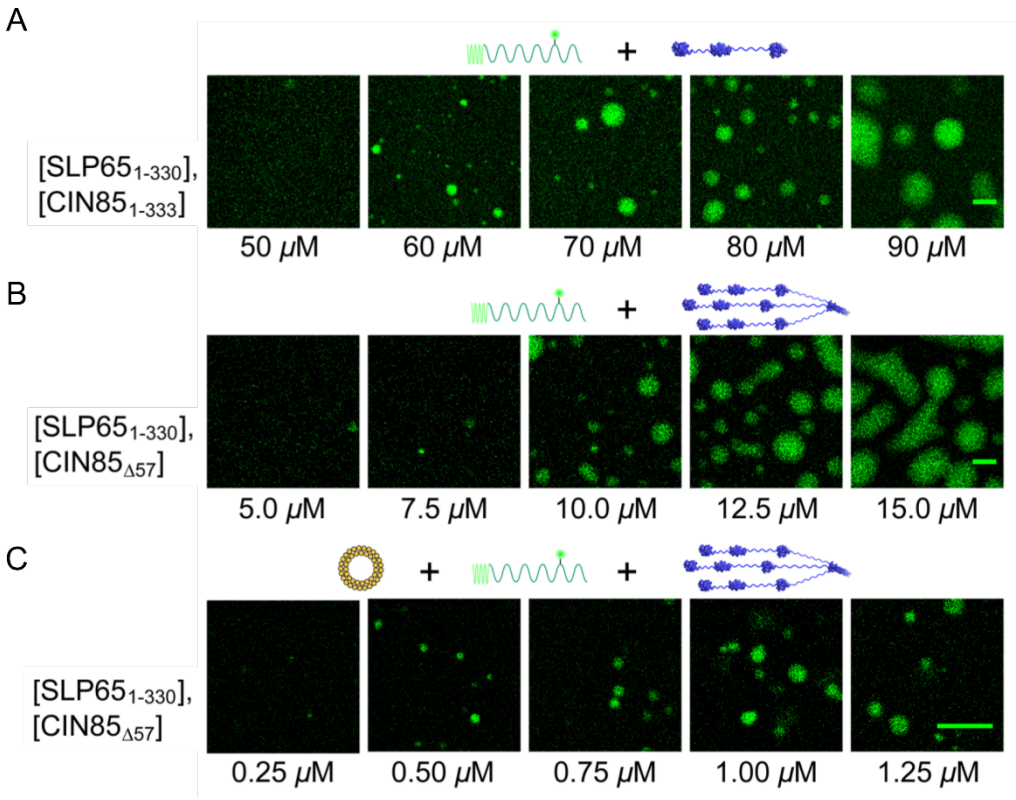

Figure 25: Phase separation of SLP65 with CIN85 and SUVs. A mixture of varying concentrations of Atto 430LS-tagged SLP65 molecule encompassing the N-terminus and the proline rich motifs with the equal concentrations of either **(A)** CIN85$_{1-333}$ i.e. CIN85 lacking the C-terminus, **(B)** CIN85$_{\Delta 57}$, or **(C)** CIN85$_{\Delta 57}$ and 1 mM of SUVs was observed under the confocal microscope. Concentrations of CIN85$_{\Delta 57}$ refer to the monomeric concentration. Figure provided by Dr. Leo Wong.

What was striking was that the concentration for this phase-separation i.e. 0.5 µM is similar to the physiological concentrations of SLP65 and CIN85 inside the DG75 human B cells (data not shown). This gave us the hint that SLP65 and CIN85 could coalesce into liquid-liquid phase-separated droplets inside the cells creating membrane-less compartments that serve to promote biochemical reactions for signaling.

The results in previous section showcased that the presence of SUVs significantly reduced the threshold concentrations such that SLP65 and CIN85 could phase separate at physiological concentrations. It was thus interesting to explore if the vesicles were a part of these phase separated droplets. For this, cryo-electron tomography studies were conducted in collaboration with Dr. Philipp Erdmann at the Max Planck Institute in Munich. The technique involved vitrification of the phase-separated droplets to faithfully preserve the molecular structures and the subsequent three-dimensional imaging by electron tomography. This shed light at the molecular assembly of the various components of the droplets.

A B

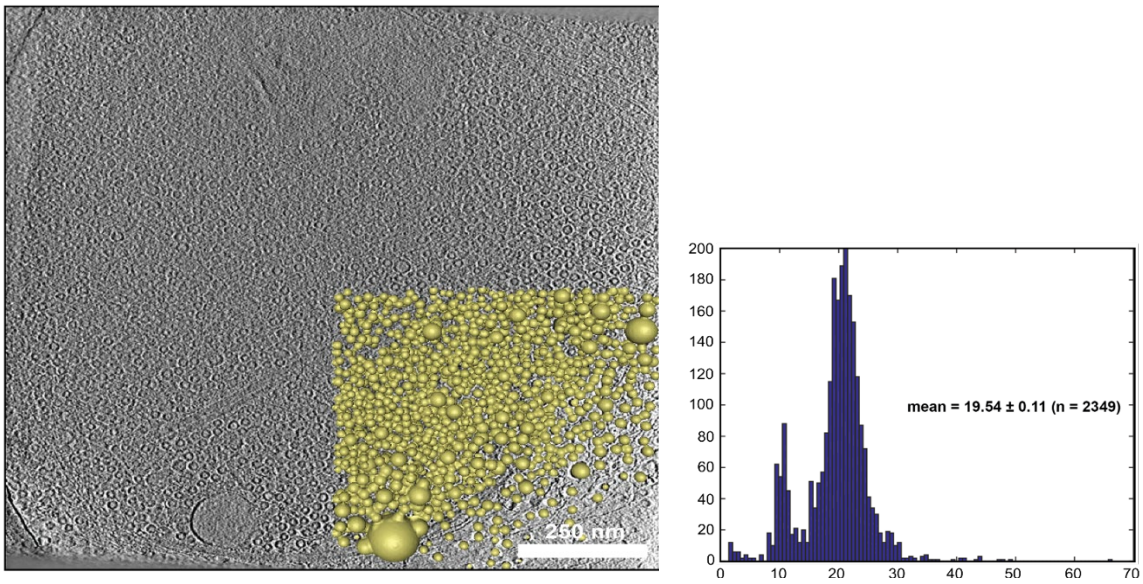

Figure 26: Vesicles are present in the phase-separated SLP65-CIN85 droplets in vitro indicating a tripartite phase-separation. (A) Cryo-electron tomograph of the droplets A mixture of 1 μM of SLP65 and 1 μM of CIN85$_{\Delta 57}$ together with 1 mM of SUVs was placed on a carbon grid and plunged frozen and subjected to Cryo-ET analyses. The cryo-tomogram represents a droplet and in yellow is the 3D rendering of the vesicles **(B)** Histogram depicts the distances between vesicles. The most populated distance is at 22 nm, the average is at 19.5 nm ± 0.1 nm. Figure provided by Dr. Philipp Erdmann.

The tomograms showed vesicles distributed inside the phase-separated droplets (Figure 26, A) with the average distance between the vesicles being 22nm (Figure 26, B). Interestingly, the vesicle concentration dropped at the periphery of the phase-separated droplets indicating that

indeed, the phase separation *in vitro* is tripartite, involving CIN85, SLP65 and the vesicles. To test if a similar model of tripartite phase-separation holds true for signaling elements inside B cells, such that the phase-separated SLP65, CIN85 and cellular vesicles constitute a functional module for B cell signaling, I used the CIN85-deficient DG75 and IIA1.6 B cells transduced with citrine-tagged CIN85 and the samples are currently in the process of being subjected to similar cryo-ET based studies.

2.3.2 Replacing the N-terminus of SLP65 with CIN85-CC circumvents the need for SLP65 vesicle targeting and interaction with CIN85

As previously mentioned, B cells deploy a dual mechanism to regulate the SLP65 function. N-terminally truncated SLP65 is unable to undergo membrane translocation and shows abrogated Ca^{2+} mobilization upon BCR-mediated B cell activation (Engelke et al. 2014). On the other hand, preventing the interaction between SLP65 and CIN85 by destroying the CIN85-SH3 domain docking proline rick motifs (PRMs) on SLP65 in turn increases the threshold for antigen stimulation to elicit an appropriate Ca^{2+} response (Kühn J., 2015).

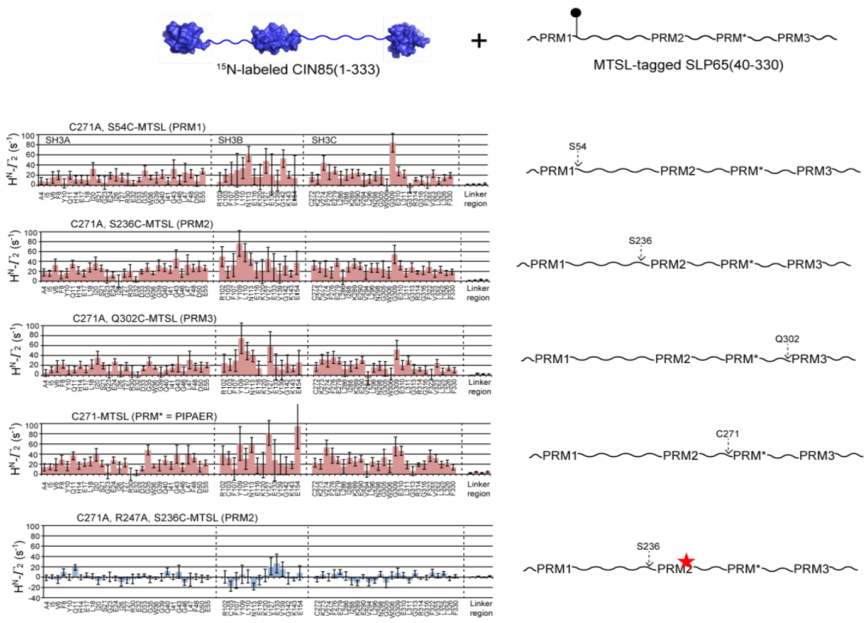

Figure 27: CIN85 SH3 domains bind promiscuously to SLP65. Paramagnetic relaxation enhancement (PRE) of the assigned 3 SH3 domains of CIN85 induced by SLP65(40-330) spin labelled at the indicated positions. The PRE-profiles show the promiscuous binding of the three SH3 domains to the four proline-rich motifs for (PRMs) of SLP65. Figure provided by Dr. Leo Wong.

In the experiments thus far, SLP65 was thought to interact with CIN85 through PRM1,2 and 3 individually (refer Figure 3 in introduction), of which the PRM 2 and 3 have been the critical players (Oellerich et al. 2011; Kühn et al. 2016). However, recently, Leo Wong in Prof. Griesinger's group established, by spin label-assisted paramagnetic relaxation enhancement, that the SH3 domains of CIN85 individually bind to four and not just three (as previously thought) proline-rich motifs (PRMs) of SLP65 in a promiscuous manner (Figure 27). Additionally, a variant of SLP65 where the coiled-coil domain of CIN85 replaces the N-terminus of SLP65 molecule in which all four CIN85 binding sites (PRM1, PRM2, PRM3 and PRM4) were disrupted was incapable of mediating phase-separation *in vitro*. Similar construct with two out of the four CIN85 binding sites disrupted (PRM2 and PRM3) however, showed wild type levels of Ca^{2+} signaling. This hinted to the possibility that perhaps the robust Ca^{2+} phenotype in cells expressing this chimera, initially thought to constitute the minimal-transducer-module for Ca^{2+} mobilization in B cells (Kühn et al. 2016), was possibly a result of remnant CIN85 interaction and hence left-over multimerization executed by the 4^{th} recently explained unmutated PRM.

To lay these speculations to rest, I created CIN85CC-ΔNSLP651,2,3,4 (R-A) variant with all the four CIN85 interaction sites mutated and transduced SLP65-deficient DT40 cells with it. I additionally expressed SLP65-wt and CIN85CC-dNSLP652,3(R-A) in SLP65-deficient cells as controls. SLP65-deficient DT40 cells were transfected with these SLP65-CIN85 chimeras as portrayed in figure 28, A. Both the constructs, one with two out four CIN85 interaction sites disrupted and the other with all four CIN85 interaction sites disrupted showed Ca^{2+} influx comparable to the SLP65-wt construct upon BCR-stimulation (Figure 28, B). Additionally, while the fluorescent speckles in resting cells were more prominent and bigger for SLP65-wt construct, the other two constructs were capable of undergoing BCR-stimulation induced plasma membrane recruitment much like SLP65-wt. This revealed a dominating role for the CIN85-CC whose presence in a SLP65 molecule lacking its N-terminus and all known CIN85 interaction sites was indeed sufficient to phenocopy the Ca^{2+} influx of the wild type protein. This also highlights the fact that the fourth PRM does not play a more governing role over PRM2 and PRM3 combined for CIN85 interaction for proper SLP65 functioning.

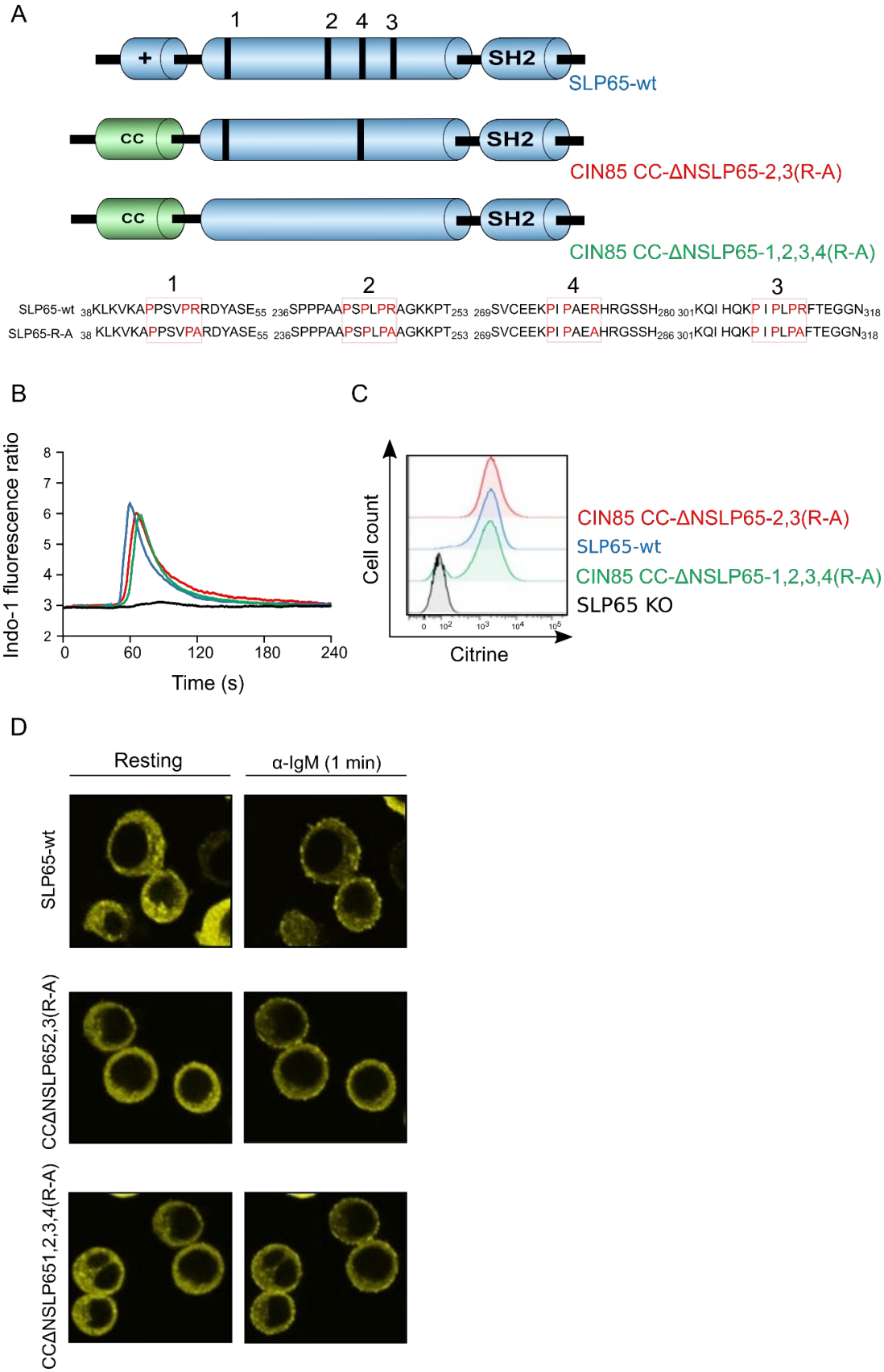

Figure 28: Oligomerization-mediated by the CIN85-CC functionally substitutes SLP65 N-terminus and complete CIN85 interaction.

(A) Slp65-deficient DT40 cells were transduced with citrine-tagged SLP65-wt or the chimeric proteins depicted. Numbers 1,2,3 and 4 depict the individual PRMs with the respective protein sequence of each mentioned below the domain architecture of the protein. The C-terminus coiled-coil domain of CIN85 was fused either to SLP65-dN-2,3(R-A) variant (red line) or the SLP65-dN-1,2,3,4(R-A) variant (green line). **(B)** The Ca^{2+} influx in transduced citrine positive cells upon stimulation with 1µg/ml α-chicken IgM $F(ab')_2$ was monitored by flow cytometry. **(C)** The histograms confirm similar expression levels of various fusion proteins in the respective cell populations. **(D)** Intracellular localization and membrane recruitment of the chimeric proteins 1min after stimulation (2µg/ml α-chicken IgM $F(ab')_2$) was observed by confocal microscopy.

2.3.3 Equipping SLP76 with oligomerizing capacity can enable it to participate in Ca^{2+} signaling cascade in B cells

SLP76 is the T cell paralog of SLP65 in which CIN85 binding sites are entirely absent. When expressed in DT40 cells lacking endogenous SLP65 it is incapable of organizing the calcium initiation complex and therefore, unable to promote calcium mobilization. In addition, unlike SLP65, it does not get recruited to the plasma membrane on activation of B cells (Kühn et al., 2016). This shows that wild type SLP76 is incapable of functionally substituting SLP65 in B cells. Interestingly, on introduction of CIN85 binding sites inherent in SLP65 into SLP76, the modified SLP76 variant successfully conducts calcium mobilization (Oellerich et al., 2011). To test if mere oligomerization of SLP76-mediated in the absence of CIN85 interaction is enough to provide it with functions similar to SLP65 in B cells, I worked with SLP76 variants fused with the split Venus protein.

Split Venus is eminently deployed in Bimolecular fluorescence complementation (BiFC) experiments to study protein-protein interactions. The two halves VN and VC undergo covalent interaction when in spatial proximity and regain a conformation that can emit a fluorescence signal. I transduced the constructs VN-SLP76 and VC-SLP76 (Figure 29, A) created by Julius Kühn either individually or simultaneously in SLP65-deficient DT40 cells and monitored the BCR-mediated Ca^{2+} influx in the transduced cells. This revealed that a VN-SLP76 – VC-SLP76 dimer enabled Ca^{2+} influx comparable to SLP65-wt (Figure 29, B). The dimerised SLP76 construct are seen as speckles in the resting cells which get recruited to the plasma membrane albeit poorly upon B cell stimulation (Figure 29, C). These results indicate that the local enrichment of SLP65 or SLP76 proteins mediated either by the CC-domain's oligomerization capacity or the dimerization property of the split Venus

protein dispenses the necessity for direct CIN85 interaction of these proteins for Ca^{2+} mobilization.

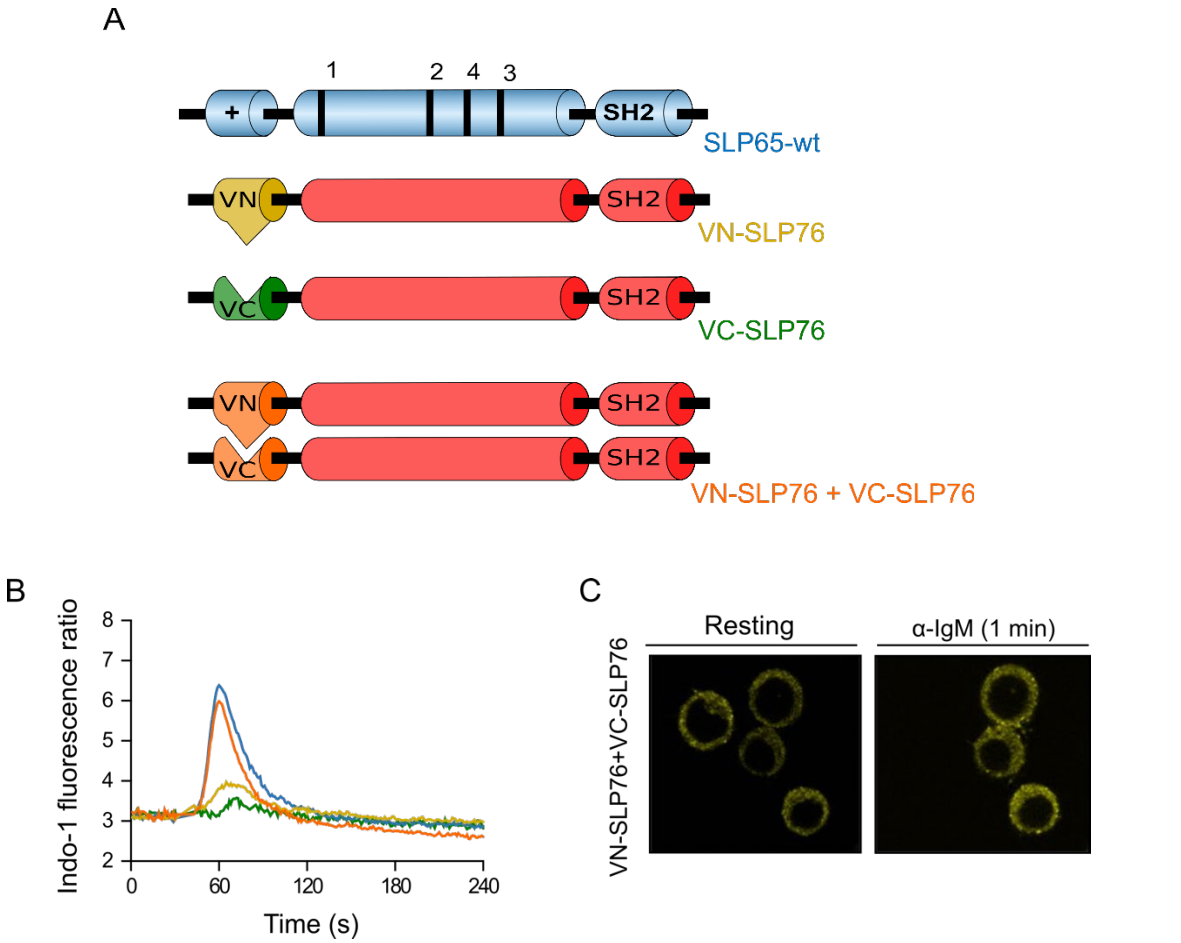

Figure 29: Dimerization confers SLP76 with the ability to function similar to SLP65. (A) Slp65-deficient DT40 cells were transduced with citrine-tagged SLP65-wt or SLP76 protein fused to parts of the Venus protein as depicted. VN-SLP76 and VC-SLP76 were transduced individually (yellow and green line) or simultaneously (orange line). **(B)** The Ca^{2+} influx in transduced cells upon stimulation with 2µg/ml α-chicken IgM F(ab´)2 was monitored by flow cytometry. **(C)** For cells expressing VN-SLP76 and VC-SLP76 simultaneously, intracellular localization and membrane recruitment 1min after BCR stimulation (2µg/ml α-chicken IgM F(ab´)2) was observed by confocal microscopy. The Venus fused SLP76 constructs were kindly provided by Dr. Julius Kühn.

2.3.4 Preventing multimerization of CIN85 impedes Ca^{2+} signaling in B cells

Building further on the knowledge of the necessity of CIN85 interaction for SLP65 to conduct Ca^{2+} mobilization, I created a set-up to be able to corroborate the previous findings but approaching the question from the side of CIN85 this time, instead of SLP65. As mentioned in the previous sections, experiments with the minimal-BCR-transducer element

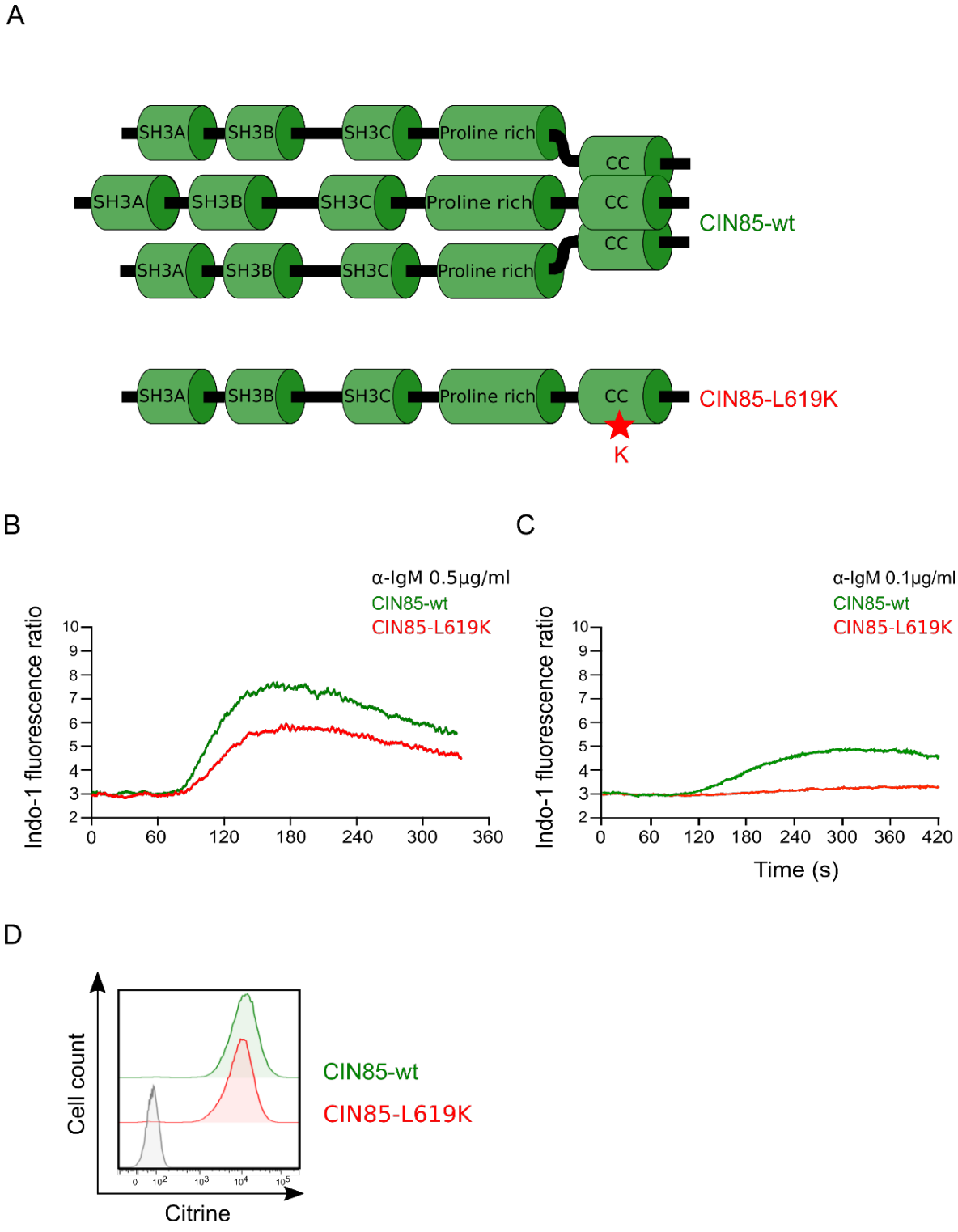

Figure 30: L619K mutation disrupts the multimerization of CIN85 and abolishes the support it provides SLP65 for its function. (A) CIN85/CD2AP-dKO DG75 cells were transduced with citrine-tagged CIN85-wt (green line) or the L619K mutant (red line) as depicted. **(B)** The Ca^{2+} influx in transduced citrine positive cells upon stimulation with 0.5 µg/ml α-human IgM F(ab´)$_2$ or **(C)** 0.1µg/ml α-human IgM F(ab´)$_2$ was monitored by flow cytometry. **(D)** The histograms confirm similar expression levels of the two citrine-tagged proteins in the respective cell populations.

represented by CIN85-CC-SLP65 fusion proteins have established that CIN85 supports SLP65-function in Ca^{2+} mobilization owing to its C-terminal effector domain. In the experiments conducted by Dr. Leo Wong and Dr. Stefan Becker, it was shown, through Multiangle laser light scattering and NMR spectroscopy experiments, that this C-terminal effector domain of CIN85 forms a coiled-coil trimer of high stability (Kühn et al., 2016). In the same study, NMR analysis showed that the position of Leu^{619} at the hydrophobic interface in the coiled-coil domain is critical for the stability of coiled-coil such that on replacing the hydrophobic residue Leu^{619} with the hydrophilic residue lysine, the trimerization gets disrupted. The Mass spectrometric analysis of the recombinant CIN85 L619K confirm this as this variant is exclusively monomeric in vitro (Kühn et al., 2016).

I mimicked this mutation into the CIN85-wt construct to create a modified CIN85-L619K variant and transduced the constructs into CIN85/CD2AP-double deficient DG75 cells that I had created previously, as explained in section 1.1 (Figure 30, A). After confirming similar protein expression levels for the wild type and L619K-variant of CIN85(Figure 30, D), I analyzed the Ca^{2+} influx in these cells upon stimulation with 0.5µg/ml α-human IgM $F(ab')_2$ and 0.1µg/ml α-human IgM $F(ab')_2$ concentrations (Figure 30, B-C) respectively. The Ca^{2+} influx mediated by the CIN85 variant harbouring the L619K mutation was significantly impaired in conducting Ca^{2+} mobilization compared to CIN85-wt at higher stimulating antigen concentration (Figure 30, B) and is almost incapable of Ca^{2+} signaling at lower stimulating antigen fragment concentration (Figure 30, C).

This corroborates the structural studies of the coiled-coiled domain of CIN85 thus far and underscores the functional significance of this critical amino acid for ensuring CIN85-mediated support to SLP65 to promote BCR-mediated Ca^{2+} mobilization in B cells.

2.3.5 A crucial balance between the affinity and the functional avidity of SLP65-CIN85 interaction sites reigns the Ca^{2+} signaling in B cells.

After mutational analyses directed towards loss of function of CIN85/SLP65 complexes, we focussed on strategies that could possibly enhance their function. A series of previous experiments revealed that the PRM2 independently executes primary SLP65-CIN85 interaction compared to the other PRMs which contribute to the avidity of interaction with

a reduced affinity (Oellerich et al., 2011). We were therefore curious to test the function of a SLP65 variant with majority of its PRMs exchanged for the PRM2 resulting in a "super-interactor" SLP65 such that the individual PRMs interacted with individual SH3 domains of CIN85 with a much greater affinity. For this, I transduced SLP65-deficient DT40 cells with both the SLP65-wt and SLP65-3XPRM2 variant, as depicted (Figure 31, A), and monitored the Ca^{2+} mobilization upon B cell stimulation (Figure 31, B). The 3XPRM2 variant of SLP65 showed a significantly reduced Ca^{2+} signaling capacity compared to SLP65-wt even though the histograms (Figure 31, B-C) and the western blot analyses (Figure 34, F) point toward a slightly higher expression level of this protein in the cells compared to SLP65-wt. The difference in Ca^{2+} flux levels is notably more prominent at lower stimulating antigen concentrations (Figure 31, C). Additionally, the fluorescent speckles in the resting cells are much more prominent for SLP65-wt which in turn get strongly recruited to the plasma membrane upon BCR-mediated stimulation of the cells. This is in stark contrast to the SLP65-3XPRM2 which is homogenously distributed in the cytosol evidently depicting a lack of ability to undergo multimerization induced clustering. On stimulation of the cells, this construct shows little to no translocation to the plasma membrane (Figure 31, E). Finally, I measured the extent of phosphorylation of the two SLP65 constructs upon stimulation of the cells over the course of 10 mins. Despite higher expression level of SLP65-3XPRM2, this variant shows reduced phosphorylation levels, especially at 5 mins time point and almost no phosphorylation after 10 mins of stimulation. I used two α-SLP65 antibody clones to detect the total SLP65 expression level in the respective cell populations due to their capacity to recognize different epitopes. The D8R3G antibody binds an epitope in the C-terminal domain of SLP65 and thus equally recognizes SLP65-wt and SLP65-3XPRM2 without any bias. However, D3P2H antibody recognizes residues around Arg282 of wild type SLP65 i.e. residues surrounding the PRM4 in the SLP65-wt (refer sequences mentioned in figure 31, A) which was now exchanged for the PRM2 in SLP65-3XPRM2 construct. The inability of this antibody to detect SLP65-3XPRM2 with sufficient efficiency thus served as a control to confirm expression of the mutated variant of SLP65.

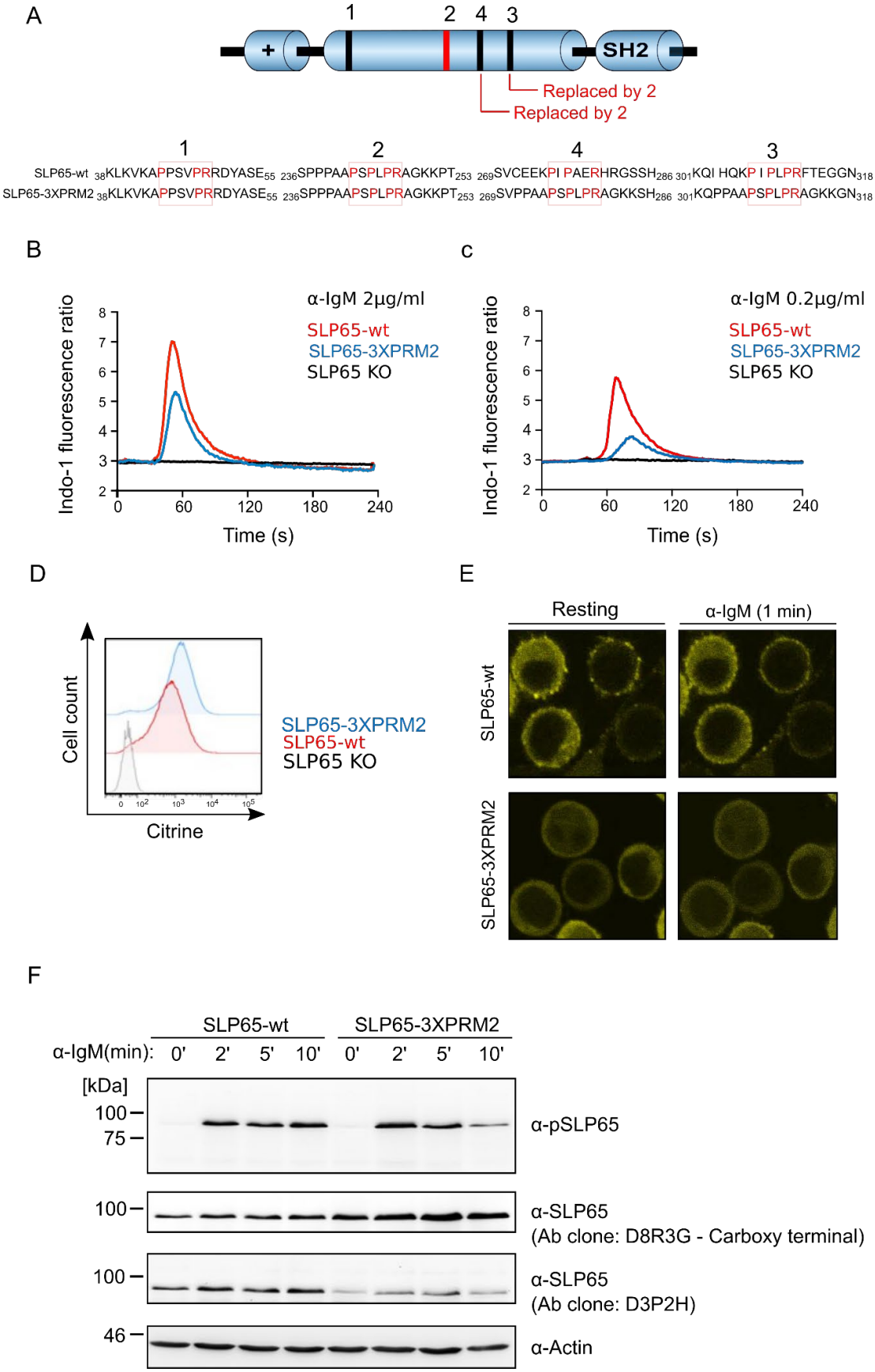

Figure 31: Increasing the affinity of the individual PRM-SH3 domain interactions reduces the signaling capacity of SLP65.

(A) SLP65-deficient DT40 cells were transduced with citrine-tagged SLP65-wt (red line) or a variant with PRM3 and PRM4 exchanged for the PRM2 (blue line). Numbers 1,2,3 and 4 depict the individual PRMs with the respective protein sequence of each mentioned below the domain architecture of the protein. The Ca^{2+} influx in transduced citrine positive cells upon stimulation with **(B)** 2µg/ml or **(C)** 0.2µg/ml α-chicken IgM F(ab´)2 was monitored by flow cytometry. Un-transduced SLP65-deficient cells served as the negative control. **(D)** The histograms indicate the expression levels of citrine-tagged wild type and 3XPRM2-variant SLP65 fusion proteins in the respective cell populations. **(E)** Intracellular localization and membrane recruitment of the SLP65 proteins 1min after stimulation (2µg/ml α-chicken IgM F(ab´)2) was observed by confocal microscopy. **(F)** Cell lysates were prepared after stimulation of SLP65-wt and SLP65-3XPRM2 expressing DT40 cells with 2µg/ml α-chicken IgM F(ab´)2. SLP65 phosphorylation was analyzed by SDS-PAGE and immunoblot analyses with antibodies against phospho-SLP65 (pSLP65). Total SLP65 was detected using two different α-SLP65 antibody clones: D8R3G which binds an epitope in the C-terminal domain of wild type-SLP65 and D3P2H which recognizes residues around Arg282 of wild type-SLP65.

2.3.6 Deletion of a 57-amino acid segment in the PRR of CIN85 does not affect the amplitude of Ca^{2+} flux in B cells

In the previous section, the reason why the phase-separation studies were performed with the $CIN85_{\Delta 57}$ construct was the difficulty in procuring large quantities of the recombinant full length-CIN85 protein. This meant that, although $CIN85_{\Delta 57}$ provided technical convenience, it did not represent a true physiological picture in terms of CIN85 structure. Therefore, as a contribution to the above-mentioned studies, and equipped with a CIN85 knock-out cell lines, I set out to test the functional capabilities of the Δ57-variant of CIN85 compared to its full-length counterpart. I created a CIN85 construct lacking 57 amino acids in the PRR, starting at residue 369 (mimicking the construct used for phase-separation studies) and transduced the construct into the CIN85-deficient DG75 cells (Figure 32, A). Additionally, the CIN85-deficient cells, and the cells expressing CIN85-wt, CIN85-ΔCC, or the EGFP mock served as important controls. The expression of the CIN85 variants and CD2AP in these cells was confirmed by immunoblot studies (Figure 32, B). Subsequently, I analyzed the Ca^{2+} flux in these cells upon BCR-mediated stimulation (Figure 32, B). The Ca^{2+} flux in the cells expressing CIN85-Δ57 and CIN85-wt was higher compared to the controls, with the CIN85-Δ57 variant even appearing to be better than CIN85-wt at conducting Ca^{2+} mobilization. This could however be explained by the differences in the expression levels of the two citrine-tagged proteins as seen in figure 32, D with the cells expressing CIN85-wt showcasing a rather broad range of citrine signal profile with more cells expressing comparatively lower levels of CIN85-wt. This helped in confirming that the CIN85-Δ57 that was used for performing most *in vitro* phase-separation studies was indeed

functional in B cells and reduced the scepticism with regard to the biological function of this protein.

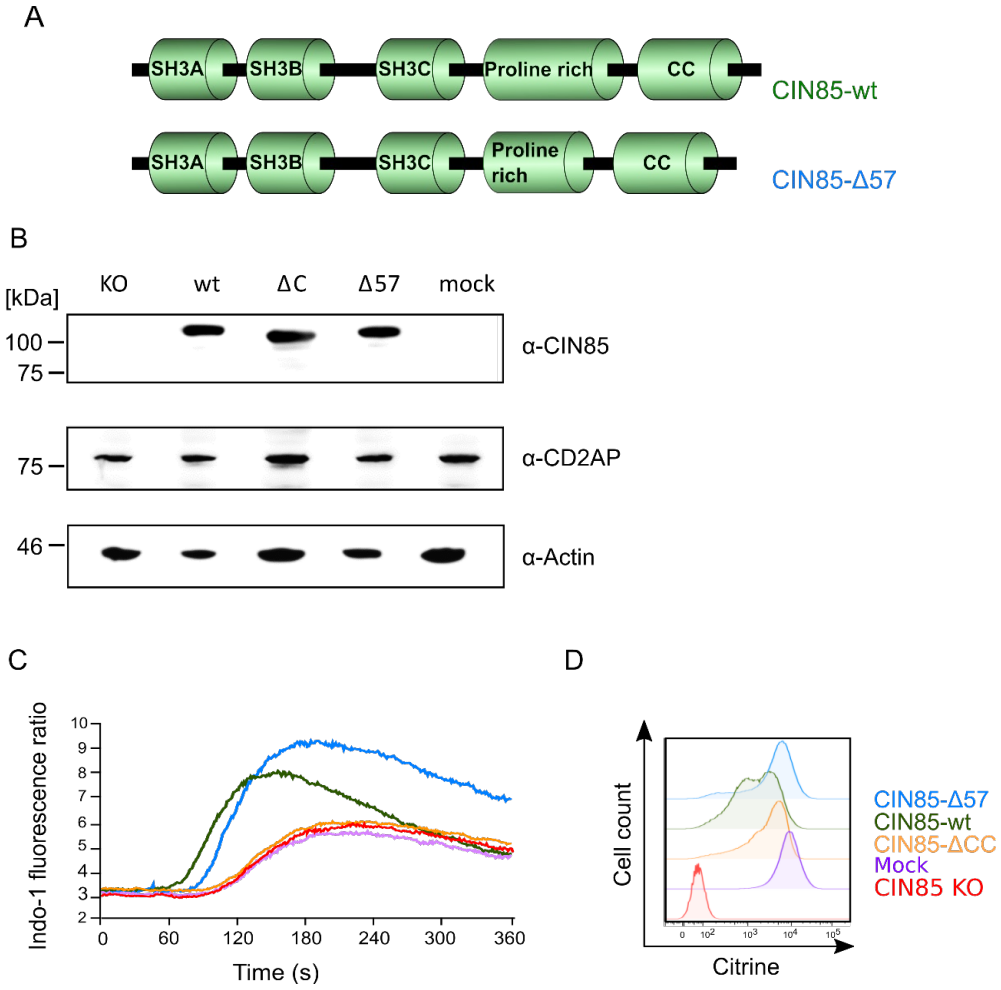

Figure 32: CIN85 lacking a 57-amino acid fragment in its PRR can conduct Ca^{2+} mobilization. (A) CIN85-deficient DG75 cells were transduced with citrine-tagged CIN85-wt (green line) or a variant lacking 57 amino acids starting at residue 369 (blue line) as depicted. **(B)** Cell lysates were prepared from DG75 cells either lacking CIN85 (KO), or expressing the following: wild type CIN85 (wt), ΔCC deletion mutant (ΔC), Δ57-variant of CIN85 (Δ57) or EGFP mock. Expression levels of CIN85 and CD2AP were analyzed by SDS-PAGE and the subsequent staining of the immunoblot with antibodies against the respective proteins. **(C)** The Ca^{2+} influx in the above-mentioned transduced citrine positive cell populations was monitored by flowcytometry upon stimulation with 0.5µg/ml α-human IgM F(ab´)2. **(D)** The histograms depict the expression levels of the various fusion proteins and the EGFP mock in the respective cell populations.

Chapter 3: Discussion

As per the basic understanding, the activation of B cells forms an integral part of an individual's capacity to mount a functional humoral response against invading pathogens, the hallmark of adaptive immunity. There are several factors controlling the intensity and the onset of this response. The chief aspects are the manner in which signals are transduced by the B cell antigen receptor and the subsequent processing of those signals by the appropriate effector systems. In my doctoral thesis, I have aimed to shed light on the contribution of the adaptor proteins CIN85 and CD2AP to the master regulator SLP65 in the process of BCR-proximal and distal signaling events.

I achieved the following objectives during the course of my work:

- Creation of CIN85-deficient and CIN85/CD2AP-double deficient human DG75 and mouse IIA1.6 sub-cell lines using the CRISPR/Cas genome engineering tool. I created a cellular model system that could facilitate the study of functional properties of these adaptor proteins in the process of BCR-mediated B cell activation.
- It was established that CIN85 lowers the stimulation threshold for BCR-mediated B cell activation i.e. it predisposes B cells to respond to lower antigen concentrations. Additionally, this positive regulation of the SLP65-mediated Ca^{2+} mobilization is a feature for both the human DG75 and mouse IIA1.6 cells.
- The influence of CIN85 to the process of PKCβ membrane localization was studied and the key observation made that the presence of CIN85 promotes PKCβ membrane recruitment.
- Amphiphysin 2/BIN 1 occupies an identical interaction module with SLP65 as do the steady interactors CIN85 and CD2AP. It thus appears as a novel SH3-domain harbouring SLP65-interaction partner, that can dock onto the atypical proline/arginine motifs on SLP65 in the absence of the significant binding companions.
- SLP65/CIN85 clusters were discerned to exist as micron sized, phase separated droplets, concentrated as part of the membrane-less signaling organelles, primed for activation upon BCR-ligation.

3.1 Not all heroes wear capes: The importance of CIN85/CD2AP adaptor proteins in BCR signaling

While SLP65 is the master regulator for BCR-signaling, via the assembly of Ca^{2+} initiation complex, it is dependent on the constitutive interaction with CIN85/CD2AP for its function. This complex encompasses a functional unit as demonstrated by the mutational analyses in cultured B cells. The importance of CIN85-SLP65 interaction for the immune system has been demonstrated by studies performed on mice harbouring B cell-specific deletion of CIN85 (Kometani et al., 2011). The patients harbouring deletion in the CIN85 encoding gene showcased varying levels of defect in their serum antibody titers which further highlighted the significance of CIN85. The primary cells pose a limitation to the scope of genetic and mechanistic analyses owing to the scarcity of cellular reserve.

For studying the signaling contribution of the adaptor proteins CIN85 and CD2AP and the mechanism of their complex formation with SLP65, it was imperative to create knock-out cell lines that could facilitate biochemical and mutational studies. Two cell lines, each from a different species were chosen, namely, the human DG75 and the mouse IIA1.6 cell line. Majority of the understanding of the BCR-signaling events stem from the studies performed in the chicken DT40 cells due to the technical advantage of having a strong grasp over the genetic system; this facilitated convenient targeted genomic modifications and subsequent analysis of phenotypes. However, DT40 being a chicken cell line, poses a disadvantage, in that the observations made fail to accurately reflect the true physiological picture of the higher order mammalian systems. Therefore, in order to investigate and mimic the patient conditions as described in section 1.3.2., the creation of cellular model systems using the abovementioned human and mouse B cell lines was undertaken.

Physiologically the most significant role of CIN85 and CD2AP adaptor proteins was discerned to be their support to SLP65 in BCR-mediated Ca^{2+} mobilization specifically at low stimulating antigen concentrations. This is of utmost significance physiologically as an early response to low antigen levels would facilitate early clearance of the pathogen, significantly reducing the risk of the pathogen-caused damage to the host.

A significant reduction in NF-κB pathway activation has been reported in several studies (Kometani et al., 2011; Oellerich et al., 2011). Similar observations could not be reported in the knock-out system generated in this study owing to several technical limitations. DG75 B cell line which is a Burkitt's lymphoma cell line exhibits a deregulated c-Myc expression which in addition to other genomic modifications aide the signaling pathways that are meant to facilitate anti-apoptotic factors like NF-kB (Nagel et al., 2014). The pathway activation axis does not involve signals transduced by the BCR as antigen stimulation had no effect on the basal levels of phosphorylated IκBα. On the other hand, IIA1.6 cells, did show stimulation dependent activation of this pathway. However, only mild differences, if any, were seen. This could be explained by the fact that more prominent defect in the serum IgM levels of the patients were reported, indicating a more prominent role of CIN85 in NF-kB activation in naïve B cells, instead of the class-switched memory B cells. IgG-BCR expressing B cells can transduce fortified signals due to the presence of a facilitating ITT motif in addition to the canonical ITAM motif, which could modulate signals transmitted for the NF-kB activation (Figure 33).

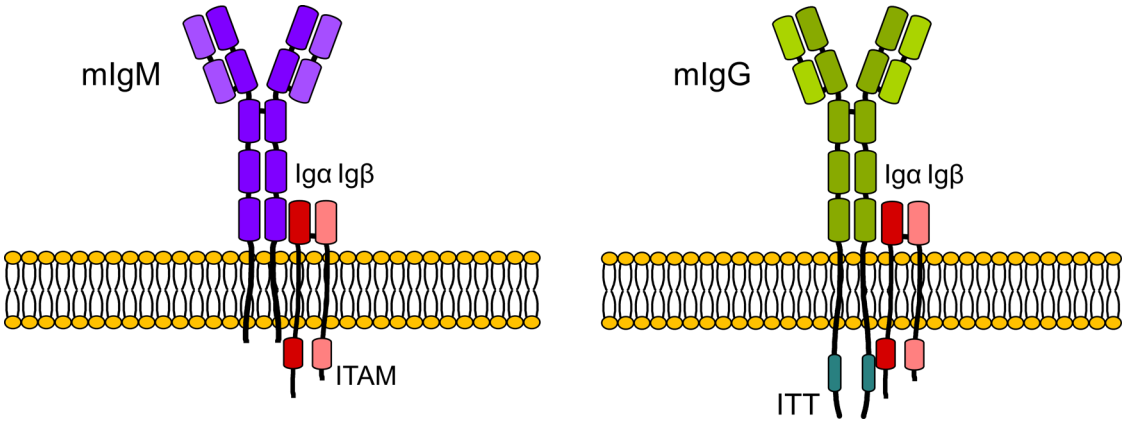

Figure 33: Human DG75 cells and the mouse IIA1.6 cells represent B cells of different developmental stages. The main signal transduction unit for the mIgM BCRs is the ITAM signaling motif that participates in canonical BCR-signaling. On the contrary the IgG BCRs on the surface of IIA1.6 cells represent class switched cells that in addition to the conventional ITAM motif are also equipped with an ITT motif to reinforce the signals that are generated from the canonical ITAM signaling.

However, the DG75 cells could be used to monitor the plasma membrane recruitment of an upstream NF-kB pathway element, PKCβ, where it was observed that the presence of CIN85 positively regulates the plasma membrane recruitment and thus the activation of this enzyme (Section 2.1.2). Additionally, mice lacking B cell-specific CIN85 expression and mice

lacking PKCβ expression exhibit similar phenotypes. PKCβ deletion resulted in low IgM and a subtype of IgG, IgG3 levels, a disturbed B1 B cell compartment and reduced T Cell dependent responses (Leitges et al., 1996).

In B lymphocytes, internalization of the BCRs is critical to a process called antigen presentation. The BCRs recognize the antigen and internalize it by endocytosis (Batista & Neuberger, 2000; Suzuki et al., 2009). Once internalized these antigens are degraded into antigenic peptides that are loaded onto major histocompatibility complex (MHC) class II molecules and presented to primed T lymphocytes (Mitchison, 2004).

CIN85 has commonly been implicated in the ligand-induced internalization of tyrosine kinases receptors by formation of a complex involving endophilins, CIN85 and Cbl (Petrelli et al., 2002; Soubeyran et al., 2002; Szymkiewicz et al., 2002). Deformation of the cell membranes and cytoskeletal remodelling is essential for cell surface receptors (Doherty & McMahon, 2009; Johannes et al., 2015). Endophilins modify membrane phospholipids and mediate invagination of the plasma membrane. Via their SH3 domains, endophilins bind the proline rich regions of CIN85. Simultaneously, CIN85 interacts with the C-terminus of Cbl which has been reported in multiple sources to be involved in receptor internalization, with Cbl mutants inhibiting this process (Lee et al., 1999; Levkowitz et al., 1999; Zeng et al., 2005; Huang et al., 2006). Stepping beyond the RTKs, it has also been established that ablation of Cbl impacts BCR endocytosis and the underlying cytoskeletal dynamics (Jacob et al., 2008). CIN85 is the cognate adaptor that interacts with Cbl and connects Cbl to the endocytic machinery.

Upon ligand-induced activation of EGF receptors, Cbl binds to phosphorylated receptors and promotes receptor ubiquitination. Cbl is also tyrosine-phosphorylated in this complex leading to translocation of CIN85/endophilin in the vicinity of active EGF receptors, whereby endophilins together with dynamin and Amphiphysin control the clathrin-mediated internalization (Dikic I., 2002)

Using the CIN85/CD2AP-double deficient cells I generated, I proceeded to test if the model for internalization of RTKs is also applicable to the BCRs on the surface of B cells. I

observed that for both human DG75 and IIA1.6 cells, the presence of CIN85 did not impact the cell surface-BCR internalization, indicating that in B cells, CIN85 possibly is not involved in the receptor internalization process. Similar reports came from studies in mice with B cell specific CIN85 ablation. Kometani et al., 2011, additionally, putting these results in context of other studies reported where BCR-downregulation is inhibited in Cbl-deficient B cells (Kitaura Y. et al., 2007), it can be interpreted that the normal BCR internalization levels in CIN85/CD2AP deficient cells is due to the fact that this process occurs in a Cbl dependent but a CIN85 independent manner. This could in turn possibly hold true because of differential signalosome participation of CIN85 where it preferentially associates with SLP65 rather than Cbl in BCR signaling context. My results nevertheless allow for the alternative possibility that CIN85 and CD2AP participate, redundantly, in BCR endocytosis.

At a cellular level, a novel strategy to monitor the impact of CIN85 on cell-viability was undertaken in a co-culture setup where the CIN85-deficient cells and cells expressing CIN85 were cultured together in the same dish under appropriate culture conditions. The respective population abundance was then monitored over time via flowcytometry. The advantage conferred by a co-culture system of this kind, was the possibility to simulate the B cell compartment of the patients' mother. The immunodeficient patients previously mentioned, carry a deletion mutation in the only *CIN85* gene which is located on the X chromosome, reportedly resulting in manifestation of the clinical symptoms. Their mother however, who is hemizygous for the gene deletion, with one healthy and one mutated allele of *CIN85*, exhibits no clinical symptoms. Taking into consideration the chromosome silencing as part of X-chromosome inactivation in females which reduces the number of actively transcribed X chromosomes to one per cell, and the fact that the inactive chromosome is randomly selected (The Lyon Hypothesis, Rédei 2008), the B cell compartment of the mother would consist of a heterogenous mixture of two cell populations: Cells expressing CIN85 and the cells that lack CIN85 expression. The co-culture system I created aimed to replicate this chimeric cellular state. Such a system could give an indication as to the survival advantage, if any, conferred upon the CIN85 expressing cells in a competitive environment.

The human DG75 and the mouse IIA1.6 cells deficient in CIN85 expression were mixed with the respective citrine-tagged CIN85 expressing counterparts in a 1:1 ratio and the differences in the cell viability monitored over time by monitoring the abundance of non-fluorescent and fluorescent cells via flowcytometry. The DG75 cells showed no difference in the rate of cell growth or viability over the time points analysed, however, for the IIA1.6 cells, there was a slight decrease in the abundance of the CIN85-negative cells after co-culturing.

These observations when studied in the context of clinical symptoms, paves the way to explore two aspects: one, the possibility that the immunodeficiency of patients correlates to the poor viability of B cells, resulting in shorter lifespans and a higher turnover which becomes especially relevant with regard to the IgG type memory B cells, represented by the IIA1.6 established cell line, indicative of B cell-developmental stage specific differences. The second aspect relates to the mixed B cell compartment of the mother/females, such that, over the years, due to a survival advantage conferred upon the wild-type CIN85 expressing B cells, this population takes over the other in making up the peripheral B cell compartment. Additional clarity could come from checking the mother's peripheral B cell populations to check for the previously mentioned heterogeneity with regard to CIN85 expression or a complete overtake by a single compartment. Also, additional measurements at time points longer than 72 hrs, might present a more accurate indication, reflective of the true physiological state in terms of the viability/growth rate differences.

3.2 Amphiphysin 2 (BIN 1): The hidden player?

In the past, the interaction studies indicated that DT40 cells expressing a variant of SLP65 incapable of interaction with CIN85 and CD2AP could not support B cell signaling. It was additionally observed that the NF-kB pathway activation was abrogated (Oellerich et al., 2011). In human DG75 B cells, the deletion of SLP65 rendered the cells completely incapable of mounting a Ca^{2+} response (Schulz K., 2016).

Upon simulating a similar absence of interaction, while approaching with the absence of CIN85 and CD2AP the results were confounding. While the presence of CIN85 significantly

improves the Ca^{2+} signaling, it's absence, combined with the absence of CD2AP, does not abrogate signaling to the same extent as in the case of SLP65-deficiency (Section 2.1.1). The explanation for this could be possible functional redundancies offered by additional signaling elements in the B cells that potentially substitute for the absence of these adaptor proteins, can support SLP65 function thus enabling B cells to mount appropriate immune response.

Having the CIN85 and CD2AP dKO cells at our disposal, it was possible to detect any interaction partners of SLP65 that have so far remained undetected due to the abundance of the more significant binding partners. An identical mass spectrometric approach as the one previously used in order to establish the highly specific interaction between SLP65 and CIN85/CD2AP was used for identification of any additional stimulation independent interaction partners that could have so far been an enigma.

A new molecule that could interact with SLP65 with high affinity was reported. The results were corroborated from both DG75 as well as the IIA1.6 cell lines from the Forward as well as the Reverse SILAC labeling experiments (Section 2.2). In both the cases, this protein was the premier candidate that could partake in interaction with SLP65 using exactly the same interaction modules as CIN85 and SLP65. This protein was Amphiphysin2/BIN1, part of the Bin1/Amphiphysin/RVS167 (BAR) family of proteins. Interestingly, the domain architecture of Amphiphysin 2 also revealed similarity to CIN85 and CD2AP (Figure 34). It has an SH3 domain on its C-terminus which possibly enabled interaction with the proline/arginine rich motifs of SLP65. Similar to CIN85, the human BIN1 gene also undergoes alternative splicing in a cell-type-specific manner (Ellis et al., 2012; Fugier et al., 2011; Nicot et al., 2007). Additionally, CD2AP and BIN1 have displayed overlapping functions. Both have been shown to be involved in endocytic trafficking related processes (Ubelmann et al., 2017).

So far, the more established function of Amphiphysin 2/Bin 1 is reported to be with regard to the ability to interact with Myc and conduct tumor suppressive functions in muscle cells (Wechsler-Reya et al., 1998). The functional confirmation of the possible participation of this protein in BCR-signaling is confirmed from experiments

(Pirkuliyeva S., 2015) where the BAR domain when used to replace the N-terminal domain of SLP65 functions just as well as on replacing the SLP65 N-terminal domain with the coiled-coil domains of CIN85 and CD2AP (Kühn J., 2015). In these experiment, it was also shown that on combined actions of replacement of the N-terminal domain with the BAR domain and the disruption of the proline/arginine motifs in SLP65, the cells lose the capacity to mobilise Ca^{2+}. (Pirkuliyeva S., 2015). This would additionally prevent any other signaling molecules to interact with SLP65 (including BIN1) that could provide functional support. Mere plasma membrane recruitment of SLP65 is not sufficient to support its function but multimerization mediated localised enrichment is essential for proper B cell activation. The would mean that merely recruiting SLP65 to the plasma membrane via its BAR domain would not be enough for Amphiphysin 2 to support its function entirely, there should be a way for it to organise SLP65 containing micro-clusters. In this regard, reports have been published on the mechanism of BAR-family proteins to mediate multimerization via membrane binding activities with the coordination of additional domains, thus accomplishing scaffolding and signaling functions (McDonald & Gould, 2016). Amphiphysin2/BIN1 thus harbours properties that make it the golden candidate for investigations into its participation in supporting SLP65 function and thus regulating BCR-signaling events.

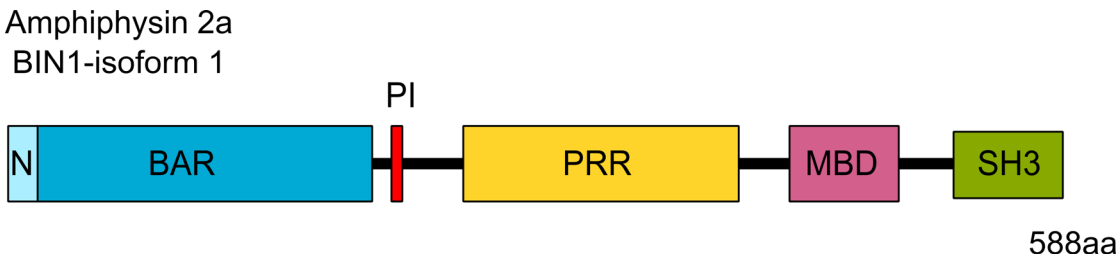

Figure 34: Domain architecture of Amphiphysin 2a or BIN1-isoform 1. Protein domains of Amphihysin 2a also known as the BIN1 isoform 1. N represents the N-terminal amphipathic helix which is followed by the BAR domain named so from the proteins Bin, Amphiphysin and Rvs. This is followed by the phosphoinositide binding site (represented as PI); PRR represents the proline rich region followed by the Myc-binding domain marked as MBD and the SH3 domain. The domain organization is adapted from (Wu et al., 2014).

3.3 The Savvy Separator: Biophysical process behind SLP65-CIN85 complex formation

This journey began with the initial evidence that the B-cell antigen receptor signals through a so-called preformed transducer module of SLP65 and CIN85, as has been referred to multiple times in my text (Oellerich et al., 2011). In our collaboration with Prof. Griesinger's group we found that SLP65-CIN85 micro-clusters in fact phase separate following the oil droplets in water analogy, thus forming membrane-less densely packed signalosomes that prime SLP65 to efficiently respond to signals transduced by the BCR. Additionally, Cryo-EM studies hinted that this phase separation is in fact tripartite involving SLP65, CIN85 and vesicles (Section 2.3.1). This mechanism of organizing signaling molecules into intracellular compartments is rather common. Studies in T cells indicate that phase-separated signaling elements proximal to the T cell antigen receptor (TCR) promote T cell activation (Su et al., 2016). The TCR-proximal signaling mechanisms are quite similar to the BCR signaling events, representing a common biological principle governing the intracellular signaling in these cells. This is a prudent mechanism as for enzymatically inert adaptor proteins, that cannot amplify signals by catalyzing biochemical reactions, a one-to-one interaction mediated signal transduction would be highly inefficient in physiological considerations. However, supramolecular assembly of multivalent proteins into signalosomes could enable efficient signaling with multiple proteins mediating respective functions being enriched in these clusters, positioned for immediate activation upon B cell stimulation (Rosen, 2014). Additionally, not just signal promoting but signal inhibiting elements could further fine tune signal transduction in cells (Strzyz, 2019).

Mutational analyses aided in investigating the factors that could either contribute to an increase in the micro-cluster forming capacity or factors that could negatively influence clustering events. I observed that due its ability to form stable coiled-coil trimers, the C-terminal domain of CIN85 is crucial for multimerizing SLP65. Disrupting all the CIN85 interaction sites and replacing the N-terminal domain of SLP65 with just the coiled-coil domain of CIN85 is enough for supporting wild type levels of Ca^{2+} signaling. In terms of quantitative considerations, a CIN85 coiled-coil domain-mediated oligomerization of a

SLP65 molecules which is incapable of interacting with additional CIN85 molecules is sufficient to support phase-separation and Ca^{2+} signaling in B cells. Due to SLP65-N terminus representing the membrane binding moiety for vesicle recruitment, these results indicated that the coiled-coil domain of CIN85 has the capacity to somehow support vesicle interaction to support tripartite phase separation. Indications of the ability of CIN85 coiled-coil domain to bind to membrane lipids have been reported (Kühn et al., 2016).
Expressing a variant of CIN85 incapable of forming stable trimers (L619K) reduced Ca^{2+} mobilization capacity emphasizing the essential step of efficient organization of SLP65 into signaling competent micro-clusters.

A "super-interactor" variant of SLP65: SLP65-3XPRM2 that interacted with CIN85 with supposedly increased affinity showed unexpected results of reduced Ca^{2+} signaling. It additionally showed reduced levels of phase-separation in *in vitro* studies (results not showed). This could be explained on takins the stoichiometry of interacting molecules into consideration. A stronger affinity-based interaction would result in one SLP65 molecule being allowed to interact with one CIN85 molecule in a rigid one-on-one interaction preventing the otherwise dynamic binding, involving interplay of several SLP65 and CIN85 molecules necessary for the formation of the multimolecular signaling complexes.
It would be of interest to corroborate these results by testing if a similar effect is rendered from the side of CIN85, where multiple dominant affinity SH3 domains mediate interactions with SLP65. Therefore, the qualitative and quantitative aspects of droplet formation hold much interest as well as the ways in which their assembly is regulated. Stepping away from its interaction with SLP65, it is reasonable to assume that CIN85 undertakes similar droplet formations enriching signaling elements that participate in other downstream signaling pathways, creating separate effector systems the composition and biophysical properties of which govern the effector functions performed.

To encapsulate, the results of my PhD study shed light on the involvement of CIN85 and CD2AP adaptor proteins in BCR-mediated signaling events. CIN85-facilitates SLP65 multimerization. More specifically, the C-terminal coiled-coil domain which forms stable CIN85-trimers mediates this action, and the prevention of this step, hampers B cell activation, especially when the simulating antigen concentrations are low. CIN85 demonstrates cell-type specific functions. While in most cell types it is involved in ligand induced internalization of receptor, in B cells, CIN85 seems to have an exclusive role of scaffolding effector molecules downstream of the BCR, increasing their local concentrations. It is subject to functional redundancy presented by CD2AP and in the absence of both the adaptor proteins, a new player might step into the picture in the cells attempt to safeguard it's signaling capabilities.

Chapter 4: Methods and Materials

4.1 Materials

4.1.1 Technical devices

Device	Manufacturer
Agarose gel electrophoresis system	Peqlab
Amaxa Nucleofector ™	Lonza
Amnis ImageStream®X MarkII Imaging	Merck
Cell culture incubator heracell®	Heraeus
Confocal laser scanning microscope tcs sp2	Leica microsystems
Countess ™ cell counter	Invitrogen
Electrophoresis power supply eps 301	Amersham biosciences
Electrophoresis system Hoefer se600	Amersham
Freezer platilab 340	Angelantoni industrie
Ice machine	Ziegra
Incubation shaker unitron	Infors
Incubator kelvitron® t	Heraeus
Laminar flow cabinet hera safe	Heraeus
Light microscope telaval 31	Zeiss
LSR II	Becton Dickinson
Magnetic stirrer m21/1	Framo Gerätetechnik
Mastercycler epgradient	Eppendorf

Mini protean tetra cell	Bio-rad laboratories
Nanodrop 2000	Thermo scientific
Neubauer improved counting chamber	Laboropotik
pH-meter	Inolab®
Pipettes	Eppendorf
Rocking shaker	Neolab
Thermomixer comfort	Eppendorf
ChemoCam Imager	Intas
Vortex Genie 2	Scientific Industries
Water Bath	Schütt Labortechnik
Water Purification System Milli-Q	Sartorious

Table 2: Technical devices used in this study

4.1.2 Software and Databases

Name	Producer	Application
Snapgene Viewer	GSL Biotech	Visualise protein and DNA sequences, plasmid mapping and primer designing
FlowJo 7.6.5	TreeStar	Flowcytometry data analysis
FACSDiva	BD Biosciences	Flowcytometry data acquirement
ImageJ	W.Rasband; NIH	Image processing
Perseus 1.5.5.0	Cox and Mann, 2008	Interpreting protein quantification and interaction data
GraphPad Prism	GraphPad Software Inc.	Data analysis and graphing

Chemostar professional	Intas	Western blot data acquirement
Leica confocal software	Leica	Microscopy data acquirement
Microsoft office 2010	Microsoft	Text processing
Mendeley	Elsevier	Citation management
Benchling	Sajith, Ashutosh Singhal and Cory Li; MIT	DNA and protein sequence analysis and editing
NCBI database	NCBI	Genomic and proteomic data analysis
Ensembl	EMBI-EBI	Genome browsing
Uniprot	Uniprot Consortium	Protein information

Table 3: Software and databases

4.1.3 Other digital and online tools

Name	Application
http://tools.genome-engineering.org	Designing CRISPR guide sequences
http://multalin.toulouse.inra.fr/multalin/	Sequence alignment
http://bioinfo.ut.ee/primer3-0.4.0/	Primer selection

Table 4: Digital tools used in this study

4.1.4 Additional materials and their supplier

Material	Supplier
6X DNA loading dye	Thermo Fischer Scientific
5X Phusion HF Buffer	New Englands Biolabs
10X NEBuffers Cutsmart bufers	New England Biolabs

Cell culture material	Greiner, Sarstedt, Nunc
GeneRuler^{TM} 1 kb DNA ladder	Thermo Fischer Scientific
Indo-1 AM	Invitrogen
Nitrocellulose filter Hybond ECL^{TM}	GE Healthcare
Whatman Gel Blotting Paper	GE Healthcare
Puromycin	InvivoGen
Polybrene	Sigma
NP-40 (IGEPAL CA-630)	Sigma-Aldrich
NuPAGE LDS sample buffer (4X)	Invitrogen
NuPAGE sample reducing buffer (10X)	Invitrogen
Prestained broad range protein marker (11-190 kDa)	New England Biolabs
RPMI 1640 + Glutamax	Gibco
SILAC RPMI 1640 Medium	Thermo Scientific
Streptavidin-Sepharose beads	GE Healthcare
Streptavidin APC	BD Biosciences
TransIT™ 293 Transfection Reagent	Mirus

Table 5: Consumables

4.1.5 Antibodies

For western blotting purposes, the primary antibodies were used at a 1:1000 dilution and secondary antibodies were used at a 1:10000 dilution. For cell surface BCR staining, fluorophore labelled antibodies were used at a 1:100 dilution for the flowcytometric analysis. Stimulating F(ab')$_2$ concentrations for B-cell stimulation are mentioned in the respective figure legends.

Target, host species	Manufacturer (Cat. no.)
Primary antibodies	
α-CIN85 (D1A4), Rabbit monoclonal Ab	CST (12304)
α-CD2AP, Sheep polyclonal Ab	Novus Biologicals (AF4474)
α-pSLP65 (Y96). Rabbit polyclonal Ab	CST (3601)
α-SLP65 (D3P2H), Rabbit monoclonal Ab	CST (36438)
α-SLP65 (D8R3G), Rabbit monoclonal Ab	CST (12168)
α-pIκBα (Ser32) (14D4), Rabbit monoclonal Ab	CST (2859)
α-IκBα,, Rabbit polyclonal Ab	CST (4814)
α-β-Actin (8H10D10), Mouse monoclonal Ab	CST (3700)
Secondary Antibodies	
α-mouse IgG2a-HRP	Southern Biotech (1081-05)
α-mouse IgG2b-HRP	Southern Biotech (1091-05)
α-rabbit IgG-HRP	Southern Biotech (4030-05)
α-goat IgG-HRP	Southern Biotech (6160-05)
α-sheep IgG-HRP	Southern Biotech (6150-05)
Antibodies for FACS	
Biotin tagged α-mouse IgG	Southern Biotech (1030-08)
Biotin tagged α-human IgM	Southern Biotech (2020-08)
α-Human IgM-APC, mouse IgG_1	Southern Biotech (902011)
α-Mouse IgG_{2a}-CY5, mouse IgG_1, goat	Southern Biotech (108015)
Antibodies used for B cell stimulation	
Goat α-Human IgM $F(ab')_2$	Jackson ImmunoResearch (109-006-129)

Goat α-Mouse IgM F(ab')$_2$	Jackson ImmunoResearch (115-006-020)
Mouse α-Chicken IgM F(ab')$_2$ (M4)	Biozol (8310-01)

Table 6: Antibodies used for western analysis

4.1.6 Vectors and constructs

Vector backbone	Insert	Source
Vectors used for cloning		
pCR2.1	-	Invitrogen
pCR2.1	CIN85CCdNSLP652,3	Julius Kühn
pCitN1	-	Michael Engelke
pMSCVpuro	-	BD Biosciences Clontech
pMSCVpuro	Citrine	Sona Pirkuliyeva
pMSCVpuro	NCitCIN85	Vanessa Bremes
Vectors used for retroviral transduction and exogenous expression of proteins		
pMSCVpuro	EGFP	Christoffer Hitzing
pMSCVpuro	NCitCIN85	Vanessa Bremes
pMSCVpuro	NCitCIN85d57	This study
pMSCVpuro	NCitCIN85 ΔCC	Vanessa Bremes
pMSCVpuro	NCitCIN85Q541E	This study
pMSCVpuro	NCitCIN85T266I	This study
pMSCVpuro	NCitCIN85R413Q	This study
pMSCVpuro	NCitCIN85L619K	This study
pMSCVpuro	NCitCD2AP	Vanessa Bremes

pMSCVpuro	CCitSLP65	Vanessa Bremes
pMSCVpuro	CCitdNSLP65M2,3	Julius Kühn
pMSCVpuro	CCitdNSLP65M1,2,3,4	This study
pMSCVpuro	PKCβII	Kathrin Schulz

Table 7: Vectors and expression constructs used in this study

4.1.7 Primers and oligonucleotides

Primer name	Primer sequence 5' – 3'
M13 Fwd	TGTAAAACGACGGCCAGT
M13 Rev	CAGGAAACAGCTATGACC
pMSCV Fwd	CCCTTGAACCTCCTCGTTCGACC
pMSCV Rev	GAGACGTGCTACTTCCATTTGTC
EGFP-C Fwd	GTCCTGCTGGAGTTCGTG
CMV Fwd	CGCAAATGGGCGGTAGGCGTG
CCdNSLPM2,3 Fwd	TAAGCAAGATCTATGGAAGGAAAACCAAAG ATG
CCdNSLPM2,3 Rev	TGCTTAACCGGTCCTGAAACTTTAACTGCATA
BamH1SLP653XPRM2 Fwd	GGATCCGATGGACAAGCTTAATAAAAT
SLP653XPRM2NotI Rev	GCGGCCGCTTATGAAACTTTAACTGCATA
CIN85d57 Fwd	TAAGCAGGATCCGGTGGAGGCCATAGTGGAGTTT
CIN85d57 Rev	TGCTTAGCGGCCGCTCATTTTGATTGTAGAGCTTT
CIN85Q541E Fwd	CTGTTACCATATCCGAAGTGTCTGACAACA
CIN85Q541E Rev	TGTTGTCAGACACTTCGGATATGGTAACAG

CIN85T266I Fwd	AAATGGACAGCAGGATAAAGAGCAAGGATT
CIN85T266I Rev	AATCCTTGCTCTTTATCCTGCTGTCCATTT
CIN85R413Q Fwd	CCAATTCTCTCAGCCAACCTGGCGCACTGC
CIN85R413Q Rev	GCAGTGCGCCAGGTTGGCTGAGAGAATTGG
CIN85 L619K Fwd	ACACAGGTCCGCGAGAAGAGGAGCATCATCGAGAC
Cin85 L619K Rev	GTCTCGATGATGCTCCTCTTCTCGCGGACCTGTGT
BamH1NCitCIN85FL Fwd	TAAGCAGGATCCGATGGTGGAGGCCATAGTGGAG
NCitCIN85FLNot1 Rev	TGCTTAGCGGCCGCTCATTTTGATTGTAGAGCTTT
mCIN85 Ex3 Fwd	CTCAGTCGTTCTCCTGATGCTCA
mCIN85 Ex3 Rev	CATACAAGGGTTTTCAAATGTGCC
hCIN85 Ex3 Fwd	CCATAGTTACATAAGGTCGCCTCAC
hCIN85 Ex3 Rev	CAGGGAGGGAACCTCTTTTTCC
mCD2AP Ex2 Fwd	TGAGCCGGTGCACAGAAG
mCD2AP Ex2 Rev	CCATAAGTGCTGATTCGCTGT
hCD2AP Ex2 Fwd	TGCCTCGGCCTCCCAAAGTGCTGGG
hCD2AP Ex2 Rev	CACTTAACCTCTCAATCTAAATATC
mCIN85-CRISPR guide oligo Fwd	CACCGCCACTGGATACATCGTGCAT
mCIN85-CRISPR guide oligo Rev	AAACATGCACGATGTATCCAGTGGC
hCIN85-CRISPR guide oligo Fwd	CACCGTCCACTGGGCACTTCGTGCA
hCIN85-CRISPR guide oligo Rev	AAACTGCACGAAGTGCCCAGTGGAC

mCD2AP-CRISPR guide oligo Fwd	CACCGCAGAAATGTGAAAAAACTAC
mCD2AP-CRISPR guide oligo Rev	AAACGTCTTTACACTTTTTTGATGC

Table 8: Primers used in this study (Fwd for Forward, Rev for reverse)

4.1.8 Chemical reagents

The chemicals and reagents used in this study were supplied by Invitrogen, Merck, Carl Roth, or Sigma unless mentioned otherwise.

4.1.9 Buffers and Solutions used in this study

Buffer/Solution	Composition
TAG lysis buffer	10 mM Tris pH 8.0, 50 mM KCl, 0.45% NP-40, 0.45% tween-20, add dH_2O
Tris acetate EDTA (1X TAE)	40 mM Tris-acetate pH8.0, 10 mM NaOAc, 1 mM EDTA, add. ddH_2O
B cell lysis buffer	137.5 mM NaCl, 50 mM Tris pH 7.8, 1 mM Na_3VO_4, 0.5 mM EDTA pH 8.0, 10% glycerol, 1X protease inhibitor cocktail, 1% NP-40 detergent, add. ddH_2O
Phosphate buffer saline (1X PBS)	137 mM NaCl, 27 mM KCl, 8.6 mM $Na_2HPO_4.12H_2O$, 1.4 mM KH_2PO_4 , add. ddH_2O
Krebs ringer solution (1X)	140 mM NaCl, 4 mM KCl, 10 mM Dglucose, 10 mM HEPES pH 7.4, 1 mM $CaCl_2$

10% Resolving gel for SDS-PAGE	375 mM Tris pH 8.8, 0.1% SDS, 10% Acrylamide and bisacrylamide, 0.00065% APS, 0.001% TEMED, add. ddH_2O
5% Stacking gel for SDS-PAGE	125 mM Tris pH6.8, 0.1% SDS, 5% Acrylamide and bisacrylamide, 0.001% APS, 0.001% TEMED, add. ddH_2O
SDS-PAGE running buffer (1X)	25 mM Tris, 192 mM glycine, 0.1% (w/v) SDS, add ddH_2O
Blotting buffer (1X)	39 mM Glycine, 48 mM Tris, 0.0375% (w/v) SDS, 0.01% (w/v) NaN_3, 20% (v/v) methanol, add. ddH_2O
Blocking solution	5% BSA, 0.01% NaN_3, add. 1X TBS-T
Tris buffer saline with tween (1X TBS-T)	20 mM Tris pH 7.6, 137 mM NaCl, 0.1% tween-20, add. ddH_2O
2X Laemlli buffer	62.5 mM TrisHCL pH 6.8, 2% SDS, 20% glycerol, 5% β-mercaptoethanol, 0.025% bromophenolblue, add. ddH_2O
ECL solution A	200 ml 0.1 M Tris pH 8.6, 50 mg luminol
ECL solution B	50 ml DMSO, 55 mg para-hydroxycoumaric acid

Table 9: Buffers and solutions used in this study

4.1.10 Enzymes and their suppliers

Enzymes	Supplier
All the restriction endonucleases	New England Biolabs
Calf intestinal phosphatase	New England Biolabs
Phusion® DNA polymerase	New England Biolabs

Taq DNA polymerase	New England Biolabs
Proteinase K	Macherey-Nagel
T4 DNA ligase	New England Biolabs

Table 10: Enzymes used in this study

4.1.11 Synthetic peptides

- Central PXXXPR motif of human SLP65 – Test peptide
  Biotin – KSPPPAAPSPLPRAGKKPT
- Binding incompetent version – Control peptide
  Biotin – KSPPPAAPSALPAAGKKPT

Preparation: A 1 mM stock solution of the peptides was prepared in 1X sterile PBS. A part of the stock solution was aliquot for use and the remaining stored away at -20° C.

Bought from: Thermo Fischer Scientific.

4.1.12 Bacterial Strains

One Shot Top10F' chemically competent E. coli (Invitrogen) were used for primary cultures for plasmid isolation. The E. coli were grown in lysogeny broth (LB) medium constituting 10 g/l tryptone, 5 g/l yeast extract, 5 g/l NaCl (pH7). Before inoculating the bacteria, the LB medium was autoclaved for 30 min at 121°C, 1.25 bar. Agar plates were prepared by adding 2% agar-agar to the LB medium. For bacterial antibiotic selection, 100µg/ml ampicillin or 50µg/ml kanamycin was used.

4.1.13 Cell lines used in this study

DG75 (DSMZ: ACC 83)

Human Burkitt lymphoma B cell line was established from the pleural effusion of a 10 year-old boy with Burkitt's lymphoma in 1975. This cell line shows suspension-cell properties in

culture and expresses IgM-BCRs on the cell surface (Ben-bassats et al., 1977). Following are the sub-cell lines established from these cells:

- DG75 cells deficient in CIN85 expression, referred to as DG75 CIN85-KO in this study
- DG75 cells with a combined deficiency of CIN85 and CD2AP expression referred to as DG75 CIN85/CD2AP-dKO in this study.

IIA1.6 (CVCL: 0J27)

IIA1.6 is a mouse reticulum cell sarcoma-cell line. It is a FcγR-negative descendant of the more prevalent mouse B cell line called A20 (Donnou et al., 2012). These cells express cell surface IgG-BCRs and exhibit a semi-adherent nature in culture. Following are the sub-cell lines established from these cells:

- IIA1.6 cells deficient in CIN85 expression, referred to as IIA1.6 CIN85-KO in this study
- IIA1.6 cells with a combined deficiency of CIN85 and CD2AP expression referred to as IIA1.6 CIN85/CD2AP-dKO in this study.

DT40 (ATCC: CRL-2111)

DT40 is an avian leukosis virus (ALV) induced bursal lymphoma cell line derived from a Hyline SC chicken (Baba & Humphries, 1984). This cell line has suspension culture properties and expresses cell surface IgM-BCRs. It shows a high ratio of targeted to random DNA integration, thus allowing for convenient genome alterations.

4.2 Methods

4.2.1 Molecular Biology based methods

If not stated otherwise standard molecular biology methods were performed as recommended by the manufacturer's protocol or as described in "Molecular Cloning: A Laboratory Manual" (Sambrook & Russell, 2001).

4.2.1.1 Isolation of genomic DNA

Genomic DNA extraction from the established B cell lines was performed by harvesting $1x10^6$ cells, washing once with 1XPBS, and finally lysing the cells in 100 µl TAG-lysis buffer containing 1 µl proteinase K (20 mg/ml). Temperature conditions: 56°C for 3 hrs. Subsequent heat inactivation of the enzyme: 95°C for 15 min. Samples were either directly used for polymerase chain reaction (PCR) or stored at 4°C until further use.

4.2.1.2 Polymerase chain reaction

Standard PCR protocol

Each PCR sample was prepared according to the instructions given below. The PCR products were then used to perform agarose gel electrophoresis and purification procedure to extract DNA sample from the gel is described further below.

PCR sample

Component	**Amount**
ddH_2O	15.07 µl
5X Phusion buffer	5 µl
10 mM dNTPs	1 µl
100 ng/µl Template DNA	1 µl
10 µM Primer Fwd	1 µl
10 µM Primer Rev	1 µl
DMSO	0.63 µl
Phusion polymerase	0.3 µl
Total	25 µl

PCR Program:

Step	**Temperature**	**Time**
Initial denaturation	98°C	5 min
35 cycles		

(Table continued on the next page)

Denaturation	98°C	30 sec
Annealing	x °C (*)	10 sec
Elongation	72°C	30 sec/kb plasmid
Final Elongation	72°C	10 Min
Stop	11°C	∞

* Annealing temperature = Tm primer – 3-5°C

Site directed mutagenesis protocol

For introducing specific point mutations in DNA sequence, amplification of plasmid was performed using complementary primers encompassing the desired mutation. The master mix prepared according to the instructions give below was split into two 50 µl reactions for PCR. One containing 1 µl Pfu polymerase and the other without any Pfu polymerase served as negative control.

Master mix

Component	**Amount**
ddH_2O	82 µl
10X Pfu Buffer	10 µl
10 mM dNTPs	2 µl
100 ng/µl Template DNA	2 µl
10 µM Primer Fwd	2 µl
10 µM Primer Rev	2 µl
Total	100 µl

PCR Program:

Step	**Temperature**	**Time**
Initial denaturation	94°C	2 min
35 cycles		
Denaturation	94°C	30 sec
Annealing	55°C	1 min
Elongation	68°C	2min/kb plasmid

(Table continued on the next page)

Final Elongation	68°C	10 Min
Stop	4°C	∞

The reactions were divided into two parts of 25 µl each. One was directly loaded onto the agarose gel for visualization and the other was treated with 1 µl DpnI to digest the template plasmid at 37 °C for 1 hour. The template plasmid being methylated gets removed and the PCR products remain intact. The sample was then used to transform competent bacteria, followed by plasmid purification and sequence validation.

4.2.1.3 Enzymatic digestion of DNA

1µg of DNA was incubated with 0.5-1µl of the appropriate restriction endonuclease and the respective NEBuffer in a total volume of 25 µl, made up with ddH_2O at either the conditions and duration specified by the manufacturer or at 37 °C, O/N. For cloning purposes, 1 µl of CIP was added on top in the same restriction sample and the sample was incubated further for 1 hr. This prevented re-ligation of the vector. Samples could then be mixed with the DNA loading dye and run on the agarose gel for visualization.

4.2.1.4 Agarose gel electrophoresis

The restriction fragments or the PCR amplicons were separated based on size using agarose gel electrophoresis making use of agarose gels that were in the range of 1-2% agarose composition. The gels contained 0.1 % (v/v) Ethidium Bromide and were run in 1X TAE running buffer. Prior to loading on the gel, the DNA samples were mixed with 1X DNA loading dye. Additionally, 10 µl of 1 kb DNA ladder was loaded onto the gel. Electrophoresis was performed at 1.2 V/cm^2 and the resolved DNA bands were viewed under the UV light. The appropriate bands were excised from the gel and the DNA purified using the kit: Promega Wizard® SV Gel and PCR Clean-Up System, as per manufacturer's protocol.

4.2.1.5 DNA ligation

Ligation of DNA fragments for cloning purposes was performed using the vector and insert amounts suggested by the NEBioCalculator, considering the vector and insert DNA lengths. 1 µl of T4 DNA enzyme and 1 µl of 10X T4 ligase buffer was added to the ligation mixture and the final volume was adjusted to 10 µl with ddH_2O. The sample was incubated at RT for 3 hrs or at 14 °C O/N. All the ligation mixture was used for transformation of the competent bacterial cells, which were then plated on the LB agar plates containing appropriate antibiotic.

4.2.1.6 Transformation of chemically competent bacteria

An aliquot of competent TOP10F' bacteria was thawed on ice, 50 ng of plasmid DNA added and the cells incubated on ice for about 20 min. The bacterial cells were then subjected to a heat-shock at 42°C for 90 sec, after which the cells were instantly placed on ice again for 2 min. After 2 min, 500 µl of RT antibiotic free LB-medium was added to the cells for recovery and incubated at 37° C for about 1 hr with constant shaking. The cells were then pelleted by centrifugation at 16,000 g for 1 min and the supernatant discarded. The pellet was resuspended in 100 µl of RT antibiotic free LB-medium and the cells were then directly plated onto a LB-agar plate with the correct antibiotic and incubated O/N at 37 °C for colonies to grow.

4.2.1.7 Isolation of plasmid DNA

4 ml of LB-Ampicillin/Kanamycin was inoculated with a transformed bacterial colony and grown at 37 °C, at about 180 rpm speed of agitation for aeration, O/N. The next morning, the cultures were used for plasmid purification using the kit: Invisorb® spin plasmid mini two (Invitek) as per the manufacturer's instructions. The DNA was finally eluted in 40 µl ddH_2O.

4.2.1.8 DNA sequencing

Sequence confirmation of the constructs and purified PCR products was done using the

services provided by the Microsynth Seqlab (Sequence Laboratories in Göttingen). Samples were prepared by combining 700 ng – 1.2 µg DNA, 30 picomol appropriate primer and ddH_2O to a final volume of 15 µl.

4.2.1.9 CRISPR/Cas9 Genome editing

The CRISPR/Cas-based gene editing was performed according to the instructions given in Cong & Zhang, 2014. pSpCas9(BB)-2A-GFP vector was used for gene targeting providing the advantage of encoding several elements like GFP (to aid sorting of transfected cells), the guide sequence, as well as the Cas9 coding sequence, all in one construct. The guide sequences for gene targeting were designed using the online tool - http://tools.genome-engineering.org. Guide sequences with a high score were selected, indicating fewer off-target effects. Additionally, the guides were selected such that, the Cas9 cleavage site overlapped with the binding site of a restriction endonuclease.

4.2.2 Cell Biology

Cells were cultured at 37° C temperature, 5% CO_2, in humidified conditions in the culture media listed below.

Cell line	Culture medium
DT40	RPMI-1640 (+GlutaMax) medium, supplemented with 10% FCS, Penicillin/Streptomycin and 1% chicken serum.
DG75	RPMI-1640 (+GlutaMax) medium, supplemented with 10% FCS, Penicillin/Streptomycin, 1mM Sodium Pyruvate, 50mM β-mercaptoethanol
IIA1.6	RPMI-1640 (+GlutaMax) medium, supplied with 10% FCS, Penicillin/Streptomycin, 1mM Sodium Pyruvate, 50mM β-mercaptoethanol
Platinum-E (retroviral packaging cell line)	DMEM supplemented with 10 % FCS and Penicillin/Streptomycin.

Table 11: Cell line specific cell culture media composition

For isotopic labeling of amino acids in the cells, for mass spectrometry-based experiments, the cells were cultured in the appropriate medium from below:

Heavy SILAC medium

SILAC RPMI-1640 Medium containing 10% dialyzed FCS, 1% penicillin/streptomycin, 0.115 mM $^{13}C_6{}^{15}N_4$ L-arginine (+10), and 0.27 mM $^{13}C_6{}^{15}N_2$ L-lysine (+8).

Light SILAC medium

SILAC RPMI-1640 Medium containing 10% dialyzed FCS, 1% penicillin/streptomycin and the corresponding non-labelled amino acids (Sigma).

For the DG75 and IIA1.6 cells, the incorporation of the labelled amino acids was performed according to Oellerich et al., 2009. To ensure complete labeling, the cells were cultured in the respective medium for at least 7 days.

4.2.2.1 Freezing and thawing of eukaryotic cells

For freezing the cells, about 8-10 million cells were harvested by centrifugation at 300 g, 5 min, RT. The supernatant was discarded and the pellet was resuspended in 2 ml freezing medium (FCS + 10% DMSO). The resuspended cells were transferred into cryo-vials, 1 ml volume in each and short-term storage of cells was done at -80 °C while the long-term storage was done at -140 °C. For thawing the frozen cells, the cryo-vials were heated in the 37 °C water-bath. Subsequently, the thawed contents were added to 10 ml cell culture medium in a 15 ml falcon tube. The DMSO was removed by centrifuging the cells at 300 g, 4 min and the supernatant discarded and the cell pellet resuspended in fresh 10 ml culture medium and seeded onto a 10 cm dish. The culture was allowed to grow to a confluence of about 50-70 % (depending on the cell line) before further use.

4.2.2.2 Amaxa Nucleofection

For transient transfection of DG75 and IIA1.6 cell lines with the respective CRISPR/Cas constructs, the Amaxa® Cell Line Nucleofector® Kit V was used following the manufacturer's instructions.

4.2.2.3 Retroviral transduction of cells

The Plat-E packaging cell line was used to produce ecotropic viral particles carrying the DNA to be transfected into the cells. These viral particles could only infect the mouse cells (IIA1.6 cells), however, when pseudo-typed with the vesicular stomatitis virus surface protein (VSV-G) they could infect cells of species that do not carry the ecotropic vector, like, the humans (DG75 cells). On infecting the target cells these viruses deliver the genetic material of interest.

The adherent Plat-E cells were cultured to about 60-80% confluence on a 6 cm dish. The culture medium was carefully aspirated from the dish and replaced with the transfection solution. The transfection solution consisted of 250 µl RPMI with no FCS (pre-warmed to 37 °C), 8 µl Trans-IT transfection reagent, about 4µg of plasmid DNA and if required 0.5 µg of pCMV-VSV-G. Before drop-wise pouring on the cells, the transfection solution was incubated at room temperature for about 35 min. The next day, culture was topped up with 1.5 ml fresh target cell medium and the cells were continued to grow under the appropriate culture conditions. For infecting the target cells, the supernatant was carefully collected from the pelleted Plat-E cells (centrifugation at 300g for 4 min) and carefully decanted over a 2ml culture of 1 million cells. Additionally, 3 µg/ml Polybrene solution was added to culture dish and mixed carefully, subjecting minimal mechanical stress to the cells. The next day, the polybrene containing medium was removed from the culture by centrifuging the cells and discarding the supernatant. The cells were re-plated and depending on the cell density, antibiotic selection was started with 2 µg/ml puromycin. In case of heterogenous cell population due to incomplete selection, the cells were additionally sorted via fluorescent activated cell sorting (FACS).

4.2.2.4 Cell sorting

Cells were sorted using the Fluorescence associated cell sorter (FACS), at the Cell Sorting Facility of the Universal Medical centre, Göttingen with the aid of Sabrina Becker. Approximately 6 million cells were washed once with 500 µl 1X PBS. Sorted cells were collected in the appropriate culture medium (R10), pelleted and then resuspended again in 200 µl of fresh medium and finally plated in a well of the 96-well round bottom plate. The

cells were cultured and expanded under the appropriate culture conditions.

4.2.3 Biochemistry

4.2.3.1 Preparation of cell lysates

B cells at a density of 0.5-1 million cells/ml in a culture dish were harvested by centrifugation at 300 g, RT for 4 min. The cell pellet was then resuspended in an appropriate volume of 1X PBS and the cells were counted either manually with the hemocytometer or using an automated cell counter countess. The cells were then harvested from appropriate volume of cell suspension, resuspended in medium containing no FCS (R0) and starved for 30 min at 37 °C with sporadic mixing. The cells were pelleted again and resuspended in 200 µl R0 per 5 million cells and stimulated with the appropriate anti-BCR antibody for the specified time points or left untreated for unstimulated samples. The cells were centrifuged again at 300 g, 4 °C, for 4 min and the media aspirated carefully. The cells were lysed in 20 µl lysis buffer (containing 1% NP40 detergent) per 1 million cells on ice for 20 min and the cell debri was pelleted by centrifugation at 20000 g , 4 °C for 20 min. The supernatant comprised the cell lysate and was mixed with 1X laemlli buffer, boiled at 95 °C for 5 min finally loaded on the SDS-PAGE gel for western blotting analyses. The left-over sample could be stored at -20 °C.

4.2.3.2 Affinity purification for mass spectrometric analyses

The cells that were grown in the Heavy or the Light SILAC medium (the composition mentioned in section 4.2.2) for at least a week were harvested by centrifugation at 300 g, 4 min, RT. The cell pellet was then resuspended in 1X PBS and cell-counting was done. Appropriate volume of the cell suspension was centrifuged to pellet about 30 million cells which were lysed in 600 µl lysis buffer for about 30 min. The cell debris were pelleted by centrifugation at 20000 g, for 20 min, 4 °C, and the cell lysates were mixed with 1 µM final concentration of the biotinylated peptides. In the forward SILAC labeling, the heavy amino acid labelled cells were treated with 1 µM of test peptide whereas the light amino acid labelled cells were treated with the control peptides. In the reverse SILAC labeling, this

treatment was reversed with heavy labelled cells treated with the control peptides and light labelled cells treated with the test peptides. Additionally, 200 µl streptavidin beads were added and the samples were incubated O/N on a rotating tube mixer at 4 °C. The beads were then washed thrice with lysis buffer at 500 g, 4 min, 4 °C. In the end, the heavy and the light labelled cells were combined and mixed with 120 µl of 1X LDS boiling buffer, prepared from 10X NuPAGE sample reducing buffer and 4X NuPAGE LDS sample buffer in ddH_2O. The samples were then boiled at 95 °C for 5 min and sent for mass spectrometry analysis to the Proteomics Core Facility at the University Medical Center Goettingen. At the mass spec. facility, the samples were subjected to SDS-PAGE and the gel bands were treated and analysed via tandem mass spectrometry (MS/MS). The data was processed using the Perseus software, the significance requirements taken into consideration and scatter-plots generated. The proteins that had a H/L normalized ratio of more than 2.0 in the case of forward labeling experiment and less than 2.0 in the case of reverse labeling experiment were considered to be the relevant binding partners of the test peptides.

4.2.3.3 SDS-PAGE

SDS-PAGE was employed for size-based separation of proteins. 10% polyacrylamide resolving gel and 5% polyacrylamide stacking gel were used. The gels were cast and run in 1X SDS running buffer. Before loading onto the gel, the samples were boiled in laemlli buffer at 95 °C for 5 min. The mini gel BioRad system was used to run the gels at the current and voltage settings of 15 mA, 250 V for the separating gel and 20 mA, 250 V for the resolving gel.

4.2.3.4 Immunoblot / western blot analysis

The proteins separated via SDS-PAGE were observed by immunoblotting and ECL-based detection. The equipment assembly consisted of the anode of the blotting chamber at the bottom, this was followed by two layers of whatman paper over it, a nitrocellulose membrane, the gel, and two more layers of whatman paper finally on top. It is important to note that all the layers were pre-soaked in blotting buffer. The bubbles impeding the transfer were removed from between the layers with the rolling motions of a pipette over the assembled layers. Finally, the cathode was placed on the top of the layers and protein transfer

was carried out at 16 V, 240 mA for 50 min. After the completion of blotting process, the membrane was blocked at room temperature for 60 min with blocking solution. The membrane was then used for incubation with the primary antibody O/N. The next day, the membrane was washed three times, 5 min each, incubated with Horse radish peroxidase (HRP) conjugated-secondary antibody for 60 min and washed three times again, for 10 min each followed by ECL-mediated detection. The ECL solution was prepared with 4 ml ECL solution A, 1.2 µl H_2O_2 and 400 µl ECL solution B and carefully poured on the surface of the membrane. The production of chemiluminescent oxidized luminol catalysed by HRP was detected using the ChemoCam Imager, Intas.

4.2.4 Optical methods

4.2.4.1 Confocal microscopy

The intracellular localization of citrine-tagged variants of proteins was observed via confocal laser scanning microscopy (Leice) as described in (Lösing et al., 2012). 1 – 2 million cells were harvested by centrifugation at 400 g for 3 min and washed twice with 1 ml Krebs-Ringer solution, containing 1mM $CaCl_2$ and finally resuspended in 800 µl Krebs-Ringer solution. The sample was distributed amongst two wells of a microscope chamber with 400 µl added to each. Prior to the imaging, the cells were rested in the wells for about 30 min to allow them to settle to the bottom of the well.

4.2.4.2 Ca^{2+} mobilization

Ca^{2+} flux and changes in the intracellular Ca^{2+} concentrations on BCR ligation was monitored with the help of the flowcytometer as described in Stork et. al. The Ca^{2+} sensitive dye INDO-1, that was used, has emission maximum at 475 nm in its free form and at 400 nm in its Ca^{2+} bound form. 1.5 – 2x10^6 cells were pelleted by centrifugation at 300 g for 4 min and resuspended in 700 µl RPMI-1640 medium with 5% FCS. Next, 2.1 µl pluronic acid (5%) and 0.7 µl INDO-1 AM was added to each sample, which was then incubated at 30 °C for 25 min. After this, 800 µl RPMI-1640 containing 10 % FCS was added and the samples were further incubated at 37 °C for 10 min. The cells were then pelleted and washed twice with Krebs-Ringer solution containing 1mM CaCl2 and finally resuspended in 600 µl

Krebs-Ringer solution. The cells were then rested for at least 25 °C to ensure a stable baseline for fluorescence signals. The fluorescence intensity for INDO-1 violet and blue was recorded for 30 sec. The ratio of these values gave an indication of the levels of intracellular Ca^{2+} concentrations. After the baseline acquisition, the cells were stimulated with the stimulating antibody and the fluorescence signal was recorded.

4.2.4.3 Analysis of cell surface-BCR expression level

To quantify the expression level of membrane bound IgM (for DG75 cells) and IgG (for IIA1.6 cells) BCRs, 1-1.5 million cells were harvested by centrifugation at 300 g, 4min and washed with 1X cold PBS. The cell pellet was then resuspended in 100 µl of 1X PBS and 1 µl of either anti-human IgM-APC or anti-mouse IgG-CY5 was added. The cells were then incubated on ice, in the dark for about 20 min. This was followed by centrifugation of the samples 300 g, 4 °C, 4 min and the washing away of the unbound antibodies using cold PBS and centrifuging again 300 g, 4 °C, 4 min. Finally, the cells were resuspended in 300 µl cold PBS and analysed via flowcytometry.

Bibliography

Abudula, A., Grabbe, A., Brechmann, M., Polaschegg, C., Herrmann, N., Goldbeck, I., … Wienands, J. (2007). SLP-65 Signal Transduction Requires Src Homology 2 domain-mediated Membrane Anchoring and a Kinase-independent Adaptor Function of Syk. *Journal of Biological Chemistry*, *282*(39), 29059–29066. https://doi.org/10.1074/jbc.M704043200

Arpin, C., Dechanet, J., Van Kooten, C., Merville, P., Grouard, G., Briere, F., … Liu, Y. (1995). Generation of memory B cells and plasma cells in vitro. *Science*, *268*(5211), 720–722. https://doi.org/10.1126/science.7537388

Baba TW, Humphries EH. Differential response to avian leukosis virus infection exhibited by two chicken lines. *Virology*. 1984;135(1):181-188. https://doi.org/10.1016/0042-6822(84)90128-4

Batista FD, Neuberger MS. B cells extract and present immobilized antigen: implications for affinity discrimination. *EMBO J*. 2000;19(4):513-520. https://doi.org/10.1093/emboj/19.4.513

Ben-bassats, H., Goldblum, N., Mitrani, S., Goldblum, T., Yoffey, J. M., Cohen, M. M., … Klein, G. (1977). Establishment in continuous culture of a new type of lymphocyte from a "burkitt-like" malignant lymphoma (line d.g.-75). *International Journal of Cancer*, *19*(1), 27–33. https://doi.org/10.1002/ijc.2910190105

Bhattacharyya, S., Deb, J., Patra, A. K., Thuy Pham, D. A., Chen, W., Vaeth, M., … Serfling, E. (2011). NFATc1 affects mouse splenic B cell function by controlling the calcineurin--NFAT signaling network. *The Journal of Experimental Medicine*, *208*(4), 823–839. https://doi.org/10.1084/jem.20100945

Bonilla, F. A., Fujita, R. M., Pivniouk, V. I., Chan, A. C., & Geha, R. S. (2000). Adapter proteins SLP-76 and BLNK both are expressed by murine macrophages and are linked to signaling via Fcgamma receptors I and II/III. *Proceedings of the National Academy of Sciences of the United States of America*, *97*(4), 1725–1730. https://doi.org/10.1073/pnas.040543597

Borinstein, S. C., Hyatt, M. A., Sykes, V. W., Straub, R. E., Lipkowitz, S., Boulter, J., & Bogler, O. (2000). SETA is a multifunctional adapter protein with three SH3 domains that binds Grb2, Cbl, and the novel SB1 proteins. *Cellular Signalling*, *12*(11–12), 769–779. https://doi.org/10.1016/S0898-6568(00)00129-7

Brack, C., Hirama, M., Lenhard-Schuller, R., & Tonegawa, S. (1978). A complete immunoglobulin gene is created by somatic recombination. *Cell*, *15*(1), 1–14. https://doi.org/10.1016/0092-8674(78)90078-8

Bremes, V. (2012) CIN85/CD2AP-based protein complexes in B cell antigen receptor signaling. Cellular and Molecular Immunology, Georg-August University of Göttingen, Göttingen. **http://hdl.handle.net/11858/00-1735-0000-000D-EFE1-5**

Coico R., Sunshine G., B. E. (2003). *Immunology: a short course, 5th edition*. Wiley-Liss publication, **ISBN-10** 0-471-22689-0 **ISBN-13** 978-0-471-22689-5 https://doi.org/10.1016/j.clim.2003.11.008

Cong, L., & Zhang, F. (2014). Genome engineering using crispr-cas9 system. In *Chromosomal Mutagenesis: Second Edition* (pp. 197–217). Springer Fachmedien. https://doi.org/10.1007/978-1-4939-1862-1_10

Coope, H. J., Atkinson, P. G., Huhse, B., Belich, M., Janzen, J., Holman, M. J., … Ley, S. C. (2002). CD40 regulates the processing of NF-kappaB2 p100 to p52. *EMBO J*, *21*, 5375–5385, https://doi.org/10.1093/emboj/cdf542.

Cooper, M. D. (2015). The early history of B cells. *Nature Reviews Immunology*, *15*(3), 191–197. https://doi.org/10.1038/nri3801

Coughlin, J. J., Stang, S. L., Dower, N. A., & Stone, J. C. (2005). RasGRP1 and RasGRP3 Regulate B Cell Proliferation by Facilitating B Cell Receptor-Ras Signaling. *The Journal of Immunology*, *175*(11), 7179–7184. https://doi.org/10.4049/jimmunol.175.11.7179

Dal Porto, J. M., Gauld, S. B., Merrell, K. T., Mills, D., Pugh-Bernard, A. E., & Cambier, J. (2004). B cell antigen receptor signaling 101. *Molecular Immunology*, *41*(6–7), 599–613. https://doi.org/10.1016/J.MOLIMM.2004.04.008

Damen, J. E., Ware, M. D., Kalesnikoff, J., Hughes, M. R., & Krystal, G. (2001). SHIP's C-terminus is essential for its hydrolysis of PIP3 and inhibition of mast cell degranulation. *Blood*, *97*(5), 1343–1351. https://doi.org/10.1182/blood.v97.5.1343

Dikic, I. (2002, October 2). CIN85/CMS family of adaptor molecules. *FEBS Letters*. https://doi.org/10.1016/S0014-5793(02)03188-5

Doherty GJ, McMahon HT. Mechanisms of endocytosis. *Annu Rev Biochem*. 2009;78:857-902. https://doi.org/10.1146/annurev.biochem.78.081307.110540

Donnou, S., Galand, C., Touitou, V., Sautès-Fridman, C., Fabry, Z., & Fisson, S. (2012). Murine models of B-cell lymphomas: promising tools for designing cancer therapies. *Advances in Hematology*, *2012*, 701704. https://doi.org/10.1155/2012/701704

Dustin, M. L., Olszowy, M. W., Holdorf, A. D., Li, J., Bromley, S., Desai, N., … Shaw, A. S. (1998). A Novel Adaptor Protein Orchestrates Receptor Patterning and Cytoskeletal Polarity in T-Cell Contacts. *Cell*, *94*(5), 667–677. https://doi.org/10.1016/S0092-8674(00)81608-6

Ellis, J. D., Barrios-Rodiles, M., Çolak, R., Irimia, M., Kim, T., Calarco, J. A., … Blencowe, B. J. (2012). Tissue-Specific Alternative Splicing Remodels Protein-Protein Interaction Networks. *Molecular Cell*, *46*(6), 884–892. https://doi.org/10.1016/j.molcel.2012.05.037

Engelke, M., Engels, N., Dittmann, K., Stork, B., & Wienands, J. (2007). Ca^{2+} signaling in antigen receptor-activated B lymphocytes. *Immunological Reviews*, *218*(1), 235–246. https://doi.org/10.1111/j.1600-065X.2007.00539.x

Engelke, M., Pirkuliyeva, S., Kühn, J., Wong, L., Boyken, J., Herrmann, N., … Wienands, J. (2014). Macromolecular assembly of the adaptor SLP-65 at intracellular vesicles in resting B cells. *Science Signaling*, *7*(339), 1–9, https://doi.org/10.1126/scitranslmed.2005104.

Engels, N., Wollscheid, B., & Wienands, J. (2001). Association of SLP-65 / BLNK with the B cell antigen receptor through a non-ITAM tyrosine of Ig-α. *European Journal of Immunology*, *31*(7), 2126–2134. https://doi.org/10.1002/1521-4141(200107)31:7<2126::AID-IMMU2126>3.0.CO;2-O

Fiala, G. J., Kaschek, D., Blumenthal, B., Reth, M., Timmer, J., & Schamel, W. W. A. (2013). Pre-Clustering of the B Cell Antigen Receptor Demonstrated by Mathematically Extended Electron Microscopy. *Frontiers in Immunology*, *4*, 427. https://doi.org/10.3389/fimmu.2013.00427

Fitzsimmons, C. M., Falcone, F. H., & Dunne, D. W. (2014). Helminth Allergens, Parasite-Specific IgE, and Its Protective Role in Human Immunity. *Frontiers in Immunology*, *5*. https://doi.org/10.3389/fimmu.2014.00061

Flajnik, M. F., & Masanori, K. (2008). Origin and evolution of the adaptive immune system: genetic events and selective pressures Martin. *Bone*, *23*(1), 1–7. https://doi.org/10.1038/nrg2703

Fu, C., Turck, C. W., Kurosaki, T., & Chan, A. C. (1998). BLNK: a central linker protein in B cell activation. *Immunity*, *9*(1), 93–103. https://doi.org/10.1016/s1074-7613(00)80591-9.

Fugier, C., Klein, A. F., Hammer, C., Vassilopoulos, S., Ivarsson, Y., Toussaint, A., … Charlet-Berguerand, N. (2011). Misregulated alternative splicing of BIN1 is associated with T tubule alterations and muscle weakness in myotonic dystrophy. *Nature Medicine*, *17*(6), 720–725. https://doi.org/10.1038/nm.2374

Gavin, A.-C., Aloy, P., Grandi, P., Krause, R., Boesche, M., Marzioch, M., … Superti-Furga, G. (2006). Proteome survey reveals modularity of the yeast cell machinery. *Nature*, *440*(7084), 631–636. https://doi.org/10.1038/nature04532

Goitsuka, R., Fujimura, Y., Mamada, H., Umeda, A., Morimura, T., Uetsuka, K., …

Kitamura, D. (1998). BASH, a novel signaling molecule preferentially expressed in B cells of the bursa of Fabricius. *Journal of Immunology (Baltimore, Md. : 1950)*, *161*(11), 5804–5808. http://www.ncbi.nlm.nih.gov/pubmed/9834055

Good, M. C., Zalatan, J. G., & Lim, W. A. (2011). Scaffold Proteins: Hubs for Controlling the Flow of Cellular Information. *Science*, *332*(6030), 680–686. https://doi.org/10.1126/science.1198701

Gout, I., Middleton, G., Adu, J., Ninkina, N. N., Drobot, L. B., Filonenko, V., … Buchman, V. L. (2000). Negative regulation of PI 3-kinase by Ruk, a novel adaptor protein. *The EMBO Journal*, *19*(15), 4015–4025. https://doi.org/10.1093/emboj/19.15.4015

Hangartner, L., Zellweger, R. M., Giobbi, M., Weber, J., Eschli, B., McCoy, K. D., … Hengartner, H. (2006). Nonneutralizing antibodies binding to the surface glycoprotein of lymphocytic choriomeningitis virus reduce early virus spread. *The Journal of Experimental Medicine*, *203*(8), 2033–2042. https://doi.org/10.1084/jem.20051557

Havran, W. L., DiGiusto, D. L., & Cambier, J. C. (1984). mIgM:mIgD ratios on B cells: mean mIgD expression exceeds mIgM by 10-fold on most splenic B cells. *Journal of Immunology (Baltimore, Md. : 1950)*, *132*(4), 1712–1716. http://www.ncbi.nlm.nih.gov/pubmed/6421926

Havrylov, S., Rzhepetskyy, Y., Malinowska, A., Drobot, L., & Redowicz, M. J. (2009). Proteins recruited by SH3 domains of Ruk/CIN85 adaptor identified by LC-MS/MS. *Proteome Science*, *7*. https://doi.org/10.1186/1477-5956-7-21

Hayashi, K., Nittono, R., Okamoto, N., Tsuji, S., Hara, Y., Goitsuka, R., & Kitamura, D. (2000). The B cell-restricted adaptor BASH is required for normal development and antigen receptor-mediated activation of B cells. *Proceedings of the National Academy of Sciences of the United States of America*, *97*(6), 2755–2760. https://doi.org/10.1073/pnas.040575697

Honjo, T., Kinoshita, K., & Muramatsu, M. (2002). M OLECULAR M ECHANISM OF C LASS S WITCH R ECOMBINATION : Linkage with Somatic Hypermutation. *Annual Review of Immunology*, *20*(1), 165–196. https://doi.org/10.1146/annurev.immunol.20.090501.112049

Huang ZY, Barreda DR, Worth RG, et al. Differential kinase requirements in human and mouse Fc-gamma receptor phagocytosis and endocytosis. *J Leukoc Biol*. 2006;80(6):1553-1562. https://doi.org/10.1189/jlb.0106019

Hutchings, N. J., Clarkson, N., Chalkley, R., Barclay, A. N., & Brown, M. H. (2003). Linking the T Cell Surface Protein CD2 to the Actin-capping Protein CAPZ via CMS and CIN85. *Journal of Biological Chemistry*, *278*(25), 22396–22403. https://doi.org/10.1074/jbc.M302540200

Ishiai, M., Kurosaki, M., Pappu, R., Okawa, K., Ronko, I., Fu, C., … Kurosaki, T. (1999). BLNK required for coupling Syk to PLC gamma 2 and Rac1-JNK in B cells. *Immunity*, *10*(1), 117–125. https://doi.org/10.1016/S1074-7613(00)80012-6

Jacob M, Todd L, Sampson MF, Puré E. Dual role of Cbl links critical events in BCR endocytosis. *Int Immunol*. 2008;20(4):485-497 https://doi.org/10.1093/intimm/dxn010

Johannes L, Parton RG, Bassereau P, Mayor S. Building endocytic pits without clathrin. *Nat Rev Mol Cell Biol*. 2015;16(5):311-321. https://doi.org/10.1038/nrm3968

Jumaa, H., Wollscheid, B., Mitterer, M., Wienands, J., Reth, M., & Nielsen, P. J. (1999). Abnormal development and function of B lymphocytes in mice deficient for the signaling adaptor protein SLP-65. *Immunity*, *11*(5), 547–554. https://doi.org/10.1016/S1074-7613(00)80130-2

Kabak, S., Skaggs, B. J., Gold, M. R., Affolter, M., West, K. L., Foster, M. S., … Clark, M. R. (2002). The direct recruitment of BLNK to immunoglobulin alpha couples the B-cell antigen receptor to distal signaling pathways. *Molecular and Cellular Biology*, *22*(8), 2524–2535. https://doi.org/10.1128/mcb.22.8.2524-2535.2002

Keller, B., Shoukier, M., Schulz, K., Bhatt, A., Heine, I., Strohmeier, V., & Speckmann, C. (2018). Germline deletion of CIN85 in humans with X chromosome – linked antibody deficiency. *Journal of Experimental Medicine*, 1–10. https://doi.org/10.1084/jem.20170534

Kitaura, Y., Jang, K. I., Wang, Y., Han, Yoon-Chi, Inazu, T., Cadera, J. E., Schlissel, M., Hardy, R. R., Gu, H. (2007). Control of the B Cell-Intrinsic Tolerance Programs by Ubiquitin Ligases Cbl and Cbl-b. *Immunity*, 26, 567-578. https://doi.org/10.1016/j.immuni.2007.03.015

Kometani, K., Yamada, T., Sasaki, Y., Yokosuka, T., Saito, T., Rajewsky, K., … Kurosaki, T. (2011). CIN85 drives B cell responses by linking BCR signals to the canonical NF-κB pathway. *The Journal of Experimental Medicine*, *208*(7), 1447–1457. https://doi.org/10.1084/jem.20102665

Kong, M. S., Hashimoto-Tane, A., Kawashima, Y., Sakuma, M., Yokosuka, T., Kometani, K., … Saito, T. (2019). Inhibition of T cell activation and function by the adaptor protein CIN85. *Science Signaling*, *12*(567), eaav4373. https://doi.org/10.1126/scisignal.aav4373

Kowanetz, K., Szymkiewicz, I., Haglund, K., Kowanetz, M., Husnjak, K., Taylor, J. D., … Dikic, I. (2003). Identification of a Novel Proline-Arginine Motif Involved in CIN85-dependent Clustering of Cbl and Down-regulation of Epidermal Growth Factor Receptors. *Journal of Biological Chemistry*, 278(41), 39735-39746 https://doi.org/10.1074/jbc.M304541200

Kühn, J., Wong, L. E., Pirkuliyeva, S., Schulz, K., Schwiegk, C., Fünfgeld, K. G., … Wienands, J. (2016). The adaptor protein CIN85 assembles intracellular signaling clusters for B cell activation. *Science Signaling*, *9*(434), 1–15. https://doi.org/10.1126/scisignal.aad6275

Kühn, J. (2015) Multimolecular adaptor protein complexes in B cell receptor signaling. Cellular and Molecular Immunology, Georg-August University of Göttingen, Göttingen. http://hdl.handle.net/11858/00-1735-0000-0022-6043-B

Kurakin, A. V., Wu, S., & Bredesen, D. E. (2003). Atypical Recognition Consensus of CIN85/SETA/Ruk SH3 Domains Revealed by Target-assisted Iterative Screening. *Journal of Biological Chemistry*, *278*(36), 34102–34109. https://doi.org/10.1074/jbc.M305264200

Kurosaki, T, & Tsukada, S. (2000). BLNK: connecting Syk and Btk to calcium signals. *Immunity*, *12*(1), 1–5. https://doi.org/10.1016/S1074-7613(00)80153-3

Kurosaki, Tomohiro. (2002). Regulation of B-cell signal transduction by adaptor proteins. *Nature Reviews Immunology*, *2*(5), 354–363. https://doi.org/10.1038/nri801

Lee PS, Wang Y, Dominguez MG, et al. The Cbl protooncoprotein stimulates CSF-1 receptor multiubiquitination and endocytosis, and attenuates macrophage proliferation. *EMBO J*. 1999;18(13):3616-3628. https://doi.org/10.1093/emboj/18.13.3616

Lee, K.-H., Dinner, A. R., Tu, C., Campi, G., Raychaudhuri, S., Varma, R., … Shaw, A. S. (2003). The Immunological Synapse Balances T Cell Receptor Signaling and Degradation. *Science*, *302*(5648), 1218–1222. https://doi.org/10.1126/science.1086507

Leitges, M., Schmedt, C., Guinamard, R., Davoust, J., Schaal, S., Stabel, S., & Tarakhovsky, A. (1996). Immunodeficiency in Protein Kinase Cbeta -Deficient Mice. *Science*, *273*(5276), 788–791. https://doi.org/10.1126/science.273.5276.788

Levkowitz G, Waterman H, Ettenberg SA, et al. Ubiquitin ligase activity and tyrosine phosphorylation underlie suppression of growth factor signaling by c-Cbl/Sli-1. *Mol Cell*. 1999;4(6):1029-1040. https://doi.org/10.1016/s1097-2765(00)80231-2

Lösing, M., Goldbeck, I., Manno, B., Oellerich, T., Schnyder, T., Bohnenberger, H., … Engelke, M. (2012). The Dok-3/Grb2 protein signal module attenuates Lyn kinase-dependent activation of Syk kinase in B cell antigen receptor microclusters. *The Journal of biological chemistry*, *288*(4), 2303–2313. http://www.jbc.org/cgi/doi/10.1074/jbc.M112.406546

McDonald, N. A., & Gould, K. L. (2016). Linking up at the BAR: Oligomerization and F-BAR protein function. *Cell Cycle (Georgetown, Tex.)*, *15*(15), 1977–1985.

https://doi.org/10.1080/15384101.2016.1190893

Medzhitov, R., & Janeway, C. (2000). Innate immune recognition: mechanisms and pathways - Medzhitov - 2002 - Immunological Reviews - Wiley Online Library. *Immunological Reviews*, *173*, 89–97. https://doi.org/10.1034/j.1600-065X.2000.917309.x

Minegishi, Y., Rohrer, J., Coustan-Smith, E., Lederman, H. M., Pappu, R., Campana, D., … Conley, M. E. (1999). An Essential Role for BLNK in Human B Cell Development. *Science*, *286*(5446), 1954–1957. https://doi.org/10.1126/science.286.5446.1954

Mitchison NA. T-cell-B-cell cooperation. *Nat Rev Immunol*. 2004;4(4):308-312. https://doi.org/10.1038/nri1334

Molfetta, R., Belleudi, F., Peruzzi, G., Morrone, S., Leone, L., Dikic, I., … Paolini, R. (2005). CIN85 Regulates the Ligand-Dependent Endocytosis of the IgE Receptor: A New Molecular Mechanism to Dampen Mast Cell Function. *The Journal of Immunology*, *175*(7), 4208–4216. https://doi.org/10.4049/jimmunol.175.7.4208

Nagel, D., Vincendeau, M., Eitelhuber, A. C., & Krappmann, D. (2014). Mechanisms and consequences of constitutive NF-κB activation in B-cell lymphoid malignancies. *Oncogene*, *33*(50), 5655–5665. https://doi.org/10.1038/onc.2013.565

Narita, T., Amano, F., Yoshizaki, K., Nishimoto, N., Nishimura, T., Tajima, T., … Taniyama, T. (2001). Assignment of SH3KBP1 to human chromosome band Xp22.1-->p21.3 by in situ hybridization. *Cytogenetics and Cell Genetics*, *93*(1–2), 133–134. https://doi.org/10.1159/000056966

Nicot, A.-S., Toussaint, A., Tosch, V., Kretz, C., Wallgren-Pettersson, C., Iwarsson, E., … Laporte, J. (2007). Mutations in amphiphysin 2 (BIN1) disrupt interaction with dynamin 2 and cause autosomal recessive centronuclear myopathy. *Nature Genetics,* 39(9), 1134-1139. https://doi.org/10.1038/ng2086

Niiro, H., Jabbarzadeh-Tabrizi, S., Kikushige, Y., Shima, T., Noda, K., Ota, S. -i., … Akashi, K. (2012). CIN85 is required for Cbl-mediated regulation of antigen receptor signaling in human B cells. *Blood*, *119*(10), 2263–2273. https://doi.org/10.1182/blood-2011-04-351965

Niiro, Hiroaki, & Clark, E. A. (2002). Regulation of B-cell fate by antigen-receptor signals. *Nature Reviews Immunology*, *2*(12), 945–956. https://doi.org/10.1038/nri955

Nishizuka, Y. (1992). Intracellular signaling by hydrolysis of phospholipids and activation of protein kinase C. *Science*, *258*(5082), 607–614. https://doi.org/10.1126/science.1411571

Oellerich, T., Bremes, V., Neumann, K., Bohnenberger, H., Dittmann, K., Hsiao, H.-H., … Geahlen, R. (2011). The B-cell antigen receptor signals through a preformed transducer module of SLP65 and CIN85. *The EMBO Journal*, *30*(17), 3620–3634. https://doi.org/10.1038/emboj.2011.251

Oellerich, T., Grønborg, M., Neumann, K., Hsiao, H. H., Urlaub, H., & Wienands, J. (2009). SLP-65 phosphorylation dynamics reveals a functional basis for signal integration by receptor-proximal adaptor proteins. *Molecular & cellular proteomics : MCP*, *8*(7), 1738–1750. https://doi.org/10.1074/mcp.M800567-MCP200

Okkenhaug, K., & Vanhaesebroeck, B. (2003). PI3K in lymphocyte development, differentiation and activation. *Nature Reviews Immunology*, *3*(4), 317–330. https://doi.org/10.1038/nri1056

Parkin, J., & Cohen, B. (2001). An overview of the immune system. *The Lancet*, *357*(9270), 1777–1789. https://doi.org/10.1016/S0140-6736(00)04904-7

Pirkuliyeva, S. (2015) Structural and functional elucidation of the primary transducer module of the B cell antigen receptor. Cellular and Molecular Immunology, Georg-August University of Göttingen, Göttingen. http://hdl.handle.net/11858/00-1735-0000-0022-6062-7

Petrelli, A., Gilestro, G. F., Lanzardo, S., Comoglio, P. M., Migone, N., & Giordano, S. (2002). The endophilin–CIN85–Cbl complex mediates ligand-dependent downregulation of c-Met. *Nature*, *416*(6877), 187–190. https://doi.org/10.1038/416187a

Pogue, S. L., Kurosaki, T., Bolen, J., & Herbst, R. (2000). B Cell Antigen Receptor-Induced Activation of Akt Promotes B Cell Survival and Is Dependent on Syk Kinase. *The Journal of Immunology*, *165*(3), 1300–1306. https://doi.org/10.4049/jimmunol.165.3.1300

Rédei, G. P. (Ed.). (2008). Lyon Hypothesis BT - Encyclopedia of Genetics, Genomics, Proteomics and Informatics (p. 1130). Dordrecht: Springer Netherlands. https://doi.org/10.1007/978-1-4020-6754-9_9660

Reth, M. (2001). Oligomeric antigen receptors: a new view on signaling for the selection of lymphocytes. *Trends in Immunology*, *22*(7), 356–360. Retrieved from http://www.ncbi.nlm.nih.gov/pubmed/11429318

Reth, Michael. (1992). Antigen Receptors on B Lymphocytes. *Annual Review of Immunology*, *10*(1), 97–121. https://doi.org/10.1146/annurev.iy.10.040192.000525

Rosen, M. K. (2014). Phase Separation of Multi-Valent Signaling Proteins. *Biophysical Journal*, *106*(2), 36a. https://doi.org/10.1016/j.bpj.2013.11.271

Rowley, R. B., Burkhardt, A. L., Chao, H. G., Matsueda, G. R., & Bolen, J. B. (1995). Syk protein-tyrosine kinase is regulated by tyrosine-phosphorylated Ig alpha/Ig beta immunoreceptor tyrosine activation motif binding and autophosphorylation. *The Journal of Biological Chemistry*, *270*(19), 11590–11594. https://doi.org/10.1074/jbc.270.19.11590

Saijo K, Mecklenbräuker I, Santana A, Leitger M, Schmedt C, Tarakhovsky A. Protein kinase C beta controls nuclear factor kappaB activation in B cells through selective regulation of the IkappaB kinase alpha. *J Exp Med*. 2002;195(12):1647-1652. doi:10.1084/jem.20020408

Sakamuro D, Elliott KJ, Wechsler-Reya R, Prendergast GC. BIN1 is a novel MYC-interacting protein with features of a tumour suppressor. *Nat Genet*. 1996;14(1):69-77. https://doi.org/10.1038/ng0996-69

Schulz, K. (2016) CIN85 in proximal and distant B cell antigen receptor signaling. Cellular and Molecular Immunology, Georg-August University of Göttingen, Göttingen. http://hdl.handle.net/11858/00-1735-0000-0028-8700-3

Shih, N. Y., Li, J., Karpitskii, V., Nguyen, A., Dustin, M. L., Kanagawa, O., … Shaw, A. S. (1999). Congenital nephrotic syndrome in mice lacking CD2-associated protein. *Science (New York, N.Y.)*, *286*(5438), 312–315. https://doi.org/10.1126/science.286.5438.312

Shinohara, H., Maeda, S., Watarai, H., & Kurosaki, T. (2007). IκB kinase β–induced phosphorylation of CARMA1 contributes to CARMA1–Bcl10–MALT1 complex formation in B cells. *The Journal of Experimental Medicine*, *204*(13), 3285–3293. https://doi.org/10.1084/jem.20070379

Sommer, K., Guo, B., Pomerantz, J. L., Bandaranayake, A. D., Moreno-García, M. E., Ovechkina, Y. L., & Rawlings, D. J. (2005). Phosphorylation of the CARMA1 Linker Controls NF-κB Activation. *Immunity*, *23*(6), 561–574. https://doi.org/10.1016/j.immuni.2005.09.014

Soubeyran, P., Kowanetz, K., Szymkiewicz, I., Langdon, W. Y., & Dikic, I. (2002). Cbl–CIN85–endophilin complex mediates ligand-induced downregulation of EGF receptors. *Nature*, *416*(6877), 183–187. https://doi.org/10.1038/416183a

Strzyz, P. (2019). Phase separation tunes signal transduction. *Nature Reviews Molecular Cell Biology*, *20*(5), 263–263. https://doi.org/10.1038/s41580-019-0121-7

Su TT, Guo B, Kawakami Y, et al. PKC-beta controls I kappa B kinase lipid raft recruitment and activation in response to BCR signaling. *Nat Immunol*. 2002;3(8):780-786. https://doi.org/10.1038/ni823

Su, X., Ditlev, J. A., Hui, E., Xing, W., Banjade, S., Okrut, J., … Vale, R. D. (2016). Phase

separation of signaling molecules promotes T cell receptor signal transduction. *Science (New York, N.Y.)*, *352*(6285), 595–599. doi:10.1126/science.aad9964

Sutherland CL, Heath AW, Pelech SL, Young PR, Gold MR. Differential activation of the ERK, JNK, and p38 mitogen-activated protein kinases by CD40 and the B cell antigen receptor. *J Immunol*. 1996;157(8):3381-3390. https://www.jimmunol.org/content/157/8/3381

Suzuki K, Grigorova I, Phan TG, Kelly LM, Cyster JG. Visualizing B cell capture of cognate antigen from follicular dendritic cells. *J Exp Med*. 2009;206(7):1485-1493. https://doi.org/10.1084/jem.20090209

Szymkiewicz, I., Kowanetz, K., Soubeyran, P., Dinarina, A., Lipkowitz, S., & Dikic, I. (2002). CIN85 Participates in Cbl-b-mediated Down-regulation of Receptor Tyrosine Kinases. *Journal of Biological Chemistry*, *277*(42), 39666–39672. https://doi.org/10.1074/jbc.M205535200

Take, H., Watanabe, S., Takeda, K., Yu, Z.-X., Iwata, N., & Kajigaya, S. (2000b). Cloning and Characterization of a Novel Adaptor Protein, CIN85, That Interacts with c-Cbl. *Biochemical and Biophysical Research Communications*, *268*(2), 321–328. https://doi.org/10.1006/bbrc.2000.2147

Tibaldi, E. V., & Reinherz, E. L. (2003). CD2BP3, CIN85 and the structurally related adaptor protein CMS bind to the same CD2 cytoplasmic segment, but elicit divergent functional activities. *International Immunology*, *15*(3), 313–329. https://doi.org/10.1093/intimm/dxg032

Ubelmann, F., Burrinha, T., Salavessa, L., Gomes, R., Ferreira, C., Moreno, N., & Guimas Almeida, C. (2017). Bin1 and CD 2 AP polarise the endocytic generation of beta-amyloid. *EMBO Reports*, *18*(1), 102–122. https://doi.org/10.15252/embr.201642738

Wang, C., Deng, L., Hong, M., Akkaraju, G. R., Inoue, J., & Chen, Z. J. (2001). TAK1 is a ubiquitin-dependent kinase of MKK and IKK. *Nature*, *412*(6844), 346–351. https://doi.org/10.1038/35085597

Wechsler-Reya, R. J., Elliott, K. J., & Prendergast, G. C. (1998). A Role for the Putative Tumor Suppressor Bin1 in Muscle Cell Differentiation. *Molecular and Cellular Biology*, *18*(1), 566–575. https://doi.org/10.1128/MCB.18.1.566

Wienands, J., Schweikert, J., Wollscheid, B., Jumaa, H., Nielsen, P. J., & Reth, M. (1998). SLP-65: a new signaling component in B lymphocytes which requires expression of the antigen receptor for phosphorylation. *The Journal of Experimental Medicine*, *188*(4), 791–795. https://doi.org/10.1084/jem.188.4.791

Winslow, M. M., Gallo, E. M., Neilson, J. R., & Crabtree, G. R. (2006). The Calcineurin

Phosphatase Complex Modulates Immunogenic B Cell Responses. *Immunity*, *24*(2), 141–152. https://doi.org/10.1016/j.immuni.2005.12.013

Woof, J. M., & Kerr, M. A. (2004). IgA function--variations on a theme. *Immunology*, *113*(2), 175–177. https://doi.org/10.1111/j.1365-2567.2004.01958.x

Wu, T., Shi, Z., & Baumgart, T. (2014). Mutations in BIN1 associated with centronuclear myopathy disrupt membrane remodeling by affecting protein density and oligomerization. *PloS One*, *9*(4), e93060. https://doi.org/10.1371/journal.pone.0093060

Xu, S., Tan, J. E.-L., Wong, E. P.-Y., Manickam, A., Ponniah, S., & Lam, K.-P. (2000). B cell development and activation defects resulting in xid-like immunodeficiency in BLNK/SLP-65-deficient mice. *International Immunology*, *12*(3), 397–404. https://doi.org/10.1093/intimm/12.3.397

Yam-Puc, J. C., Zhang, L., Zhang, Y., & Toellner, K.-M. (2018). Role of B-cell receptors for B-cell development and antigen-induced differentiation. *F1000Research*, *7*, 429. https://doi.org/10.12688/f1000research.13567.1

Zeng S, Xu Z, Lipkowitz S, Longley JB. Regulation of stem cell factor receptor signaling by Cbl family proteins (Cbl-b/c-Cbl). *Blood*. 2005;105(1):226-232. https://doi.org/10.1182/blood-2004-05-1768

Zhang, Y., Wienands, J., Zürn, C., & Reth, M. (1998). Induction of the antigen receptor expression on Blymphocytes results in rapid competence for signaling of SLP-65 and Syk. *The EMBO Journal*, *17*(24), 7304–7310. https://doi.org/10.1093/emboj/17.24.7304

Zúñiga-Pflücker, J. C. (2004). T-cell development made simple. *Nature Reviews Immunology*, *4*(1), 67–72. https://doi.org/10.1038/nri1257

Acknowledgements

I am very fortunate to have performed my PhD study at the Institute of Cellular and Molecular Immunology. There are many people who contributed to my success that I would like to express my profound gratitude to.

First and foremost, Prof. Wienands, I am grateful to you for being my mentor during the course of my PhD study. Your invaluable suggestions, especially in guiding me with this thesis kept me focused on the goals. I would carry fond memories of our discussions, especially the ones that occasionally stepped out of the technical realm of Science and additionally touched upon aspects of the philosophy of science. Thank you !

I am grateful for the insightful suggestions and the motivating words I received throughout my PhD from Prof. Blanche Schwappach and Prof. Steven Johnson as part of my thesis committee meetings.

I would also like to thank our collaborators Prof. Griesinger and the members of his group who I have enjoyed working with.

My heartfelt gratitude to the two post-docs of the department, Michael and Niklas. Thank you for taking out time for discussions with me whenever I came to you, despite your busy schedules and priorities. Just a few minutes of conversation with you helped me learn so much.

I thank Gabi Sonntag and Ines Heine for the great technical assistance and I would also like to acknowledge all the other present and past members of the lab for the great times through the years. Marcel, you would always told me to focus on the silver lining and were always immensely encouraging, thank you!

I am also grateful to Frau Teuteberg and Anika Schindler for their assistance to the department. Anika, I want to profusely thank you for going out of your way, many times, to help me with several complicated administrative matters, especially in the hectic days towards the end. You were always supportive with bright solutions and reminders and English translations. Thank you for being so helpful !

Elsa, I thank you for providing support in several matters in challenging times. Our discussions over Ethiopian food have always brought immense perspective into my life. Matthias, political and pop-culture debates with you have been so enriching for me. Our sarcastic banter definitely kept my spirits high in the lab. Thank you for giving me a listening

ear when I needed it and for being supportive at multiple instances. In several matters, you both have been my family away from family and I would always treasure our friendship in my heart.
I want to thank Lishika, Ipsita and Shikha for the vibrant discussions on our whatsapp group 'Social Kinetics'. You all kept me up to date with all the major events and political activities in India and never made me feel like I was missing out on anything. Shradha, the connection with you is unbreakable, thank you for constantly reminding me that. As a co-expatriate and an old friend, LInk, conversations with you are always comforting. Devesh and Deepika di, thank you for encouraging me over our skype sessions. Shriraj, thank you for the laughs and for making me realise what I was truly capable of.

To my extended family and family-friends sitting in India, your blessings have given me all the strength to come this far in my journey.

Finally, and most importantly I would like to thank my parents. You are my true squad. I owe all of my accomplishments, big or small, to you. You have been cheering me on at every step of the way, forever encouraging me to embark on adventures. Your unconditional love and support enabled the contemplation, hours of research and writing necessary to complete my study. Your faith in me is what drives me forward.

To Göttingen, I thank you for this memorable experience!

List of abbreviations

°C	degree Celsius	g	times gravity
µ	micro	GEF	Guanine nucleotide exchange factor
A	ampere	GFP	Green fluorescent protein
aa	amino acid	GC	Germinal center
α	anti	HRP	Horse radish peroxidase
A	Alanine or Adenine	Ig	Immunoglobulin
Ag	antigen	Igα	Immunoglobulin α
ADCC	Antibody-dependent cell-mediated cytotoxicity	Ig β	Immunoglobulin β
CD	Cluster of differentiation	Ig	Immunoglobulin
CRAC	Ca^{2+} release-activated channel	IP_3	Inositol-1,4,5,-triphosphate
CIN85	Cbl-interacting protein of 85 kDa	IP_3R	Inositol-1,4,5,-triphosphate receptor
CD2AP	CD2 Associated Protein	ITAM	Immunoreceptor tyrosine-based activation motif
DAG	Diacylglycerol	ITT	Immunoglobulin tail tyrosine
ddH_2O	Double distilled water	kDa	Kilo Dalton
Δ	deletion/truncation	MAPK	Mitogen activated protein kinase
dKO	Double knock out	NFAT	Nuclear factor or activated T cells
ERK	Extracellular signal regulated kinase	NF-κB	Nuclear factor kappa of activated B cells
ER	Endoplasmic reticulum	NP-40	Nonidet P-40 or octylphenoxypolyethoxyethanol
$F(ab')_2$	Dimer of antigen binding fragment	PBS	Phosphate buffered saline
FACS	Fluorescence activated cell sorting	PI3K	Phosphoinositide 3-kinase
FcγR	Fc epsilon receptor		

PIP_3	Phosphatidyl-inositol-3,4,5-trisphosphate	Sos	Son of sevenless
SH3	Src homology 3 domain	Syk	Spleen tyrosine kinase
sKO	Single knock out	V(D)J	Variable (V), Diversity (D), Joining (J) gene segments of the Ig heavy chain or Ig light chain
SLP65	Src homology 2 domain containing protein of 65 kDa	wt	Wild-type

Deoxyribonucleotides

G	deoxyguanosine monophosphate
A	deoxyadenosine monophosphate
T	deoxythymidine monophosphate
C	deoxycytidine monophosphate

Single-letter Amino Acid Code

Amino acid	**Three letter code**	**One letter code**
alanine	ala	A
arginine	arg	R
asparagine	asn	N
aspartic acid	asp	D
asparagine or aspartic acid	asx	B
cysteine	cys	C
glutamic acid	glu	E
glutamine	gln	Q
glutamine or glutamic acid	glx	Z
glycine	gly	G
histidine	his	H

isoleucine	ile	I
leucine	leu	L
lysine	lys	K
methionine	met	M
phenylalanine	phe	F
proline	pro	P
serine	ser	S
threonine	thr	T
tryptophan	trp	W
tyrosine	tyr	Y
valine	val	V

List of Figures

List of Tables